

## **INFORMATION TO USERS**

The most advanced technology has been used to photograph and reproduce this manuscript from the microfilm master. UMI films the text directly from the original or copy submitted. Thus, some thesis and dissertation copies are in typewriter face, while others may be from any type of computer printer.

The quality of this reproduction is dependent upon the quality of the copy submitted. Broken or indistinct print, colored or poor quality illustrations and photographs, print bleedthrough, substandard margins, and improper alignment can adversely affect reproduction.

In the unlikely event that the author did not send UMI a complete manuscript and there are missing pages, these will be noted. Also, if unauthorized copyright material had to be removed, a note will indicate the deletion.

Oversize materials (e.g., maps, drawings, charts) are reproduced by sectioning the original, beginning at the upper left-hand corner and continuing from left to right in equal sections with small overlaps. Each original is also photographed in one exposure and is included in reduced form at the back of the book. These are also available as one exposure on a standard 35mm slide or as a 17" x 23" black and white photographic print for an additional charge.

Photographs included in the original manuscript have been reproduced xerographically in this copy. Higher quality 6" x 9" black and white photographic prints are available for any photographs or illustrations appearing in this copy for an additional charge. Contact UMI directly to order.



University Microfilms International  
A Bell & Howell Information Company  
300 North Zeeb Road, Ann Arbor, MI 48106-1346 USA  
313/761-4700 800/521-0600



**Order Number 8926182**

**Mechanics of interface fracture**

**Suo, Zhigang, Ph.D.**

**Harvard University, 1989**

**U·M·I**  
300 N. Zeeb Rd.  
Ann Arbor, MI 48106



HARVARD UNIVERSITY  
THE GRADUATE SCHOOL OF ARTS AND SCIENCES



THESIS ACCEPTANCE CERTIFICATE  
(To be placed in Original Copy)

The undersigned, appointed by the  
Division of Applied Sciences  
Department  
Committee

have examined a thesis entitled  
"Mechanics of Interface Fracture."

presented by Mr. Zhigang Suo

candidate for the degree of Doctor of Philosophy and hereby  
certify that it is worthy of acceptance.

Signature .....

Typed name Professor J. Hutchinson

Signature .....

Typed name Professor B. Budiansky

Signature .....

Typed name Professor J. L. Sanders

Francis Spaepen  
Professor F. Spaepen

Date May 12, 1989



# **Mechanics of Interface Fracture**

A thesis presented

by

**ZHIGANG SUO**

to

Division of Applied Sciences

in partial fulfillment of the requirements

for the degree of

Doctor of Philosophy

in the subject of

Engineering Sciences

Harvard University

Cambridge, Massachusetts

May 12, 1989

© 1989 by Zhigang Suo

All rights reserved.

## **Abstract**

The present work attempts to summarize our knowledge on the mechanics of interface fracture. Emphasis is placed on the analytical and numerical results obtained in the recent years. The materials considered are limited to linearly elastic ones, but nonlinear behaviors are allowed in a small zone around crack tips. Various fundamental issues involved in the definition of interfacial toughness are discussed. An engineering fracture mechanics scheme is stated, including data conversion in the experimental determination of toughness and assessment of a given interface by using the measured toughness. A collection of basic solutions is presented. These solutions are intended to calibrate fracture specimens, evaluate structures and model fracture behaviors at microscopic levels. The parallel results for anisotropic bimaterials are also presented. A brief survey of the elements of anisotropic elasticity is included with application to crack analysis as our goal. Efforts have been made to demonstrate the similarity of the solution structures between isotropic and anisotropic bimaterials. Throughout the work key problems waiting for further development are identified and discussed.

*dedicated to my father*

## Preface

Four years ago in the early May in 1985, I was introduced by Professor Xing Ji, the head then of the Department of Engineering Mechanics, Xi'an Jiaotong University, to Professor John W. Hutchinson who was a visitor of the University. Both men have played significant roles in my intellectual development. At that time and for a year after, I worked for Professor Ji on Boundary Element Methods. I learned a great deal of basic techniques of programming and mathematics that prove to be very useful in my later work. It was purely because of the incident mentioned in the beginning I was luckily admitted by Harvard, and came to this wonderful country in the full of 1986.

The last three years of my life may be typical for many former residents of the Bullpen. I took Professor F. Spaepen's Applied Physics 282 in my first semester, which, I was told later by Professor J.R. Rice, was a survey of at least five standard courses of the materials science major. At that time, I barely knew the classification of crystals, not to mention the phase diagrams. The research usually starts in the first summer for the Bullpen fellows, and I was no exception. The first problem Professor Hutchinson assigned me is the inhomogeneous conic singularities. My newly-wed wife joined me from China that summer, and I did not work out anything until one week before Professor Hutchinson came back from his summer visit of UCSB. He brought back a long list of *important* problems, including interface cracking, thin film decohesion, and crack kinking. He told me to concentrate on these exciting problems, and forget the conic problems (later we were informed that the conic singularities had been worked out by L.M. Keer and co-workers). In the following few months I managed to learn the pathological singularity at an interface crack tip, toughness loci and integral equations, primarily from the preprint of Rice's JAM article of 1988, and many discussions with Professor Hutchinson. We worked out several problems on that list before the Chinese New Year of 1988, which yielded three co-authored papers.

Professor Hutchinson is a truly remarkable advisor. Working for him is a fun itself. He worked with me on the same problem when I started, and let me explore by myself when I felt comfortable with the problem area. The transition from a theoretically motivated person to a theoretically *and* experimentally motivated person is a painful process. He guided me with many of his thought experiments and many real ones conducted by his experimentalist colleagues.

I have also been strongly influenced, directly or indirectly, by several other highly distinguished scholars, among whom Professors B. Budiansky, A.G. Evans and J.R. Rice deserve special thanks. Some ideas elaborated here actually originated from their thinking. My sincere appreciation is extended to Professors Budiansky, Hutchinson, Rice, Sanders and Spaepen who reviewed this work recently, and to Professor K.S. Kim and Drs. H.C. Cao, V. Gupta and J.S. Wang who taught me a lot about fracture behaviors and experimental details.

I am indebted to Ms. Marion Remillard for her helps though the years, and many beautiful preprints she edited for me. My fellow Bullpeners are great people who have made the past three years even more enjoyable.

I will spend more time with my wife, Denian and our one-year old son, Daniel, and write more frequently to my parents and friends in China after my graduation. I own them a lot in many ways.

This work is dedicated to my father.

Z.S.

Science Center Basement

May, 1989

## CONTENTS

<b>Abstract</b>	<b>i</b>
<b>Preface</b>	<b>ii</b>
<b>I. Introduction</b>	<b>1</b>
<b>II. Elasticity Theory of Interface Fracture</b>	<b>4</b>
A. Bimaterial Elasticity 4	
B. Crack Tip Fields 7	
1. Asymptotic Solutions. 2. The Notion of K-Annulus. 3. A Dimensional Dilemma.	
C. $\varepsilon$ -Effects 11	
D. Interface Fracture Mechanics 14	
1. Interfacial Toughness: a $G_c - \psi$ Curve. 2. Utility of a $G_c - \psi$ Curve. 3. A Simplified Approach for Interface Fracture Mechanics. 4. Scales in Application of Interface Fracture Mechanics.	
<b>III. Solutions and Specimens</b>	<b>20</b>
A. Collinear Cracks 20	
1. General Formulation. 2. Examples.	
B. Singularity/Crack Interactions 25	
1. Singularities in a Homogeneous Material. 2. Singularities in a Bimaterial.	
3. Singularity/Crack Interaction.	
C. Sandwiches 31	
1. A Universal Relation for Sandwich Specimens. 2. Data Extraction Scheme for Sandwiches.	
3. Requirement of Small-Scale-Yielding.	
D. Double-Layers 36	
1. Mathematical Development. 2. Applications.	
<b>IV. Elements of Anisotropic Elasticity</b>	<b>43</b>
A. LES Representation 44	

B.	Hermitian Matrices <b>B</b> and <b>H</b>	48
C.	In-Plane Rotation	50
D.	Anti-Plane Deformations	52
E.	In-Plane Deformations of Orthotropic Solids	53
F.	Symmetric Tilt Double-Layers	58
	1. Edge-Loaded Double-Layers. 2. Clamped Double-Layers.	
<b>V.</b>	<b>Interface Cracks in Anisotropic Media</b>	<b>62</b>
A.	An Eigenvalue Problem	63
	1. Structure of Eigenpairs. 2. Effects of in-Plane Rotations.	
B.	Crack Tip Fields	67
	Case 1. Non-Oscillatory Fields. Case 2. Oscillatory Fields. 3. Crack Tip Fields for Orthotropic Bimaterials. 4. Interface Fracture Mechanics of Anisotropic Bimaterials.	
C.	Collinear Cracks	75
	Case 1. <b>H</b> is real. Case 2. <b>H</b> is not real.	
D.	Singularity/Crack Interactions	79
	1. Line Force and Dislocation in a Homogeneous Medium. 2. A singularity in a Bimaterial. 3. Singularity/Crack Interaction.	
<b>Bibliography</b>		<b>84</b>
<b>Figure Captions</b>		<b>88</b>

## I. Introduction

The fundamental objective of the interface fracture mechanics is to seek a meaningful definition of *toughness*, a material property that characterizes the resistance of a bimaterial interface to fracture. The definition should be as simple and useful as it could be.

A student of thermodynamics, telling himself that fracture of an interface is nothing but a separation of two solids, may think that toughness is the energy difference between the sum of the two separated surfaces and the well bonded interface. Under a microscope, he should see, however, much more is going on along with the separation process: micro-cracking, dislocation nucleation, void growth, zig-zag propagation, etc. All dissipate energy and all contribute to resist further cracking. Thus, toughness is a macroscopic measure of the total resistance of all these microscopic contributions. Is it possible to collect all the information at the microscopic level and then assemble them? People have tried and are still trying, without decisive advance yet.

Like many other material properties such as yield strength, toughness should be defined and measured independently. Any hope that it can be related to other more 'basic' material properties seems to be out of the reach of the present state of science. In other words, one can measure and use toughness, both at a macroscopic level, but one does not pretend to have understood how each microscopic process contributes to the toughness. Fracture mechanics, in this sense, is largely a phenomenological theory.

Unlike many other material properties, toughness cannot be defined by a uniform deformation, since cracking inherently involves severely distorted deformation. The quantification of toughness is a significant contribution to the modern mechanics of materials made by G.R. Irwin. About forty years ago, in his pioneering work Irwin identified the three independent singular fields at a crack tip in a homogeneous, isotropic body, which have since been referred to as the three *modes* of singularities. For a given.

material, each mode is universal for all cracked specimens under arbitrary loadings, except for a normalizing constant, or *stress intensity factor*, which depends on the specific specimen geometry and external loading. Based on this mathematical artifact, Irwin was able to define a material property, *toughness*, a loosely termed jargon among metallurgists then, as the critical value (or combinations) of the stress intensity factor that a material can sustain. The toughness so defined can be measured by conventional mechanical test machines and can be readily used to assess structural failure quantitatively.

During the last four decades, Irwin's agenda has been pursued for both brittle and ductile solids. Here we will only keep track of the development for brittle solids.

Williams (1959) discovered the so-called oscillatory near-tip behavior for an interface crack between two isotropic materials. There are still three independent singularity fields in the sense that the near-tip fields are universal for a given material pair except for one complex and one real normalizing factors. The two in-plane modes are coupled and oscillatory, and scaled by a complex stress intensity factor. The mode III field has a square root singularity and is scaled by a real stress intensity factor. The subject of the present work is to extend Irwin's fracture mechanics, on the basis of Williams interface crack tip field, to assess brittle bimaterial interface failure.

In another direction, Stroh (1958), Sih, Irwin and Paris (1965), among others, investigated the crack tip fields in an anisotropic homogeneous body. Again the near-tip fields can be normalized by three stress intensity factors, and moreover, for this situation, the three modes can be separately defined.

The next logical target, a crack along an interface between dissimilar anisotropic media, has been tackled by several authors (Clements 1971, Gotoh 1967, Qu and Bassani 1988, Suo 1989, Tewary et al. 1989a, Ting 1986, Wang 1984, Willis 1971). Several basic crack problems have been solved, and calculation of the oscillatory index has been emphasized. Moreover, the recent work of Suo (1989) identified the precise structure of

the near tip field scaled by one real and one complex stress intensity factors.

The time has come that one can present a rather complete elastic theory of interface fracture mechanics, while there still remains many major works to be done on both the theoretical and experimental sides. The writer takes this opportunity to review what has already been known to the community and discusses in passing what remains to be learned. The plan of this work is as follows.

Interface toughness is defined in Chapter II. Here we try to convey that it is a curve, rather than a number, that fully characterize the resistance of an interface to fracture. The interface fracture mechanics scheme is then stated, which is essentially the same as that in Rice (1988). A simplified scheme proposed earlier (Suo and Hutchinson 1989) is also discussed.

Some basic crack solutions are presented in Chapter III. They are intended as a small compilation to assist the practitioners of the interface fracture mechanics in specimen calibration, structural assessment, and microscopic modelling.

Theoretical breakthrough has taken place recently in anisotropic bimaterial interface fracture. We are now in the position to be able to present the structure of the crack tip fields, and thus to define toughness in the similar spirit as for isotropic bimaterials. A collection of exact crack solutions is also given. It is hoped that the rigorous fracture mechanics will be adopted in the near future, so that toughness data can be reported independent of test specimens in bicrystal and composite material research.

## **II. Elasticity Theory of Interface Fracture**

In this chapter we review, briefly, the fundamentals of interface fracture mechanics. Two frequently asked questions are in our mind when writing this chapter: what makes a interface fracture mechanics scheme possible and, how does this scheme differ from the classical fracture mechanics?

The chapter begins with a short account of bimaterial elasticity, introducing several composite elastic moduli that will be used throughout this work. Since these bimaterial constants are now adopted by several research groups, it is suggested that they be used consistently in the subsequent development of interface fracture mechanics to avoid possible notational confusion. Full crack-tip fields are then presented and certain features of which are discussed. The complex scaling factor of the crack tip fields, or the *stress intensity factor*, is used to define the *toughness locus* which correlates fracture behaviors of specimens under different external conditions. In closing we try to state the scheme of interface fracture mechanics that has been accepted recently by the majority workers in this field. Emphasis is placed on how to convert experimentally measured data to the toughness for a given specimen, and how to use the toughness to assess a given structure containing the same interface.

Some issues discussed here may also be found in previous articles, e.g., Rice (1988), Hutchinson (1989) and Rice, Wang and Suo (1989). We feel these issues are worth repeating in order to appreciate the chapters that follow.

### **A. BIMATERIAL ELASTICITY**

A *bimaterial*, as will be referred to throughout this work, is a composite of two homogeneous materials, either isotropic or anisotropic, with continuity of traction and displacement across *interfaces* maintained. In this and the next chapter attention will be restricted to plane strain deformations in isotropic bimaterials.

As shown in Muskhelishvili (1953), for such 2D elasticity problems, stresses, displacements and resultant forces on an arc in each material can be represented by two *holomorphic functions*,  $\phi(z)$  and  $\psi(z)$ , i.e.,

$$\begin{aligned}\sigma_{yy} + \sigma_{xx} &= 2[\phi'(z) + \bar{\phi}'(\bar{z})] \\ \sigma_{yy} - \sigma_{xx} + 2i\sigma_{xy} &= 2[z\bar{\phi}''(z) + \psi'(z)] \\ 2\mu(u_x + iu_y) &= (3 - 4\nu)\phi(z) + z\bar{\phi}'(\bar{z}) + \bar{\psi}(\bar{z}) \\ i(f_x + if_y) &= \phi(z) + z\bar{\phi}'(\bar{z}) + \bar{\psi}(\bar{z})\end{aligned}\tag{2.1}$$

where  $\mu$  and  $\nu$  are shear modulus and Poisson's ratio of the material. It proves efficient for solving straight crack problems to use another complex potential:

$$\omega(z) = z\phi'(z) + \psi(z)\tag{2.2}$$

In terms of  $\phi(z)$  and  $\omega(z)$ , the representation (2.1) can be rewritten as

$$\begin{aligned}\sigma_{yy} + \sigma_{xx} &= 2[\phi'(z) + \bar{\phi}'(\bar{z})] \\ \sigma_{yy} + i\sigma_{xy} &= \bar{\phi}'(\bar{z}) + \omega'(z) + (\bar{z} - z)\phi''(z) \\ -2i\mu(u_y + iu_x) &= (3 - 4\nu)\bar{\phi}(\bar{z}) - \omega(z) - (\bar{z} - z)\phi'(z) \\ i(f_x + if_y) &= \bar{\phi}(\bar{z}) + \omega(z) + (\bar{z} - z)\phi'(z)\end{aligned}\tag{2.3}$$

In general, the stress field in a bimaterial should depend on three dimensionless elastic moduli combinations  $\nu_1, \nu_2$  and  $\mu_1/\mu_2$ . Subscripts 1 and 2 refer to the two materials. For traction prescribed boundary value problems, however, Dundurs (1969) proved that the in-plane stresses in the bimaterial depend on only *two* dimensionless moduli combinations

$$\alpha = \frac{(1 - \nu_2)/\mu_2 - (1 - \nu_1)/\mu_1}{(1 - \nu_2)/\mu_2 + (1 - \nu_1)/\mu_1}, \quad \beta = \frac{1}{2} \frac{(1 - 2\nu_2)/\mu_2 - (1 - 2\nu_1)/\mu_1}{(1 - \nu_2)/\mu_2 + (1 - \nu_1)/\mu_1}\tag{2.4}$$

They are referred to as the Dundurs' parameters. Two other expressions suggest the roles that  $\alpha$  and  $\beta$  play:

$$\alpha = \frac{\bar{E}_1 - \bar{E}_2}{\bar{E}_1 + \bar{E}_2}, \quad \varepsilon = \frac{1}{2\pi} \ln \frac{1 - \beta}{1 + \beta}\tag{2.5}$$

Here  $\bar{E}$  is the plane strain tensile modulus, being related to  $\mu$  and  $\nu$ , and Young's modulus  $E$  by

$$\bar{E} = \frac{E}{1 - \nu^2} = \frac{2\mu}{1 - \nu} \quad (2.6)$$

Thus  $\alpha$  measures the relative stiffness of the two materials. Material 1 is stiffer than material 2 if  $\alpha > 0$ . The so-called *oscillatory index*,  $\epsilon$ , which is responsible for various pathological behaviors at an interface crack tip as to be discussed shortly, can hardly be interpreted intuitively.

All three nondimensional parameters  $\alpha$ ,  $\beta$  and  $\epsilon$  change signs as materials 1 and 2 switch, and vanish when the two materials have identical elastic constants. By requiring  $0 < \nu < 1/2$  and  $\mu > 0$ , Dundurs showed that  $\alpha$  and  $\beta$  are confined to the parallelogram of Fig. 2.1a. Data by Suga et al. (1988) on over a hundred of material pairs suggest that the values of  $\beta$  are even more restricted, i.e.,  $|\beta| < .25$ , implying that  $|\epsilon| < .08$ . Their results are plotted in Fig. 2.1b.

Table 2.1 Dundurs parameters and the oscillatory index.

bimaterial	$\alpha$	$\beta$	$\epsilon$
Al / Al <sub>2</sub> O <sub>3</sub>	-.69	-.143	.046
Au / Al <sub>2</sub> O <sub>3</sub>	-.62	-.053	.017
Cu / Al <sub>2</sub> O <sub>3</sub>	-.47	-.096	.031
Nb / Al <sub>2</sub> O <sub>3</sub>	-.55	-.056	.018
Fe / Al <sub>2</sub> O <sub>3</sub>	-.30	-.065	.021
Au / MgO	-.53	-.062	.020
Ni / MgO	-.13	-.079	.025
Cu / Si	-.04	.038	-.012
epoxy / Al	-.90	-.218	.071

For later convenience, an average stiffness  $E^*$  is defined in the sense

$$\frac{1}{E^*} = \frac{1}{2} \left( \frac{1}{\bar{E}_1} + \frac{1}{\bar{E}_2} \right) \quad (2.7)$$

Representative values of these parameters are given in Table 2.1. The elastic constants used for the calculations are taken from Hirth and Lothe (1982) for all single elements and Suga et. al (1988) for all compounds.

## B. CRACK TIP FIELDS

### 1. Asymptotic Solutions

Consider a semi-infinite traction-free crack lying along the interface between two homogeneous isotropic half planes, with material 1 above and material 2 below (see Fig. 2.2). Also depicted in the figure are two coordinate systems ( $x, y$ ) and ( $r, \theta$ ). It is important to realize that *no* specific length or load are present in the problem. Singular fields are sought to satisfy continuity of traction and displacement vectors across the bonded portion of the interface, as well as the traction-free condition along the crack faces. This is a homogeneous boundary value problem, or an eigenvalue problem.

The problem was posed and solved by Williams (1959) via separation of variables. Presented here is the solution expressed by the complex potentials (Rice 1988)

$$\begin{cases} \phi_1'(z) \\ \phi_2'(z) \end{cases} = \frac{\bar{K}_z^{-1/2-i\varepsilon}}{2\sqrt{2\pi} \cosh \pi\varepsilon} \begin{cases} e^{-\pi\varepsilon} \\ e^{\pi\varepsilon} \end{cases} \quad (2.8)$$

$$\begin{cases} \omega_1'(z) \\ \omega_2'(z) \end{cases} = \frac{K_z^{-1/2+i\varepsilon}}{2\sqrt{2\pi} \cosh \pi\varepsilon} \begin{cases} e^{\pi\varepsilon} \\ e^{-\pi\varepsilon} \end{cases}$$

The branch cut for the multi-valued functions is along the crack line so that for a complex number  $\gamma$ ,  $z^\gamma = (re^{i\theta})^\gamma = e^{\gamma(\ln r + i\theta)}$ . The complex amplitude  $K$ , referred to as the *complex stress intensity factor*, can not be determined by the eigenvalue problem itself. Other numerical factors are embedded to ensure that  $K$  recovers the classical mode I and mode II stress intensity factors, i.e.,  $K = K_I + iK_{II}$ , when  $\varepsilon = 0$ . It is interesting to note that, apart possibly from  $K$ , the near-tip solution does not depend on the other Dundurs' parameter  $\alpha$ . Also observe that potentials in material 2 can be obtained by replacing the

combination  $\pi\varepsilon$  to  $-\pi\varepsilon$  everywhere in the potentials for material 1. For this reason we will present expressions for stresses and displacements in material 1 only.

The asymptotic stress and displacement fields in material 1, derived from the potentials in (2.7), can be put into the form

$$\sigma_{ij} = \frac{1}{\sqrt{2\pi r}} \left\{ \operatorname{Re}[Kr^{ie}] \tilde{\sigma}_{ij}^I(\theta, \varepsilon) + \operatorname{Im}[Kr^{ie}] \tilde{\sigma}_{ij}^{II}(\theta, \varepsilon) \right\} \quad (2.9)$$

$$u_{ij} = \frac{1}{2\mu_1} \sqrt{\frac{r}{2\pi}} \left\{ \operatorname{Re}[Kr^{ie}] \tilde{u}_{ij}^I(\theta, \varepsilon, v_1) + \operatorname{Im}[Kr^{ie}] \tilde{u}_{ij}^{II}(\theta, \varepsilon, v_1) \right\}$$

The dimensionless angular distributions are

$$\begin{aligned} \tilde{\sigma}_{rr}^I &= -\frac{\sinh \varepsilon(\pi - \theta)}{\cosh \pi\varepsilon} \cos \frac{3\theta}{2} + \frac{e^{-\varepsilon(\pi - \theta)}}{\cosh \pi\varepsilon} \cos \frac{\theta}{2} (1 + \sin^2 \frac{\theta}{2} + \varepsilon \sin \theta) \\ \tilde{\sigma}_{\theta\theta}^I &= \frac{\sinh \varepsilon(\pi - \theta)}{\cosh \pi\varepsilon} \cos \frac{3\theta}{2} + \frac{e^{-\varepsilon(\pi - \theta)}}{\cosh \pi\varepsilon} \cos \frac{\theta}{2} (\cos^2 \frac{\theta}{2} - \varepsilon \sin \theta) \\ \tilde{\sigma}_{r\theta}^I &= \frac{\sinh \varepsilon(\pi - \theta)}{\cosh \pi\varepsilon} \sin \frac{3\theta}{2} + \frac{e^{-\varepsilon(\pi - \theta)}}{\cosh \pi\varepsilon} \sin \frac{\theta}{2} (\cos^2 \frac{\theta}{2} - \varepsilon \sin \theta) \\ \tilde{\sigma}_{rr}^{II} &= \frac{\cosh \varepsilon(\pi - \theta)}{\cosh \pi\varepsilon} \sin \frac{3\theta}{2} - \frac{e^{-\varepsilon(\pi - \theta)}}{\cosh \pi\varepsilon} \sin \frac{\theta}{2} (1 + \cos^2 \frac{\theta}{2} - \varepsilon \sin \theta) \\ \tilde{\sigma}_{\theta\theta}^{II} &= -\frac{\cosh \varepsilon(\pi - \theta)}{\cosh \pi\varepsilon} \sin \frac{3\theta}{2} - \frac{e^{-\varepsilon(\pi - \theta)}}{\cosh \pi\varepsilon} \sin \frac{\theta}{2} (\sin^2 \frac{\theta}{2} + \varepsilon \sin \theta) \end{aligned} \quad (2.10)$$

$$\tilde{\sigma}_{r\theta}^{II} = \frac{\cosh \varepsilon(\pi - \theta)}{\cosh \pi\varepsilon} \cos \frac{3\theta}{2} + \frac{e^{-\varepsilon(\pi - \theta)}}{\cosh \pi\varepsilon} \cos \frac{\theta}{2} (\sin^2 \frac{\theta}{2} + \varepsilon \sin \theta)$$

$$\tilde{u}_r^I = A \left\{ \kappa_1 \left( \cos \frac{\theta}{2} + 2\varepsilon \sin \frac{\theta}{2} \right) - e^{2\varepsilon(\pi - \theta)} \left( \cos \frac{3\theta}{2} + 2\varepsilon \sin \frac{3\theta}{2} \right) - (1 + 4\varepsilon^2) \sin \theta \sin \frac{\theta}{2} \right\}$$

$$\tilde{u}_\theta^I = A \left\{ \kappa_1 \left( -\sin \frac{\theta}{2} + 2\varepsilon \cos \frac{\theta}{2} \right) - e^{2\varepsilon(\pi - \theta)} \left( -\sin \frac{3\theta}{2} + 2\varepsilon \cos \frac{3\theta}{2} \right) - (1 + 4\varepsilon^2) \sin \theta \cos \frac{\theta}{2} \right\}$$

$$A = \frac{e^{-\varepsilon(\pi - \theta)}}{(1 + 4\varepsilon^2) \cosh \pi\varepsilon}, \quad \kappa_1 = 3 - 4v_1$$

The above expressions hold also for plane stress problems provided one reinterpreted  $\varepsilon$  and  $\kappa_1$  accordingly.

When  $\varepsilon = 0$  these angular distributions reduce to the classical results for a crack

tip in a homogeneous material. The angular distributions for stresses are contrasted for the two cases  $\epsilon = 0$  and  $\epsilon = .05$  in Fig. 2.3. It is striking that the  $\sigma_{rr}^J$  component for the two  $\epsilon$  values differ about 30% in magnitude ahead the crack tip ( $\theta = 0$ ). Recall that the normal stress in the  $x$  direction is not continuous across the interface. Indeed, one may confirm

$$[\sigma_{xx}(r, 0)]_1 - [\sigma_{xx}(r, 0)]_2 = -4(\tanh \pi\epsilon) \operatorname{Re}(Kr^{i\epsilon}) / \sqrt{2\pi r} \quad (2.11)$$

The interface traction a distance  $r$  ahead of the crack tip ( $\theta = 0$ ) is

$$\sigma_{yy} + i\sigma_{xy} = (2\pi r)^{-1/2} Kr^{i\epsilon} \quad (2.12)$$

This equation can be taken as the defining equation for the stress intensity factor. The displacement jump across the interface a distance  $r$  behind the crack tip is

$$\delta_y + i\delta_x = \frac{8Kr^{i\epsilon}}{E * (1 + 2i\epsilon) \cosh \pi\epsilon} \sqrt{\frac{r}{2\pi}} \quad (2.13)$$

The Irwin type formula is (Malyshev and Salganik 1965, Park and Earmme 1986)

$$J = G = \frac{|K|^2}{E * \cosh^2 \pi\epsilon} \quad (2.14)$$

Here  $G$  is the stain energy release per unit of newly created crack surface, and  $J$  is the Rice's (1968) conservation integral.

## 2. The Notion of K-Annulus

For a real life structure containing an interface crack, the crack tip fields must be perturbed by at least two things: the external geometry and the inelastic behavior in a zone localized around the crack tip. The field may also be perturbed because the interface is not mathematically well defined, e.g., an interface with a thin reaction layer, or a continuous transition layer resulting from diffusion, or a small zone of contact due to surface roughness, or the crack being slightly off the interface.

If all these micro-features are small in dimension compared with the external geometry, owing to the square root singularity, the above asymptotic fields are still approximately *unperturbed* in an *annulus* larger than the micro-features but smaller than

the external geometry. Within such an annulus, for any given specimen, the structure of stress fields is completely determined by the Williams solution, while the amplitude of the fields,  $K$ , obtained by solving the particular boundary value problem, uniquely characterizes the external information of the specimen. Such an annulus may be naturally termed as  $K$ -annulus.

A fracture mechanics scheme can be formulated in exactly the same spirit as Irwin did for homogeneous fracture using  $K$  as a (complex) correlating parameter. Rice and Sih (1965) postulated the following fracture criterion:

$$f(\operatorname{Re}[K], \operatorname{Im}[K]) = f_c \quad (2.15)$$

In words it reads: some combination of the real and imaginary parts of  $K$  attains a critical value. In §D we will state the interface fracture mechanics scheme in the current language, which is essentially a variant of the above statement. Indeed, it is these seemingly trivial observations, more than anything else, that make the interface fracture mechanics possible.

### 3. A Dimensional Dilemma

On dimensional grounds and by linearity, for a specimen with a characteristic length  $L$  and traction load  $T$ , the complex  $K$  will take the form

$$K = YT L^{1/2-i\varepsilon} e^{i\psi} \quad (2.16)$$

Here  $Y$  is a dimensionless *real positive* number, and  $\psi$  by definition is the phase angle of the quantity  $KL^{i\varepsilon}$ , but is often loosely (and incorrectly) called the phase angle of stress intensity factor, or even the phase angle of applied load. Both  $Y$  and  $\psi$  in general depend on the ratios of various applied loads and lengths and, for traction prescribed problem, on  $\alpha$  and  $\beta$ .

Observe the stress intensity factor has funny, material-dependent dimensions, which seem unlikely to be accepted in the engineering world in reporting data. The current practice favors to report the combination  $KL^{i\varepsilon}$ , which has the same dimension as the classical stress intensity factor (stress times square root of length). Since  $|L^{i\varepsilon}| = 1$ , and

thus  $|KL^{ie}| = |K|$ , recalling (2.14), one has

$$KL^{ie} = K |e^{i\psi}| = \cosh \pi \epsilon \sqrt{GE} * e^{i\psi} \quad (2.17)$$

The length L used here affects only the phase angle but not the amplitude of the combination  $KL^{ie}$ . However, as mentioned before, it is through K that the interface fracture mechanics correlates laboratory specimens and real structures, not through the combination with an extrinsic length L. The implication of this dilemma will be discussed in §D.

A relation of form (2.16) which connects K to the external load and geometry for a given specimen will be called as a *calibration relation* for the specimen. The length L that is used to define the phase angle  $\psi$  in (2.17) is termed as the *associated length* for  $\psi$ .

### C. $\epsilon$ -EFFECTS

Here we give a short account of several commonly observed pathological behaviors due to the non-vanishing  $\epsilon$ . In conjunction with the next section, we try to convey the idea that these behaviors are largely irrelevant to the framework of interface fracture mechanics scheme, except possibly that some of them will complicate the way people report and use toughness data.

When  $\epsilon = 0$ , the structure of the near-tip fields (stresses, displacements) in each of the two blocks are independent of the elastic constants of the other block, and thus the singular fields in each block are the same as those for a crack in the corresponding homogeneous material. The elastic interaction of the two blocks, if any, is through K, which, for a given boundary value problem in general, depends on the elastic constants of the both blocks. The energy release rate expression (2.14) is simply the average of the corresponding results for the two homogeneous materials. More importantly, the so-called *mode mixity* may be defined exactly as in the mixed mode fracture mechanics for homogeneous materials

$$M \equiv \frac{2}{\pi} \tan^{-1} \left( \frac{\sigma_{xy}}{\sigma_{yy}} \right)_{\theta=0, r \rightarrow 0} = \frac{2}{\pi} \psi \quad (2.18)$$

where  $\psi$  is the phase angle of  $K$  defined in (2.14). Pure mode I is identified as  $M = 0$  and pure mode II as  $M = \pm 1$ . Notice, however, for this case the two materials may still be *very dissimilar* in stiffness since  $\alpha$  may not vanish.

Note that the present definition of the mode mixity is slightly different from that in Shih (1974). We emphasize here that unlike a crack in a homogeneous material, an interface crack plane is not a material symmetry plane. Thus,  $M = +1$  and  $M = -1$  correspond to two entirely different fracture modes. There is no reason that the toughnesses for the two situations should be the same.

In the case  $\varepsilon \neq 0$ , since  $r^{i\varepsilon} = e^{i\varepsilon \ln r} = \cos(\varepsilon \ln r) + i \sin(\varepsilon \ln r)$ , the asymptotic solution displays several pathological behaviors. Firstly, As suggested by (2.12) the ratio  $\sigma_{xy}/\sigma_{yy}$  along the interface varies slowly as  $r$  changes and has no limit as  $r$  approaches zero. This feature is commonly referred to as the *oscillation* in the stress field. A consequence is that the above definition of the mode mixity is meaningless when  $\varepsilon \neq 0$ . A modification is taken to be

$$M(r) \equiv \frac{2}{\pi} \tan^{-1} \left( \frac{\sigma_{xy}}{\sigma_{yy}} \right)_{\theta=0} = \frac{2}{\pi} \left( \psi + \varepsilon \ln \frac{r}{L} \right) \quad (2.19)$$

where  $\psi$  and  $L$  are defined by (2.17). Clearly it is ambiguous to talk about the fracture mode of a specimen without referring to the position  $r$ . However, since  $M$  varies *slowly* with  $r$ , the mode mixity concept does make some sense if an annulus  $r_1 < r < r_2$  around the crack tip is considered. The maximum change of  $M$  over this zone is

$$M(r_2) - M(r_1) = \frac{2}{\pi} \varepsilon \ln \left( \frac{r_2}{r_1} \right) \quad (2.20)$$

For example, taking  $\varepsilon = 0.03$ ,  $r_2/r_1 = 10$ , the above yields a change of  $M$  by 0.04, which is small compared to 1.

This rotational effect will complicate the data reporting and engineering applications, as we will see in the next section.

Another commonly observed pathological feature is the interpenetration of crack faces, i.e.,  $\delta_y < 0$  predicted by (2.13). This implies that there may exist a contact zone behind the crack tip. An elementary estimate of the zone size can be obtained by calculating from (2.13) the largest  $r$  that satisfies  $\delta_y = 0$ . With phase angle  $\psi$  and the associated length  $L$  defined by (2.17), the equation for the contact zone size  $r_c$  is

$$\cos(\psi + \varepsilon \ln \frac{r_c}{L} - \tan^{-1} 2\varepsilon) = 0 \quad (2.21)$$

Here  $L$  is taken to be specimen size, say, the smallest macroscopic length of the specimen. For example, if  $\varepsilon > 0$  and  $-\pi/2 < \psi < \pi/2$ ,  $r_c$  is estimated by

$$\frac{r_c}{L} = e^{-(\psi - \tan^{-1} 2\varepsilon + \pi/2)/\varepsilon} \quad (2.22)$$

This is an exceedingly small number unless  $\psi$  approaches  $-\pi/2$ .

The complexity due to crack face contact can be circumvented by invoking the concept of a small scale process zone (physicists seem to prefer to call it *crack core*, an analogous notion of dislocation core). If the contact zone is small enough, as it is for a large range of the phase angle, there still exists a K-annulus, sufficiently large compared to the contact zone but small compared to the specimen geometry, in which the elastic field is approximately the same as the unperturbed Williams crack tip field. Thus, K uniquely captures all the external information communicated to the tip, and use of K as a correlating factor is justified. Similar to the small scale yielding for metal fracture, the contact zone, when small, does not enter interface fracture mechanics scheme explicitly.

However, the situation is much more complicated when the contact zone is large, say, comparable to the specimen geometry. The problem may be more similar to a tribology problem than to a conventional fracture mechanics problem. Bearing in mind that the crack/contact interference is still largely an unresolved problem even for homogeneous materials, we can say little here besides to appeal to the future investigators.

An important difference can be made between the small-scale-yielding and the small-scale-contact. The yielding zone size is independent of the specimen size when the specimen is large enough. Hence in principle one can always achieve the small-scale-yielding condition by using a giant specimen. By contrast, as indicated by (2.22), the ratio of the contact zone size to the specimen size is fixed for a given loading angle no matter how large the specimen is. This feature allows one to use specimens of any convenient size to conduct fracture test for very large range of the phase angle.

These pathological behaviors have frequently stood as obstacles in the development of interface fracture mechanics. However, it is now accepted that while the near-tip fields must be wrong on the scale of a localized zone (crack core), they nevertheless provide a parameter  $K$ , owing to the square root singularity, characterizing the near-tip state when the zone size is much smaller than the specimen geometry. The fracture mechanics scheme based on  $K$  is discussed in the next section.

#### D. INTERFACE FRACTURE MECHANICS

An interface fracture mechanics is stated in this section, which is a combination of the Irwin's  $K$ -annulus notion and Williams' interface crack tip field, and was first elaborated on by Rice (1988).

##### 1. Interfacial Toughness: a $G_c$ - $\psi$ Curve

Imagine a bimaterial specimen with a pre-existing interface crack. Suppose somehow one has obtained the calibration relation connecting the complex  $K$  with a measurable load  $T$  and specimen size  $L$ :

$$KL^{ie} = YT L^{1/2} e^{i\psi} \quad (2.23)$$

Note the magnitude,  $|KL^{ie}| = |K|$ , is given by  $YTL^{1/2}$ .

Load the specimen proportionally (thus  $\psi$  is fixed), record the magnitude of the loading system  $T$  at the onset of crack propagation, and then calculate  $|K|$  according to

(2.23). The value, denoted as  $|K|_c$ , is the *toughness* of the interface associated with the phase angle  $\psi$ . Repeating this procedure systematically for various  $\psi$ , e.g., by changing the relative proportions of loads, one obtains a  $|K|_c$ - $\psi$  curve, referred to as the *toughness locus* of the interface.

Notice the specific length  $L$  used should also be reported in conjunction with the toughness locus, since it affects the definition of  $\psi$ , as indicated in (2.23). If a different length  $L_1$  is used to define  $\psi_1$ , the  $G_c$ - $\psi_1$  curve will translate in  $\psi$ -axis by an amount  $\varepsilon \ln(L_1/L)$ .

Within the framework of elastic fracture mechanics, this curve is the property of the given interface in the sense that it is independent of specimen geometry and loading system. However, the toughness locus is clearly dependent on the nature of the interface and the testing environment, such as the temperature, the roughness of the free surfaces before bonding, the bonding history, chemical composition of the two materials. Systematic study of these effects is still in a rather primitive stage, and is certainly the central theme in the further development of the interface fracture mechanics.

Observe that  $|K|$  is related to the energy release rate  $G$  by (2.14), the current practice tends to report a  $G_c$ - $\psi$  curve instead, and they are equivalent.

Experimental determination of interface toughness has been attempted recently on several model systems (Argon et al. 1989, Cao and Evans 1988, Charalambides et al. 1989, Gupta et al. 1989, Oh et al. 1988, Varchenya, et al. 1988, Wang and Suo 1989). In principle, any geometry containing an interface crack, with a calibration relation connecting  $K$  and measurable loads, may be used as a specimen for measuring interface toughness. Three types of specimens, thin films under residual tension, sandwiches, and bending specimens, seem to be especially suitable for measuring toughness of brittle interface between brittle solids. The analysis of the corresponding calibration relations will be presented in the next chapter.

## 2. Utility of a $G_c$ - $\psi$ Curve

How is the interface fracture mechanics used? First of all, the  $G_c$ - $\psi$  curves may be taken to rank, quantitatively, the different interfaces. A Cr/glass interface is said to be *tougher* than a Cu/glass interface because the former exhibits higher  $G_c$  values for various  $\psi$ . A short compilation of measured toughness data is given in Table 2.2. The length L in the table is the length used to define  $\psi$ . Owing to the lack of a testing standard, these data may not be very reliable. Yet they nevertheless give a pretty good idea about the 'quality' of these interfaces. In converting  $G_c$  to  $|K|_c$  by (2.17), all elastic constants that are not reported in the original works are taken from Suga et al. (1988). A more detailed compilation of interface energy for many metal/ceramic systems is found in Evans, et al. (1989).

Table 2.2 Toughness for Some Interfaces

Interface	L(μm)	ψ(deg)	$G_c$ (Jm <sup>-2</sup> )	$ K _c$ (MPam <sup>1/2</sup> )
glass/epoxy	25	0	6	0.21 <sup>a</sup>
glass/epoxy	25	40	8	0.29 <sup>a</sup>
glass/epoxy	25	75	23	0.41 <sup>a</sup>
Al/epoxy	25	40	1	0.09 <sup>a</sup>
Al/PMMA	$10^6$	74	11.4	0.25 <sup>b</sup>
Cu/glass	1.5	0	2	0.43 <sup>c</sup>
Si/SiC	0.3	43	5.1	0.40 <sup>d</sup>

a. Cao and Evans (1988). b. Charalambides et al. (1989).

c. Oh et al. (1987). d. Argon et al. (1989)

The second use of the  $G_c$ - $\psi$  curves displays more convincingly the power of interface fracture mechanics. To assess a given structure with an interface flaw, a design engineer may first calculate the energy available for cracking (both  $G$  and  $\psi$ ) for the given structure by any established method (e.g. the finite element method), and then

compare the applied  $G$  with the material toughness  $G_c$  at the same  $\psi$ . The latter critical value may have been measured previously from a laboratory specimen. This is precisely the same as the Irwin's scheme for mixed mode fracture.

In the above discussion we have tacitly assumed that the same  $L$  is used in defining  $\psi$  for both the specimen and the structure. This may not be practical in real applications. Suppose, however,  $L$  and  $L_1$  are used to define the specimen and structure phase angles, respectively, so that

$$KL^{ie} = K(\psi)|_c e^{i\psi}, \quad KL_1^{ie} = K(\psi_1)|_c e^{i\psi_1} \quad (2.24)$$

Remember that the fracture mechanics allows one to correlate  $K$  rather than any other combinations. If under a particular loading case the structure is calculated to have  $|K|$  and  $\psi_1$ , the fracture criterion is then

$$\begin{cases} \psi = \psi_1 - \varepsilon \ln(L_1/L) \\ |K| = K(\psi)|_c \end{cases} \quad (2.25)$$

where the critical value should be read from the toughness locus.

### 3. A Simplified Approach for Interface Fracture Mechanics

Clearly, aside from the complication in data recording, the pathological behaviors do *not* present any essential difficulty in engineering application of the fracture mechanics. Rather, it is the *mode mixity* that complicates the theory. A crack in an isotropic, homogeneous body can usually adjust itself onto a path with the mode I state at the tip. For this reason, the classical fracture mechanics requires information about only one material property, namely,  $K_L$ . By contrast, the fracture mode on an interface of dissimilar materials is usually mixed. Differences in elastic moduli across an interface will disrupt the symmetry even when the geometry and loading are otherwise symmetric with respect to the crack plane. Furthermore an interface is typically brittle compared with the two bulk materials, and an interface crack, even subjected to substantial shear stresses ahead the tip, tends to stay along the interface. Consequently, instead of one material property, one needs a *curve* of toughness locus to fully characterize toughness of an interface.

Two facts have motivated several authors (He and Hutchinson 1988, Suo and Hutchinson 1989) to propose setting  $\varepsilon = 0$  in both recording and using toughness data. The first fact is that for all the calibration relations of various specimens people have known thus far,  $G$  and  $\psi$  are independent or only weakly dependent on  $\varepsilon$  (recall  $\varepsilon$  is small). Secondly, a measured  $G_c$ - $\psi$  curve is not expected to change appreciably if one shifts  $\psi$  by an angle  $\varepsilon \ln(L_1/L_2)$ , as long as  $L_1/L_2 < 100$ , say, where  $L_1$  and  $L_2$  are length scales for the laboratory specimen and the structure to be assessed, respectively. This simplification allows one to talk precisely of the mode mixity of a given specimen and to emphasize the similarity between the interface fracture mechanics and the classical mixed mode fracture mechanics for homogeneous bodies.

If one assumes the theory for  $\varepsilon \neq 0$  is an exact theory, there are two sources of the errors for the above simplified theory. One is due to the simplified calibration relation, and the other is due to the translation of the toughness locus, as discussed above.

#### 4. Scales in Applications of Interface Fracture Mechanics

Scales play a fundamental role in the development of the fracture mechanics, as in any branch of continuum science. Classical examples are the notion of the small scale crack core, homogenization of composites or damaged materials. Here we try to demonstrate, by a concrete example, how the interface fracture mechanics may be applied at different scales.

Consider two blocks of adherends joined by an interlayer of an adhesive. Suppose the adhesive is very thin and brittle compared with the adherends. One is asked to study the toughness of the assembly. The problem may be tackled at two scales.

At a relatively macroscopic level, one may think this is an interface fracture process between the two adherends, while treat the interlayer as a small scale object. At such a level, the two adherends explicitly enter the scheme of interface fracture, but the role of the adhesive, as well as damage processes in it, is contained in the macroscopically

measured toughness. This evaluation process has been used in the adhesion community for years, except that the two adherends treated are usually identical, whereas only the mixed mode homogeneous fracture mechanics is invoked. Obviously the interface fracture mechanics is ideally suited to study the adhesion of different adherends.

At a more microscopic level, one may study the cracking along the interface between the adhesive and one of the adherend. The interface fracture mechanics can be used provided the crack stays along the interface and other damage processes are confined in a crack core small compared with the thickness of the adhesive. These requirements can be realized if the interface is brittle enough.

Clearly, the existence of an unperturbed K-annulus is a prerequisite of the fracture mechanics correlation, which in turn requires a significant macro/micro length ratio. Such a requirement can be violated sometimes. Large scale crack face contact problems, as mentioned earlier, and some very thin films offer such examples. Research efforts are evidently needed in this area.

### **III. Solutions and Specimens**

This chapter contains interface stress intensity factors obtained recently for some geometries (sandwiches and double-layers). They are intended to be used as calibration relations for experimentally measuring interfacial toughness, as well as for the assessment of thin film structures. These specimens have been tested on a few model systems by several research groups.

One inherent difficulty in specimen design is that the interface toughness is a strong function of bonding processes. One can not, in principle, assess a metallic film plasma-sprayed onto a ceramic substrate by consulting the toughness locus measured from the bulk metal/ceramic system bonded by inter-diffusion. In other words, unlike fracture mechanics for homogeneous materials, there is no such thing as one standard specimen that can be used everywhere. The design of interface fracture specimens for various applications has emerged as a high priority subject waiting for further development.

Another category of solutions included here are for collinear interface cracks between two half planes of dissimilar materials, and interactions between such cracks with singularities (dislocation, line force, transformation spot, etc.). The former were obtained in 1960's by several authors. They may be of value for modelling at the microstructural level. Readers will find in Chapter V that these solutions for isotropic bimaterials can be extended almost straightforwardly to anisotropic bimaterials.

#### **A. COLLINEAR CRACKS**

We begin with a class of problems which can be tackled analytically. Consider a bimaterial consisting of two half planes with material 1 above the x-axis and material 2 below. Suppose that a set of cracks lies on the interface, and denote by  $C$  the union of the crack lines. More specifically, suppose there are  $n$  finite cracks in the intervals  $(a_j, b_j)$  and two semi-infinite cracks in the intervals  $(-\infty, b_0)$  and  $(a_0, +\infty)$ , respectively. Each

material is taken to be elastically isotropic and homogeneous, and plane strain deformation is assumed. It suffices to consider only the case of self-equilibrated traction  $\sigma_0(x) = \sigma_{yy}(x) + i\sigma_{xy}(x)$  prescribed on the crack faces since other methods of loading may be reduced to this case by superposition.

The solutions to this class of problems were published simultaneously by England, Erdogan, and Rice and Sih in 1965. Summarized below are their methods and results, which provide us with the first collection of stress intensity factors. The results will be used to examine singularity/crack interactions in the next section, and to construct solutions for anisotropic bimaterials in Chapter V.

### 1. General Formulation

Let the elastic potentials for the two half planes be

$$\phi(z) = \begin{cases} \phi_1(z), \\ \phi_2(z), \end{cases} \quad \omega(z) = \begin{cases} \omega_1(z) \\ \omega_2(z) \end{cases} \quad (3.1)$$

where the subscripts 1 and 2 indicate the two materials. Due to the method of loading,  $\sigma_{yy}$  and  $\sigma_{xy}$  are continuous across the whole x-axis, both the bonded *and* cracked portions. Recalling the Muskhelishvili representation (2.3), it follows that

$$\bar{\phi}'_1(x) + \omega'_1(x) = \bar{\phi}'_2(x) + \omega'_2(x), \quad x \in (-\infty, \infty) \quad (3.2)$$

The above equation can be rearranged as

$$\bar{\phi}'_1(x) - \omega'_2(x) = \bar{\phi}'_2(x) - \omega'_1(x), \quad x \in (-\infty, \infty) \quad (3.3)$$

The functions on the left-hand side are analytic in the lower half plane, while those on the right are analytic in the upper half plane. Hence the both sides are equal to a function analytic on the entire plane, which ought to be a polynomial of  $z$ . This polynomial must be zero to conform the vanishing stresses at infinity. With these *analytic continuation arguments*, (3.3) implies

$$\bar{\phi}'_1(z) = \omega'_2(z), \quad \bar{\phi}'_2(z) = \omega'_1(z) \quad (3.4)$$

Define the displacement jump across the x-axis

$$\delta(x) \equiv [u_y(x, 0^+) + iu_x(x, 0^+)] - [u_y(x, 0^-) + iu_x(x, 0^-)] \quad (3.5)$$

With the aid of (3.4), a direct calculation shows that the displacement jump can be expressed in terms of  $\omega_1(x)$  and  $\omega_2(x)$ :

$$\delta'(x) \equiv \frac{4i}{E^*} [(1 - \beta) \omega_2'(x) - (1 + \beta) \omega_1'(x)] \quad (3.5a)$$

The elastic moduli combinations in the above are defined in §II.A.

As inferred from (3.5a), continuity of displacement across the bonded interface requires that  $\omega_1'(z)$  and  $\omega_2'(z)$  be analytic on the whole plane except on the crack lines, and satisfy

$$\omega_2'(z) = e^{-2\pi\varepsilon} \omega_1'(z), \quad z \notin C \quad (3.6)$$

where  $\varepsilon$  is related to  $\beta$  by (2.5). Since  $\omega_1'(z)$  and  $\omega_2'(z)$  are analytic in upper and lower planes, respectively, equation (3.6) suggests that each of them can be analytically extended to the whole plane except on crack lines  $C$ .

Thus, by only invoking various continuity conditions, we have reduced the four potentials to only one, denoted as  $h(z)$ , such that

$$\omega_1'(z) = \bar{\phi}_2'(z) = h(z), \quad \omega_2'(z) = \bar{\phi}_1'(z) = e^{-2\pi\varepsilon} h(z) \quad (3.7)$$

Obviously  $h(z)$  is analytic in the whole plane except on  $C$ . We will see immediately that  $C$  actually constitutes the branch lines for this otherwise analytic functions. Now one can focus on  $h(z)$ , and once it is solved the four potentials can be obtained by (3.7).

Expressed in terms of  $h(z)$ , the traction along x-axis and the displacement jump are

$$\begin{aligned} \sigma(x) &\equiv \sigma_{yy}(x) + i\sigma_{xy}(x) = h^+(x) + e^{-2\pi\varepsilon} h^-(x) \\ \delta'(x) &= \frac{4i}{E^*} (1 + \beta) [h^-(x) - h^+(x)] \end{aligned} \quad (3.8)$$

The prescribed traction  $\sigma_0(x)$  on crack line  $C$  leads to a Hilbert problem

$$h^+(x) + e^{-2\pi\varepsilon} h^-(x) = \sigma_0(x), \quad x \in C \quad (3.9)$$

Equation (3.9) does not have a unique solution. Several auxiliary conditions needed are:

$h(z)$  approaches zero faster than  $1/z$  as  $z$  goes to infinity;  $h(z)$  conforms the near-tip field (2.7) as  $z$  approaches crack tips; and the net Burgers vector for each of the  $n$  finite cracks is zero. From (3.8) This latter statement yields

$$\int_{a_j}^{b_j} \{ h^-(x) - h^+(x) \} dx = 0, \quad j = 1, 2, \dots, n \quad (3.9a)$$

Since both the governing equation and auxiliary conditions are dependent on only one of the Dundurs parameters  $\varepsilon$ , the solutions should depend only on this moduli combination. For example, if  $\varepsilon = 0$  ( $\alpha$  may be arbitrary), the solutions are exactly the same as those for the corresponding problems in a homogeneous material.

A homogeneous solution of (3.9) is

$$\chi(z) = \prod_{j=0}^n (z - a_j)^{-1/2-i\varepsilon} (z - b_j)^{-1/2+i\varepsilon} \quad (3.10)$$

The branch cuts are chosen along the crack lines so that the product for each finite crack behaves as  $1/z$  for large  $z$ . The total solution to (3.9) is

$$h(z) = \frac{\chi(z)}{2\pi i} \int_C \frac{\sigma_0(x) dx}{\chi^+(x)(x-z)} + \chi(z) P(z) \quad (3.11)$$

where  $P(z)$  is a polynomial which should be chosen to satisfy the auxiliary conditions mentioned above. Once  $h(z)$  is solved, the four potentials can be readily obtained from (3.7).

Recalling (2.7), one can compute the stress intensity factor  $K$  for a crack running in the positive  $x$ -axis with tip at  $x = a$  from

$$K = 2\sqrt{2\pi} (1 + e^{-2\pi\varepsilon}) \lim_{x \rightarrow a^+} (x - a)^{1/2-i\varepsilon} h(x) \quad (3.12)$$

## 2. Examples

Two simple configurations are of particular importance in applications. For a *semi-infinite crack* along the whole negative  $x$ -axis, one can confirm that

$$\chi(z) = z^{-1/2+i\varepsilon}, \quad P(z) = 0 \quad (3.13)$$

$$K = -\sqrt{\frac{2}{\pi}} \cosh \pi\varepsilon \int_{-\infty}^0 \frac{\sigma_0(x)dx}{(-x)^{1/2+i\varepsilon}}$$

The potentials are available from (3.11) if the distribution  $\sigma_0(x)$  on the crack line  $(-\infty, 0)$  is prescribed. For a *finite internal crack* on the interval  $(-a, a)$  the corresponding results are

$$\chi(z) = (z - a)^{-1/2+i\varepsilon} (z + a)^{-1/2-i\varepsilon}, \quad P(z) = 0 \quad (3.14)$$

$$K = -\sqrt{\frac{2}{\pi}} \cosh \pi\varepsilon (2a)^{-1/2-i\varepsilon} \int_{-a}^a \left(\frac{a+x}{a-x}\right)^{1/2+i\varepsilon} \sigma_0(x)dx$$

The general solutions (3.13) and (3.14) embody many special cases. Two examples are given below. In formulating a Dugdale type cohesive-zone model, Ortiz and Blume (1988) solved the semi-infinite crack problem with uniformly distributed opening and shearing stresses,  $\sigma_0(x) = -\sigma - i\tau$ , in the interval  $(-R, 0)$ . The complete potentials for this problem is given by the integral (3.11), although the explicit solution can not be obtained when  $\varepsilon \neq 0$ . The stress intensity factor can be readily evaluated from (2.13), which gives

$$K = \frac{\cosh \pi\varepsilon}{1/2 - i\varepsilon} \sqrt{\frac{2R}{\pi}} R^{-i\varepsilon} (\sigma + i\tau) \quad (3.15)$$

This stress intensity is then implemented to nullify the far field applied stress intensity in their work.

As a second example, consider an internal crack of length  $2a$  with stress state  $(\sigma_y^\infty, \sigma_{xy}^\infty)$  at infinity. By superposition one can confirm that  $K$  is the same for an internal crack loaded at the crack faces with uniform traction  $\sigma_0(x) = -\sigma_y^\infty - i\sigma_{xy}^\infty$  and with zero stress at infinity. The result obtained from (3.14) is

$$K = (1 + 2i\varepsilon)(\sigma_y^\infty + i\sigma_{xy}^\infty)(2a)^{-i\varepsilon} \sqrt{\pi a} \quad (3.16)$$

The integration involved is less trivial this time, and a contour integral has been invoked.

The reader will see more applications in the next section.

## B. SINGULARITY/CRACK INTERACTIONS

This section is primarily based on an earlier note (Suo 1989) dealing with singularities (dislocation, line force, transformation spot, etc.) interacting with traction-free interface cracks. These interactive solutions are quite useful in various models for understanding material toughness at the microstructural level. The solution scheme is essentially superposing the following two solutions: a singularity embedded in a bimaterial *without* crack and, an interface crack loaded on crack faces but with no singularity embedded. The net result is a singularity interacting with a traction-free crack. The second solution has been discussed in above section. The remaining work in the process is the solution for the first problem, and evaluation of the integral involved in (3.11). A *universal constructive rule* has been found which allows one to write out the solution for a singularity in a bimaterial using the solution for the same singularity in a homogeneous material. The second difficulty is resolved via contour integrals on a complex plane.

### 1. Singularities in a Homogeneous Material

In the present context, by a singularity we mean that the associated potentials,  $\phi_0'(z)$  and  $\omega_0'(z)$ , are meromorphic functions (the only singular points are simple poles). The subscript 0 signifies the solution for a *homogeneous* material. If the singularity is at point  $z = s$ , the two potentials in general can be written as

$$\phi_0'(z) = \sum_m \frac{A_m}{(z - s)^m}, \quad \omega_0'(z) = \sum_m \frac{B_m}{(z - s)^m} \quad (3.17)$$

Listed below are potentials for various singularities embedded in a homogeneous material, all at point  $z = s$ .

*An edge dislocation with Burgers vector  $b_x$  and  $b_y$*

$$\phi_0'(z) = \frac{B}{z-s}, \quad \omega_0'(z) = \frac{\bar{B}}{z-s} + \frac{B(s^- - s)}{(z^- - s)^2} \quad (3.18)$$

$$B = \frac{\bar{E}}{8\pi i} (b_x + ib_y)$$

*A line force distributed normal to the z-plane with force per unit length  $p_x$  and  $p_y$*

$$\phi_0'(z) = -\frac{P}{z-s}, \quad \omega_0'(z) = \frac{(3-4\nu)\bar{P}}{z-s} - \frac{P(s^- - s)}{(z^- - s)^2} \quad (3.19)$$

$$P = \frac{p_x + ip_y}{8\pi(1-\nu)}$$

*A line moment distributed normal to the z-plane with moment per unit length  $M$*

$$\phi_0'(z) = 0, \quad \omega_0'(z) = \frac{M}{2\pi i(z^- - s)^2} \quad (3.20)$$

*A circular transformation strain spot*

Let a circular region of radius  $R$  and center  $z = s$  in an infinite homogeneous plane undergo a uniform transformation straining  $\epsilon_{\alpha\beta}$ . Continuity of traction and displacement across the circular boundary is maintained. This is a 2D version of the Eshelby (1953) problem, which is included in an unpublished report by Hutchinson (1974). The potentials outside the spot,  $|z - s| > R$ , are

$$\phi_0'(z) = -\frac{AR^2}{(z^- - s)^2},$$

$$\omega_0'(z) = \frac{(A+2B)R^2}{(z^- - s)^2} + \frac{2AR^2(s^- - \bar{s})}{(z^- - s)^3} - \frac{3AR^4}{(z^- - s)^4} \quad (3.21)$$

$$A = \frac{\bar{E}}{8} (\epsilon_{xx} - \epsilon_{yy} + 2i\epsilon_{xy}), \quad B = \frac{\bar{E}}{8} (\epsilon_{xx} + \epsilon_{yy})$$

## 2. Singularities in a Bimaterial

Suppose we know, somehow, the solution for an isolated singularity in an infinite homogeneous medium, designated as  $\phi_0'(z)$  and  $\omega_0'(z)$ . The aim of this sub-section is to construct the solution for the same singularity in the two bonded half planes. Without loss

of generality, suppose material 1 is above the x-axis and material 1 below, and let the singularity be embedded in material 2. The elastic constants in  $\phi_0'(z)$  and  $\omega_0'(z)$  are for material 2.

Write the solution for the two blocks formally as

$$\phi(z) = \begin{cases} \phi^1(z) + \phi_0(z), & z \in 1 \\ \phi^2(z) + \phi_0(z), & z \in 2 \end{cases} \quad \omega(z) = \begin{cases} \omega^1(z) + \omega_0(z), & z \in 1 \\ \omega^2(z) + \omega_0(z), & z \in 2 \end{cases} \quad (3.22)$$

The task below is to relate  $\phi^1(z)$ ,  $\phi^2(z)$ ,  $\omega^1(z)$  and  $\omega^2(z)$  to the known homogeneous solution  $\phi_0(z)$  and  $\omega_0(z)$ . Notice that by construction,  $\phi^1(z)$ ,  $\omega^1(z)$ ,  $\phi_0(z)$  and  $\omega_0(z)$  are analytic in the upper half plane, while  $\phi^2(z)$  and  $\omega^2(z)$  are analytic in the lower half plane. Continuity of the resultant forces across the interface requires

$$\bar{\phi}^1(x) + \omega^1(x) = \bar{\phi}^2(x) + \omega^2(x) \quad (3.23)$$

By the standard analytic continuity arguments it follows that

$$\bar{\phi}^1(z) = \omega^2(z), \quad \bar{\phi}^2(z) = \omega^1(z) \quad (3.24)$$

Continuity of displacements across the interface, with the aid of (3.24), leads to

$$(1 - \beta)\omega^2(x) - (\alpha + \beta)\bar{\phi}_0(x) = (1 + \beta)\omega^1(x) - (\alpha - \beta)\omega_0(x) \quad (3.25)$$

Invoking analytic continuity arguments again yields

$$\omega^2(x) = \Lambda\bar{\phi}_0(x), \quad \omega^1(x) = \Pi\omega_0(x) \quad (3.26)$$

Here  $\Lambda$  and  $\Pi$  measure the inhomogeneity by

$$\Lambda = \frac{\alpha + \beta}{1 - \beta}, \quad \Pi = \frac{\alpha - \beta}{1 + \beta} \quad (3.27)$$

Now with (3.24) and (3.26) one can rewrite (3.22) explicitly as

$$\phi(z) = \begin{cases} (1 + \Lambda)\phi_0(z), & z \in 1 \\ \Pi\bar{\omega}_0(z) + \phi_0(z), & z \in 2 \end{cases} \quad \omega(z) = \begin{cases} (1 + \Pi)\omega_0(z), & z \in 1 \\ \Lambda\bar{\phi}_0(z) + \omega_0(z), & z \in 2 \end{cases} \quad (3.28)$$

Equation (3.28) is a quite remarkable result in that it is a constructive rule independent of the information of the particular singularity considered. The full elastic fields for a

singularity in a bimaterial can be obtained from (3.28) if the corresponding homogeneous solution is known.

A singularity in a half plane interacting with either traction-free surface or rigidly-held surface along x-axis can be treated as special cases. For the traction-free case, the upper material is nothing which corresponds to  $\alpha = -1$ , or  $\Lambda = \Pi = -1$ . Specializing (3.28) to this case gives

$$\phi(z) = \phi_0(z) - \bar{\omega}_0(z) \quad \omega(z) = \omega_0(z) - \bar{\phi}_0(z) \quad (3.29)$$

For the rigid surface case, one can confirm  $\Lambda = 1/\Pi = 3 - 4\nu$  and

$$\phi(z) = \phi_0(z) + \frac{1}{3-4\nu} \bar{\omega}_0(z) \quad \omega(z) = \omega_0(z) + (3-4\nu)\bar{\phi}_0(z) \quad (3.30)$$

### 3. Singularity/Crack Interactions

Now the interactive solution of singularities and traction-free cracks are sought by superposing the solutions for singularity in a well bonded bimaterial (problem A) and interface cracks loaded only on crack faces (problem B). We first consider the generalized singularity of form (3.17) interacting with a semi-infinite crack or a finite internal crack. The results are then specialized to some cases of particular interest.

Suppose the homogeneous solution  $\phi_0(z)$  and  $\omega_0(z)$  of form (3.17) is known. The potentials for the same singularity in two bonded half planes without cracks (problem A) can be constructed by rule (3.28). In particular, the traction along the interface is given by

$$\sigma_{yy}(x) + i\sigma_{xy}(x) = (1 + \Lambda)\bar{\phi}'_0(x) + (1 + \Pi)\omega'_0(x) \quad (3.31)$$

The negative of this traction is loaded onto the crack faces in problem B. It follows from the results in §III.A, the four potentials induced in the crack problem can expressed by  $h(z)$ , and

$$h(z) = -\frac{\chi(z)}{2\pi} \int_C \frac{(1 + \Lambda)\bar{\phi}'_0(x) + (1 + \Pi)\omega'_0(x)}{\chi^+(x)(x - z)} dx \quad (3.32)$$

where  $\chi(z)$  is given in (3.13) for a semi-infinite crack and (3.14) for an internal crack.

Denote the Cauchy integral over crack lines in (3.32) by  $I$ . Consider a contour integral with the same integrand but over contours specified in Fig. 3.1

$$J = \frac{1}{2\pi i} \oint \frac{(1 + \Lambda)\bar{\phi}_0'(\xi) + (1 + \Pi)\omega_0'(\xi)}{\chi(\xi)(\xi - z)} d\xi \quad (3.33)$$

Evaluating residues one obtains

$$\begin{aligned} J &= \frac{1}{\chi(z)} [(1 + \Lambda)\bar{\phi}_0'(z) + (1 + \Pi)\omega_0'(z)] \\ &+ \sum_m [(1 + \Lambda)\bar{A}_m F_{m-1}(z, \bar{s}) + (1 + \Pi)B_m F_{m-1}(z, s)] \end{aligned} \quad (3.34)$$

where

$$F_m(z, s) = \frac{1}{m!} \frac{\partial^m}{\partial s^m} \left[ \frac{1}{\chi(s)(s - z)} \right] \quad (3.35)$$

On the other hand  $J$  is related to the integral along crack lines  $I$  by

$$J = J_\infty + (1 + e^{-2\pi\varepsilon}) I \quad (3.36)$$

where  $J_\infty$  is the same integrand as  $J$  integrated over circle  $|z| = R \rightarrow \infty$ . The result for the semi-infinite crack is  $J_\infty = 0$  and, for the internal crack  $J_\infty = (1 + \Lambda)\bar{A}_1 + (1 + \Pi)B_1$ .

Substitution of (3.36) into (3.32) gives

$$h(z) = - \frac{\chi(z)}{1 + e^{-2\pi\varepsilon}} (J - J_\infty) \quad (3.37)$$

The four potentials are given by substitution of (3.37) into (3.7), so that the complete solution for the interactive problem is the sum of these potentials and those in (3.22).

The stress intensity factors can be obtained by comparing (3.37) with (3.12). For the semi-infinite crack

$$K = -\sqrt{2\pi} \sum_m [(1 + \Lambda)\bar{A}_m F_{m-1}(0, \bar{s}) + (1 + \Pi)B_m F_{m-1}(0, s)] \quad (3.38)$$

$$F_m(0, s) = \frac{1}{m!} \frac{d^m}{ds^m} [s^{-1/2-i\varepsilon}]$$

and for the internal crack

$$\begin{aligned}
K = & -\sqrt{2\pi}(2a)^{-1/2-i\varepsilon} \{(1+\Lambda)\bar{A}_1 + (1+\Pi)B_1 \\
& - \sum_m (1+\Lambda)\bar{A}_m F_{m-1}(a, \bar{s}) + (1+\Pi)B_m F_{m-1}(a, s)\} \\
F_m(a, s) = & \frac{1}{m!} \frac{d^m}{ds^m} \left[ \left( \frac{s+a}{s-a} \right)^{1/2+i\varepsilon} \right]
\end{aligned} \tag{3.39}$$

As an illustration, the above solutions are specialized to two problems which may be useful in micromechanics modelling. First consider an edge dislocation with Burgers vector  $b = b_y + ib_x$  at point  $z = s$  (in material 2), interacting with a semi-infinite traction-free crack. The dislocation induced  $K$  is given by

$$K = -\frac{E * \cosh \pi\varepsilon}{4\sqrt{2\pi}} \left[ (e^{-\pi\varepsilon} \bar{s}^{-1/2-i\varepsilon} + e^{+\pi\varepsilon} s^{-1/2-i\varepsilon})b + \left(\frac{1}{2} + i\varepsilon\right)e^{+\pi\varepsilon} (s - \bar{s})s^{-3/2-i\varepsilon}b^- \right] \tag{3.40}$$

The above result can be put into a more useful form in the polar coordinates. Let  $s = \rho e^{i\phi}$  ( $-\pi < \phi < 0$ ), and (3.40) can be rewritten as

$$\begin{Bmatrix} \text{Re}[K\rho^{i\varepsilon}] \\ \text{Im}[K\rho^{i\varepsilon}] \end{Bmatrix} = -\frac{E * \cosh \pi\varepsilon}{2\sqrt{2\pi\rho}} \begin{bmatrix} k_{11} & k_{12} \\ k_{21} & k_{22} \end{bmatrix} \begin{Bmatrix} b_y \\ b_x \end{Bmatrix} \tag{3.41}$$

where

$$\begin{aligned}
k_{11} &= \cosh \varepsilon(\pi + \phi) \cos \frac{\phi}{2} + e^{\varepsilon(\pi+\phi)} \sin \phi \left( \frac{1}{2} \sin \frac{3\phi}{2} - \varepsilon \cos \frac{3\phi}{2} \right) \\
k_{12} &= \sinh \varepsilon(\pi + \phi) \sin \frac{\phi}{2} + e^{\varepsilon(\pi+\phi)} \sin \phi \left( \frac{1}{2} \cos \frac{3\phi}{2} + \varepsilon \sin \frac{3\phi}{2} \right) \\
k_{21} &= -\sinh \varepsilon(\pi + \phi) \sin \frac{\phi}{2} + e^{\varepsilon(\pi+\phi)} \sin \phi \left( \frac{1}{2} \cos \frac{3\phi}{2} + \varepsilon \sin \frac{3\phi}{2} \right) \\
k_{22} &= \cosh \varepsilon(\pi + \phi) \cos \frac{\phi}{2} - e^{\varepsilon(\pi+\phi)} \sin \phi \left( \frac{1}{2} \sin \frac{3\phi}{2} - \varepsilon \cos \frac{3\phi}{2} \right)
\end{aligned} \tag{3.42}$$

The interactive solution of a dislocation with a semi-infinite crack in a homogeneous material was solved in Thomson (1986), and was used to examine the shielding effect of dislocations around a crack tip. The solution in the present context has been used by He and Hutchinson (1988a) as kernel functions in formulating integral

equations for problems involving crack kinking out of an interface.

The next example is concerned with a circular transformation straining spot of (3.21). For simplicity we only consider pure dilatation (i.e.,  $\varepsilon_{xx} = \varepsilon_{yy} = \delta$ ,  $\varepsilon_{xy} = 0$ ). The transformation induced stress intensity factor is

$$K = \frac{\sqrt{2\pi}}{4} \delta R^2 E * e^{\pi\varepsilon} \cosh \pi\varepsilon (1 + 2i\varepsilon) \rho^{-3/2-i\varepsilon} \quad (3.43)$$

Alternatively, one can write the result in the polar coordinates  $s = \rho e^{i\phi}$  ( $-\pi < \phi < 0$ ) as

$$\begin{cases} \operatorname{Re}[K\rho^{i\varepsilon}] \\ \operatorname{Im}[K\rho^{i\varepsilon}] \end{cases} = \frac{\sqrt{2\pi}}{4} \delta R^2 \rho^{-3/2} E * e^{\varepsilon(\pi+\phi)} \cosh \pi\varepsilon \begin{cases} \cos \frac{3\phi}{2} + 2\varepsilon \sin \frac{3\phi}{2} \\ -\sin \frac{3\phi}{2} + 2\varepsilon \cos \frac{3\phi}{2} \end{cases} \quad (3.44)$$

The corresponding one-material version solution was contained in an unpublished report of Hutchinson (1974), and has been used in recent works of understanding transformation toughening in ceramics (e.g., Budiansky, et al. 1983) and impurity embrittlement (e.g., Weertman and Hack 1988).

It is interesting to note that when  $\varepsilon = 0$ , the bimaterial solutions for the above two problems are the same as the corresponding one-material solutions except that the moduli are replaced by  $E^*$ , the average modulus defined in (2.6). In the above the singularity is assumed to be in material 2. To obtain stress intensity factors when the singularity is in material 1, simply change the combination  $\pi\varepsilon$  everywhere to  $-\pi\varepsilon$ .

### C. SANDWICHES

The fracture mode of an interface of dissimilar materials is often mixed. A complete characterization of an interface requires toughness data over the full range of mode combinations. This poses a non-trivial problem to those who engaged in preparing and analyzing fracture specimens. Several fracture specimens have been analyzed and

experimentally tested. In this section and the next we will present the analytical results for these specimens. Emphasis will be placed on the final calibration relations which are useful to experimentalists. The results are also of value to those interested in thin film structures.

### 1. A Universal Relation for Sandwich Specimens

Any homogeneous fracture specimen may be converted to measure interface toughness by sandwiching a *thin* layer of second material. A generic set-up is depicted in Fig.3.2. An interlayer of material 2 is in a homogeneous body of material 1, with a pre-existing crack lying along one of the interfaces (upper interface with our convention). Each material is taken to be isotropic and linearly elastic. Attention is restricted to plane strain deformation. The problem is asymptotic in that the reference homogeneous specimen is infinite and the crack is semi-infinite, as is appropriate when the layer thickness  $h$  is very small compared with all other in-plane length scales. The crack tip field of the homogeneous problem (without the layer) is prescribed as the far field in the asymptotic problem. Thus the far field is characterized by the mode I and mode II stress intensity factors,  $K_I$  and  $K_{II}$ , induced by the loads on the reference homogeneous specimen. The interface crack tip field is characterized by the (complex) interfacial stress intensity factor  $K$ . A universal relation is developed below which connects these two sets of stress intensity factors, allowing straightforward conversion of any homogeneous specimen to a sandwich without further calibration.

A remarkable feature common to all sandwiches when the interlayer is thin is that the residual stress in the layer is *not* a driving force of the crack. Thus, in calibrating such a specimen, one needs to take account of the external loading only. To an experimentalist, this simply means that he does not have to measure the residual stress in the interlayer in order to obtain toughness.

Owing to the path-independence of Rice's J-integral, one may calculate the energy release rate  $G$  for the sandwich specimen in two different ways. In terms of the far field  $K_I$

and  $K_{II}$  use of the standard Irwin's formula gives

$$G = \frac{1}{E_1} (K_I^2 + K_{II}^2) = \frac{1}{E_1} |K_I + iK_{II}|^2 \quad (3.45)$$

Alternatively, one may obtain  $G$  in terms of the interface crack stress intensity factor  $K$  by (2.14). Comparison of the two expressions yields

$$|Kh^{i\epsilon}| = \sqrt{1 - \alpha} \cosh \pi \epsilon |K_I + iK_{II}| \quad (3.46)$$

where  $h^{i\epsilon}$  is embedded (without affecting the equation since  $|h^{i\epsilon}| = 1$ ) so that the quantity  $Kh^{i\epsilon}$  has the dimension of the classical stress intensity factors (stress times square root of length). Equation (3.46) states that the two complex quantities have the same magnitude. Thus they can differ only by a *phase angle shift*, designated as  $\omega$ , so that

$$Kh^{i\epsilon} = \sqrt{1 - \alpha} \cosh \pi \epsilon (K_I + iK_{II}) e^{i\omega} \quad (3.47)$$

Now we have obtained the desired conversion relation which connects the crack tip  $K$  and the far field  $K_I$  and  $K_{II}$ , with only one parameter,  $\omega$ , yet to be determined. Notice that this relation is universal in the sense that it does not depend on the details of the reference homogeneous specimens.

On dimensional grounds,  $\omega$  should be a nondimensional function of nondimensional quantities  $K_I/K_{II}$ , and the two Dundurs' parameters  $\alpha$  and  $\beta$ . However, by linearity  $\omega$  should not depend on  $K_I/K_{II}$ . Therefore  $\omega$  depends on  $\alpha$  and  $\beta$  only, i.e.,

$$\omega = \omega(\alpha, \beta) \quad (3.48)$$

This function was determined numerically by solving an integral equation and fully tabulated in Suo and Hutchinson (1989). From the numerical calculation this angle shift, which is due exclusively to the moduli dissimilarity, ranges between  $5^\circ$  to  $-15^\circ$ , depending on  $\alpha$  and  $\beta$ . For most material pairs this will not be a large effect. The issues in the applications of the results here will be discussed in the next two sub-sections.

## 2. Data Extraction Scheme for Sandwiches

The application of universal relation (3.47) to a particular sandwich specimen is straightforward. One may start with any specimen which has been successfully used for homogeneous crack fracture test. Proper techniques are required to sandwich a second material layer into the bulk of the specimen and ensure the crack stays along one of the interfaces, as discussed by Oh et al. (1987) and Cao and Evans (1988). Critical external loads are recorded as the crack start to propagate. To obtain an experimental point on the toughness locus, or the  $G_c$ - $\psi$  curve, for the interface under investigation, one may follow the following scheme:

- i) calculate the apparent stress intensity factors,  $K_I$  and  $K_{II}$ , from the critical external loads as if the specimen were homogeneous using, for instance, the standard handbook solutions;
- ii) obtain the interfacial toughness  $G_c$  from the standard Irwin's formula (3.45) using the critical far field  $K_I$  and  $K_{II}$  since J-integral is conservative;
- iii) the phase angle  $\psi$  is defined associated with the interlayer thickness:

$$Kh^{i\varepsilon} \equiv |Kh^{i\varepsilon}| e^{i\psi} = |K| e^{i\psi} \quad (3.49)$$

and it follows from (3.47) that  $\psi$  can also be determined with  $K_I$  and  $K_{II}$  by

$$\psi = \tan^{-1}(K_{II}/K_I) + \omega(\alpha, \beta) \quad (3.50)$$

As an example, consider the specimen shown in Fig. 3.3. A layer of material 2 with thickness  $h$  is sandwiched in a large plate of material 1, with overall length scale  $L$ . A crack of length  $2a$  is introduced at the center of the specimen along the interface. To apply the universal relation, the specimen should be devised such that  $h \ll a$  and  $L$ . Uniaxial tensile stress  $\sigma$  is applied at an angle  $\theta$  with the normal to the layer and crack. If  $L$  is large enough so that the reference homogeneous specimen can be taken as an internal crack in an infinite plane, the apparent stress intensity factors are (e.g., Tada et al., 1985)

$$K_I = \sigma \sqrt{\pi a} \cos^2 \theta, \quad K_{II} = \sigma \sqrt{\pi a} \sin \theta \cos \theta \quad (3.51)$$

The induced energy release rate calculated from (3.45) is

$$G = \frac{\pi a \sigma^2}{\bar{E}_1} \cos^2 \theta \quad (3.52)$$

and from (3.50) the phase angle is

$$\psi = \theta + \omega(\alpha, \beta) \quad (3.53)$$

Observe that for a given material pair the phase angle shift  $\omega$  is fixed, so that one may use this specimen to measure  $G_c$  over wide range of  $\psi$  by continuously varying the load direction  $\theta$ . Note this specimen is not good if  $\theta$  approaches  $\pm\pi/2$  since the driving force (3.52) goes to zero.

Sandwich set-up has been tested experimentally recently by Oh et al. (1987), Cao and Evans (1988) and Wang and Suo (1989) with various reference homogeneous specimens. The universal conversion relation determined here has reduced the labor of specimen calibration to *mixed mode homogeneous* specimens.

### 3. Requirement of Small-Scale-Yielding

The general requirements for a valid toughness measurement apply to sandwiches. Among them, plane strain condition is usually easy to satisfy. However, the requirement of small scale yielding at the crack tip is sometimes hard to be satisfied, since the interlayer is extremely thin, usually of order of a micron. This concern has been communicated to the writer by K.S. Kim and R.O. Ritchie. Lacking rigorous elastic-plastic analysis for sandwiches, one may use a self-consistence checking scheme as follows. Suppose the small-scale-yield condition is satisfied for a particular sandwich system, i.e., the plastic zone size,  $r_p$ , is very small compared with the interlayer thickness, say,  $r_p < 10h$ . The critical magnitude  $|K|_c$  can be calculated using (3.46). As indicated by the full field finite element analysis of Shih and Asaro (1988), a good estimate of  $r_p$  under the small scale yielding condition may be given as

$$r_p \approx \frac{1}{\pi} \frac{|K|_c^2}{\sigma_0^2} \quad (3.54)$$

where  $\sigma_0$  is the uniaxial yield strength of the weaker material. Now one can check the self-consistency assumption  $r_p < 10h$ .

As an illustration, Table 3.1 listed two sandwich systems taken from Oh et al. (1987) and Cao and Evans (1988). It appears that the glass/Cu/glass system may have violated the small scale yielding condition, and hence one may not accept the  $|K|_c$  value so obtained as an interfacial toughness.

Table 3.1 Estimate of  $r_p$

system	$\psi$ deg	$ K _c$ MPam <sup>1/2</sup>	$\sigma_0$ MPa	$r_p$ $\mu\text{m}$	$h$ $\mu\text{m}$
glass/Cu/glass	0	0.43	75(copper)	10.4	1.5
Al/epoxy/glass	40	0.09	60(epoxy)	2.3	25.0

When the plastic zone size is comparable to or larger than the interlayer thickness, one may still be able to calculate the J-integral from (3.45). What is missing is a parameter that measures the mode mixity under the large-scale-yielding condition. The plasticity theory of interface cracks is still not in a good shape, although some initial work has been reported in a series of articles by Shih and Asaro (1988, 1989). To study the fracture in thin film structures it is important to develop such a non-linear interface fracture mechanics.

#### D. DOUBLE-LAYERS

Another class of specimens that meet certain success is based on double-layers. Looking ahead at Figs. 3.5-3.8, one can find several loading arrangements that will be

analyzed. A desirable feature common to all these specimens is that the cracks attain the steady-state when the crack length is long enough, allowing an accurate measurement of toughness data.

This section is based on Suo and Hutchinson (1988a). Similar analyses have been done when the crack is in the substrate (Suo and Hutchinson 1988b), and when the crack is in an orthotropic material strip (Suo 1988b).

### 1. Mathematical Development

The generalized elasticity problem is introduced in Fig.3.4a, which embodies all above specimens as special cases. Each material is taken to be homogeneous, isotropic and linearly elastic. The double layer is infinitely long with a semi-infinite crack lying along the interface. The upper layer will be called as a film and the lower one a substrate. The film thickness is  $h$  and the film/substrate thickness ratio is  $\eta$ . The structure is traction-free along the upper and lower surfaces but loaded at three edges as indicated, where  $P$ 's are loads per unit width and  $M$ 's are moments per unit width. The uncracked portion far ahead the crack tip may be regarded as a composite beam with a neutral axis lying a distance  $\Delta h$  above the bottom of the beam, where

$$\Delta = \frac{1 + 2\Sigma\eta + \Sigma\eta^2}{2\eta(1 + \Sigma\eta)} \quad (3.55)$$

and

$$\Sigma \equiv \frac{\bar{E}_1}{\bar{E}_2} = \frac{1 + \alpha}{1 - \alpha} \quad (3.56)$$

The solution of  $K$  in general depends on  $P$ 's,  $M$ 's,  $h$ ,  $\eta$  and two Dundurs parameters  $\alpha$  and  $\beta$ . An exact expression for the energy release rate  $G$  can be calculated in close form, which by (2.14) gives the magnitude of the complex  $K$ . Integral equation methods have been used to determine the phase angle of  $K$ . Several analytical considerations are given below which will significantly reduce the labor of numerical computation and result compilation.

Overall equilibrium provides two constraints among the six loads. That is

$$P_1 - P_2 - P_3 = 0 \quad (3.57)$$

$$M_1 - M_2 - M_3 + P_1 h \left( \frac{1}{2} + \frac{1}{\eta} - \Delta \right) + P_2 h \left( \Delta - \frac{1}{2\eta} \right) = 0$$

Hence only four among the six are independent, say,  $P_1, P_3, M_1$  and  $M_3$ .

Since  $\sigma_{22} = \sigma_{12} = 0$  in the uncracked composite layer of Fig. 3.4b, crack can be created anywhere paralleling the interface without disturbing stress distribution. The singular fields for the problem in Fig. 3.4a are therefore the same as those for the problem in Fig. 3.4c when the problem in Fig. 3.4b is superimposed. This superposition shows that the number of load parameters controlling the crack tip singularity can be reduced to only two,  $P$  and  $M$ , given by

$$P = P_1 - C_1 P_3 - C_2 M_3 / h, \quad M = M_1 - C_3 M \quad (3.58)$$

The  $C$ 's are dimensionless numbers given by

$$C_1 = \frac{\Sigma}{A_0}, \quad C_2 = \frac{\Sigma}{I_0} \left( \frac{1}{\eta} + \frac{1}{2} - \Delta \right), \quad C_3 = \frac{\Sigma}{12I_0}$$

$$A_0 = 1/\eta + \Sigma$$

$$I_0 = \Sigma \left[ \left( \Delta - \frac{1}{\eta} \right)^2 - \left( \Delta - \frac{1}{\eta} \right) + \frac{1}{3} \right] + \frac{\Delta}{\eta} \left( \Delta - \frac{1}{\eta} \right) + \frac{1}{3\eta^3} \quad (3.59)$$

where  $A_0$  and  $I_0$  are dimensionless cross section and moment of inertia of the uncracked composite beam, respectively.

It is the problem in Fig. 3.4c that will be analyzed below. Once this solution is obtained, the solution to the general problem in Fig. 3.4a can be readily constructed by reinterpreted  $P$  and  $M$  via (3.58).

The energy release rate may be calculated exactly by taking the difference between the strain energy stored in the structure per unit length far ahead and far behind the crack tip. The result is a positive definite quadratic in  $P$  and  $M$  which can be arranged as

$$G = \frac{1}{2E_1} \left[ \frac{P^2}{hA} + \frac{M^2}{h^3 I} + 2 \frac{PM}{h^2 \sqrt{AI}} \sin \gamma \right] \quad (3.60)$$

where A and I are dimensionless numbers and the angle  $\gamma$  is restricted in the  $|\gamma| < \pi/2$  for definiteness. These quantities are given by

$$\frac{1}{A} = 1 + \Sigma \eta (4 + 6\eta + 3\eta^2), \quad \frac{1}{I} = 12(1 + \Sigma \eta^3), \quad \frac{\sin \gamma}{\sqrt{AI}} = 6\Sigma \eta^2(1 + \eta) \quad (3.61)$$

Hence the energy release rate is obtained in closed form. It is interesting to note that in all formulae above, only one Dundurs' parameter  $\alpha$  (or  $\Sigma$ ) appears. This fact suggests that the other Dundurs' parameter  $\beta$  (or  $\varepsilon$ ) may play a secondary role in the entire problem.

The magnitude of  $K$  can be readily obtained by (2.14). To solve for the phase angle of  $K$ , or more precisely, to partition the real and imaginary parts of  $Kh^{ie}$ , we may do the following. Equating the two energy release expressions (2.14) and (3.60), one can confirm that

$$|Kh^{ie}| = \sqrt{\frac{1-\alpha}{2}} \cosh \pi\varepsilon \left| \frac{P}{\sqrt{hA}} - ie^{i\gamma} \frac{M}{\sqrt{h^3 I}} \right| \quad (3.62)$$

Equation (3.62) implies that two complex numbers have the same magnitude, and thus they can only differ by a phase angle shift, designated as  $\omega$ , so that

$$Kh^{ie} = \sqrt{\frac{1-\alpha}{2}} \cosh \pi\varepsilon \left( \frac{P}{\sqrt{hA}} - ie^{i\gamma} \frac{M}{\sqrt{h^3 I}} \right) e^{i\omega} \quad (3.63)$$

From dimensional considerations and by linearity, it follows that  $\omega$  is a function of  $\alpha$ ,  $\beta$  and  $\eta$  only, i.e.,

$$\omega = \omega(\eta, \alpha, \beta) \quad (3.64)$$

Consequently, the stress intensity factor is fully determined apart from the single real function  $\omega(\eta, \alpha, \beta)$ , which is independent of any load parameters. Determination of this function requires that the crack problem be solved rigorously for a given double-layer

under only *one* loading case. This has been done in Suo and Hutchinson (1988a) using an integral equation formulation. The results are tabulated in that paper.

Now (3.63) may be rewrite in real and imaginary parts separately

$$\begin{aligned}\operatorname{Re}(Kh^{ie}) &= \sqrt{\frac{1-\alpha}{2}} \cosh \pi \epsilon \left[ \frac{P}{\sqrt{hA}} \cos \omega + \frac{M}{\sqrt{h^3 I}} \sin(\omega + \gamma) \right] \\ \operatorname{Im}(Kh^{ie}) &= \sqrt{\frac{1-\alpha}{2}} \cosh \pi \epsilon \left[ \frac{P}{\sqrt{hA}} \sin \omega - \frac{M}{\sqrt{h^3 I}} \cos(\omega + \gamma) \right]\end{aligned}\quad (3.65)$$

## 2. Applications

The general nature of the edge loads of the system in Fig. 3.4a makes it possible to solve many special problems of practical interest. The energy release rate  $G$  can be calculated in closed form as mentioned earlier, namely

$$G = \frac{1}{2\bar{E}_1} \left( \frac{P_1^2}{h} + 12 \frac{M_1^2}{h^3} \right) + \frac{1}{2\bar{E}_2} \left( \eta \frac{P_2^2}{h} + 12\eta^3 \frac{M_2^2}{h^3} - \frac{P_3^2}{A_0 h} - \frac{M_3^2}{I_0 h^3} \right) \quad (3.66)$$

where  $A_0$  and  $I_0$  are dimensionless cross section and moment of inertia of the composite beam, respectively, given in (3.59). The phase angle is defined by

$$\tan \psi = \frac{\operatorname{Im}(Kh^{ie})}{\operatorname{Re}(Kh^{ie})} = \frac{\lambda \sin \omega - \cos(\omega + \gamma)}{\lambda \cos \omega + \sin(\omega + \gamma)}, \quad \lambda = \sqrt{\frac{I}{A} \frac{Ph}{M}} \quad (3.67)$$

where (3.65) has been used and  $P$  and  $M$  are related to the general loads via (3.58).

Sample problems in Fig. 3.5 to 3.8 are chosen to illustrate the process of application. The results are quite useful themselves in several cases as we will mention in passing. The procedure for each application includes

- i) identifying the loads  $P$ 's and  $M$ 's conforming the convention of Fig. 3.4a;
- ii) calculating  $G$  by (3.66);
- iii) getting the equivalent loads  $P$  and  $M$  via (3.58) and hence the loading parameter  $\lambda$  in (3.67) and finally
- iv) calculating  $\psi$  using (3.67).

The *double cantilever specimen* in Fig. 3.5a is considered first, which was

contained in a recent article by Hutchinson (1989) to illuminate the extent of loss of symmetry due to material dissimilarity. Specializing (3.66) and (3.67) to this case gives

$$G = 12M^2h^{-3}/E^*, \quad \psi = \omega + \gamma - \pi/2 \quad (3.68)$$

where  $E^*$  is the average tensile modulus defined in (2.6), and  $\gamma$  should be calculated from (3.61) with  $\eta = 1$ . The angle  $\psi$  is plotted in Fig. 3.5b as a function of  $\alpha$  (setting  $\varepsilon = 0$ ). It is remarkable that the specimen may be severely asymmetric (large mode II stress intensity) due to the material dissimilarity.

Figure 3.6a depicts a *thin film* of material 1 with biaxial misfit tensile stress  $\sigma$  deposited on a substrate of material 2. One can confirm that the misfit stress is equivalent to following mechanical loads in Fig. 3.4a:

$$P_1 = P_3 = \sigma h, \quad M_3 = (1/2 + 1/\eta - \Delta)\sigma h^2, \quad M_1 = 0 \quad (3.69)$$

The energy release rate is thus

$$G = \frac{\sigma^2 h}{2\bar{E}_1} \left[ 1 - \frac{\Sigma}{A_0} - \frac{\Sigma (1/2 + 1/\eta - \Delta)^2}{I_0} \right] \quad (3.70)$$

The loading parameter  $\lambda$  of (3.67) for this case is

$$\lambda = -\sqrt{\frac{I}{A}} \frac{1 - C_1 - C_2(1/2 + 1/\eta - \Delta)}{C_3(1/2 + 1/\eta - \Delta)} \quad (3.71)$$

The results for a thin film on an infinitely thick substrate ( $\eta = 0$ ) are rather simple:

$$G^\infty = \frac{\sigma^2 h}{2\bar{E}_1}, \quad \psi^\infty = \omega(\eta = 0, \alpha, \beta) \quad (3.72)$$

The phase angle obtained by substituting (3.71) into (3.67) is plotted in Fig. 3.6b as a function of  $\alpha$  and  $\eta$ . The ratio of (3.70) and (3.72),  $G/G^\infty$  is plotted in Fig. 3.6c.

Argon et al. (1988) have used residual stresses in thin films as driving forces to measure interface toughness.

The *four-point bend specimen* in Fig. 3.7a was analyzed by Charalambides et al. (1989) and Suo and Hutchinson (1988a). As confirmed by finite element analysis

(Charalambides et al. 1989), when the crack is long compared with the thickness of the notched layer,  $h$ , the crack can be considered as semi-ininitely long. Specializing (3.66) and (3.67) gives

$$G = \frac{M^2}{2E_2 h^3} (12\eta^3 - 1/I_0), \quad \lambda = \sqrt{\frac{I}{A}} \frac{C_2}{C_3} \quad (3.73)$$

where  $M$  is the moment per unit width ( $M = PI$ ). The above results can be put into another form

$$Kh^{i\varepsilon} = YMh^{-3/2} e^{i\psi} \quad (3.74)$$

where  $Y$  and  $\psi$  as the functions of  $\alpha$  and  $h/H$  are plotted in Figs. 7b and 7c, with  $\beta = 0$ . Notice that the thermal mismatch stress of the two layers is a driving force of the crack, analysis of which can be found in Charalambides et al. (1988), or by superposing the results for a thin film under residual tension given above

The final example considered is the *delamination specimen* depicted in Fig. 3.8a.

The stress intensity factor is given by

$$Kh^{i\varepsilon} = YPh^{-1/2} e^{i\psi} \quad (3.75)$$

where  $Y$  and  $\psi$  as the functions of  $\alpha$  and  $h/H$  are plotted in Figs. 8b and 8c, with  $\beta = 0$ .

#### **IV. Elements of Anisotropic Elasticity**

In this chapter we try to set the stage for the possible extension of the interface fracture mechanics to anisotropic bimaterials.

A brief, yet self-contained, review is presented of a complex-variable formulation that represents the stresses and displacements in an anisotropic solid by holomorphic functions. This representation was invented independently in different countries for different purposes. The work done by the Russians early this century was summarized in the book by Lekhnitskii (1963). The problems they treated belonged to conventional structural mechanics (rods, holes and half-planes). Several English scientists (Eshelby, et al. 1953 and Stroh 1958, among others) re-invented the representation, with applications to crystal deformation in mind (dislocations, interfaces, and cracks). The appearance of the two formulations was so different that for quite a long time they had been regarded as entirely different theories for anisotropic elasticity. People involved in the early development of polymeric composites, quite naturally, embraced the Lekhnitskii formulation. Meanwhile materials science community uses exclusively the formulation due to Eshelby et al., which is better known as the Stroh formalism. In §A, both theories are presented, and their equivalence is established. Thus one can take advantage of the both theories and the associated solution methods.

Two positive definite Hermitian matrices  $\mathbf{B}$  and  $\mathbf{H}$  of dimension of compliance are introduced in §B. Some known results in dislocation and crack mechanics involving these matrices are compiled to familiarize ourselves with the notation. Then in §C we explain the notion of an in-plane rotation and the associated tensor rules. Specialized key results for the antiplane deformation and in-plane deformation, especially for orthotropic solids are given in §§D and E. They are useful in application of the solutions developed in the next chapter. The chapter concludes with close form solutions for stress intensity factors for symmetric tilt double-layers.

Aside from the last section, this chapter is largely a synthesis of the previously known results. We hope that such an organization will make the contents in the next chapter, some fundamental results of interface fracture mechanic for anisotropic bimaterials, more transparent.

#### A. LEKHNTSKII-ESHELBY-STROH (LES) REPRESENTATION

Hooke's law connecting the stresses  $\sigma_{ij}$  and strains  $\varepsilon_{ij}$  for a generally anisotropic material can be written in one of the following forms

$$\begin{aligned}\varepsilon_{ij} &= \sum_{k,l=1}^3 S_{ijkl} \sigma_{kl}, & \sigma_{ij} &= \sum_{k,l=1}^3 C_{ijkl} \varepsilon_{kl} \\ \varepsilon_i &= \sum_{j=1}^6 s_{ij} \sigma_j, & \sigma_i &= \sum_{j=1}^6 c_{ij} \varepsilon_j\end{aligned}\quad (4.1)$$

The standard correspondence  $\{\varepsilon_i\} = [\varepsilon_{11}, \varepsilon_{22}, \varepsilon_{33}, 2\varepsilon_{23}, 2\varepsilon_{31}, 2\varepsilon_{12}]^T$  and  $\{\sigma_i\} = [\sigma_{11}, \sigma_{22}, \sigma_{33}, \sigma_{23}, \sigma_{31}, \sigma_{12}]^T$  is adopted. The superscript T denotes the transpose. The fourth-order tensors S and C are referred to as the compliance and stiffness tensors, respectively. The  $6 \times 6$  matrices s and c ( $s = c^{-1}$ ) are conventional compliance and stiffness matrices. The tensor  $C_{ijkl}$  can be replaced by the matrix  $c_{ij}$  correspondingly. The relationship between  $s_{ij}$  and  $S_{ijkl}$  is analogous except that numerical factors are needed, e.g.,  $s_{11} = S_{1111}$ ,  $s_{14} = 2S_{1123}$ ,  $s_{44} = 4S_{2323}$ . To avoid confusion, in this work *no* summation is assumed implicitly for repeated indices.

It has been shown by Lekhnitskii (1963) and Eshelby et al. (1953), that for a two dimensional problem, i.e., with geometry and external loading invariant in the direction normal to x,y-plane, the elastic field can be represented in terms of *three* functions  $f_1(z_1)$ ,  $f_2(z_2)$  and  $f_3(z_3)$ , each of which is *holomorphic* in its argument  $z_j = x + \mu_j y$ . Here  $\mu_j$ , referred to as the *characteristic numbers*, are three distinct complex numbers with positive imaginary part, which can be solved as roots of a sixth-order polynomial to be listed

shortly. With these holomorphic functions, or *complex potentials*, the *representation* for displacements  $u_i$ , stresses  $\sigma_{ij}$ , and resultant forces on an arc  $T_i$  (the medium is kept on the left-hand side as an observer travels in the positive direction of the arc) is

$$\begin{aligned} u_i &= 2 \operatorname{Re} \left[ \sum_{j=1}^3 A_{ij} f_j(z_j) \right], & T_i &= -2 \operatorname{Re} \left[ \sum_{j=1}^3 L_{ij} f_j(z_j) \right] \\ \sigma_{2i} &= 2 \operatorname{Re} \left[ \sum_{j=1}^3 L_{ij} f_j'(z_j) \right] & \sigma_{1i} &= -2 \operatorname{Re} \left[ \sum_{j=1}^3 L_{ij} \mu_j f_j'(z_j) \right] \end{aligned} \quad (4.2)$$

Here,  $(\cdot)'$  stands for the derivative with respect to the associated arguments, and  $\mathbf{A}$  and  $\mathbf{L}$  are two matrices depending on elastic constants, to be defined shortly. Curiously, the derivations by Lekhnitskii and Eshelby et al., and some other authors, notably Green and Zerna (1954), gave entirely different schemes to compute the numbers  $\mu_\alpha$  and matrices  $\mathbf{A}$  and  $\mathbf{L}$ .

On the basis of two Airy-type stress functions, Lekhnitskii found that  $\mu_\alpha$  satisfy the sixth-order characteristic equation

$$l_2(\mu)l_4(\mu) - [l_3(\mu)]^2 = 0 \quad (4.3)$$

where

$$\begin{aligned} l_2(\mu) &= s_{55}\mu^2 - 2s_{45}\mu + s_{44} \\ l_4(\mu) &= s_{11}\mu^4 - 2s_{16}\mu^3 + (2s_{12} + s_{66})\mu^2 - 2s_{26}\mu + s_{22} \\ l_3(\mu) &= s_{15}\mu^3 - (s_{14} + s_{56})\mu^2 + (s_{25} + s_{46})\mu - s_{24} \end{aligned} \quad (4.4)$$

By requiring the compliance matrix to be positive definite, he was able to prove that (4.3) has no real root. If one assumes the roots are distinct, the six roots form three complex conjugate pairs, from which three  $\mu_\alpha$  with positive imaginary part can be selected. The elements of the matrices  $\mathbf{A}$  and  $\mathbf{L}$  are given by

$$\mathbf{L} = \begin{bmatrix} -\mu_1 & -\mu_2 & -\mu_3 \eta_3 \\ 1 & 1 & \eta_3 \\ -\eta_1 & -\eta_2 & -1 \end{bmatrix} \quad (4.5)$$

and

$$\begin{aligned} A_{1\alpha} &= s_{11}\mu_\alpha^2 + s_{12} - s_{16}\mu_\alpha + \eta_\alpha(s_{15}\mu_\alpha - s_{14}) \\ A_{2\alpha} &= s_{21}\mu_\alpha + s_{22}/\mu_\alpha - s_{26} + \eta_\alpha(s_{25} - s_{24}/\mu_\alpha) \\ A_{3\alpha} &= s_{41}\mu_\alpha + s_{42}/\mu_\alpha - s_{46} + \eta_\alpha(s_{45} - s_{44}/\mu_\alpha) \end{aligned} \quad (4.6)$$

for  $\alpha = 1, 2$  and

$$\begin{aligned} A_{13} &= \eta_3(s_{11}\mu_3^2 + s_{12} - s_{16}\mu_3) + s_{15}\mu_3 - s_{14} \\ A_{23} &= \eta_3(s_{21}\mu_3 + s_{22}/\mu_3 - s_{26}) + s_{25} - s_{24}/\mu_3 \\ A_{33} &= \eta_3(s_{41}\mu_3 + s_{42}/\mu_3 - s_{46}) + s_{45} - s_{44}/\mu_3 \end{aligned} \quad (4.6a)$$

where

$$\eta_\alpha = -l_3(\mu_\alpha)/l_2(\mu_\alpha), \quad \alpha = 1, 2 \quad \eta_3 = -l_3(\mu_3)/l_4(\mu_3) \quad (4.7)$$

Equations (4.5-4.7) are valid for plane stress deformation. *Plane strain* deformation can be treated by a change of compliances

$$s'_{ij} = s_{ij} - s_{i3}s_{j3}/s_{33} \quad (4.8)$$

Evidently unaware of the Russian work, Eshelby et al. (1953) presented their more elegant formalism based on the Navier-Cauchy equations. Their representation has the same structure as (4.2). However, each of the characteristic roots  $\mu_\alpha$ , as well as each column of  $\mathbf{A}$  are solved from the eigenvalue problem

$$\sum_{k=1}^3 [C_{i1k1} + \mu_\alpha(C_{i1k2} + C_{i2k1}) + \mu_\alpha^2 C_{i2k2}] A_{ik\alpha} = 0 \quad (4.9)$$

Each column of  $\mathbf{A}$  may be normalized arbitrarily. Thus  $\mu_\alpha$  are the roots with positive imaginary parts of the sixth-order polynomial

$$|C_{i1k1} + \mu_\alpha(C_{i1k2} + C_{i2k1}) + \mu_\alpha^2 C_{i2k2}| = 0 \quad (4.9a)$$

The matrix  $\mathbf{L}$  is given by

$$L_{i\alpha} = \sum_{k=1}^3 [C_{i2k1} + \mu_\alpha C_{i2k2}] A_{k\alpha} \quad (4.10)$$

Plane strain deformation is assumed in (4.9) and (4.10). For plane stress problem the following substitution has to be made

$$c'_{ij} = c_{ij} - c_{i3} c_{j3} / c_{33} \quad (4.11)$$

Now the question of equivalence of the two formulations arises naturally: are  $\mu_\alpha$ ,  $\mathbf{A}$  and  $\mathbf{L}$  defined in the two entirely different ways actually identical? The answer is yes. It is clear in Eshelby et al.(1953) that the representation (4.2) is *uniquely* determined by the elastic constants of a material (up to the three normalization factors for the matrix  $\mathbf{A}$ ), however one derives it. Therefore the Lekhnitskii derivation gives, explicitly, a specially normalized  $\mathbf{A}$ . In the remaining of the paper, the basic formula (4.2) will be referred to as the *LES representation*. Fundamental results known in different formalisms will be cited freely as needed.

Having listed the LES representation and stated the consistency of the two derivations, we now add some words about a particular method, analytic continuation, which will be used extensively in the next chapter. Stated below is a trivial observation that makes analytic continuation arguments possible:

A function  $h(z)$  of  $z = x + \mu y$  is analytic in  $y > 0$  (or  $y < 0$ ) for any  $\mu$  if it is analytic in  $y > 0$  (or  $y < 0$ ) for one  $\mu$ , where  $\mu$  is any complex number with positive imaginary part.

Consequently, when talking about a function analytic in the upper (or lower) half plane, one needs *not* refer to its argument, as long as the argument has the form  $z = x + \mu y$  ( $\text{Im}\mu > 0$ ).

Without loss of any information, we can and *will* present our solutions by the function vector  $\mathbf{f}(z)$  defined as

$$\mathbf{f}(z) = [f_1(z), f_2(z), f_3(z)]^T \quad (4.12)$$

where the argument has the generic form  $z = x + \mu y$  ( $\text{Im}\mu > 0$ ). A substitution of  $z_1, z_2$  or  $z_3$  is made for each component function when the field quantities are to be calculated from (4.2). Of particular importance is the following set of vectors defined along the  $x$ -axis

$$\begin{aligned} \mathbf{u}(x) &= \{u_j(x, 0)\} = \mathbf{Af}(x) + \bar{\mathbf{Af}}(x) \\ \mathbf{T}(x) &= \{T_j(x, 0)\} = -\mathbf{Lf}(x) - \bar{\mathbf{Lf}}(x) \\ \mathbf{t}(x) &= \{\sigma_{2j}(x, 0)\} = \mathbf{L}\mathbf{f}'(x) + \bar{\mathbf{L}}\bar{\mathbf{f}}'(x) \end{aligned} \quad (4.13)$$

The over bar denotes complex conjugation.

## B. HERMITIAN MATRICES $\mathbf{B}$ AND $\mathbf{H}$

One thing that makes the field chaotic is notation. In this work we have tried to use smallest possible set of matrices, i.e.,  $\mathbf{A}, \mathbf{L}, \mathbf{B}$  and  $\mathbf{H}$ . The first two matrices have been discussed in the last section, and the latter two will be introduced in the following. The first three are matrices only involving elastic constants of one material, while the last one,  $\mathbf{H}$ , is a bimaterial matrix. All of them, in general, are complex-valued, and  $\mathbf{B}$  and  $\mathbf{H}$  are positive-definite Hermitian matrices.

Assuming that the roots of the characteristic equation (4.3) or (4.9a) (they are equivalent) form three *distinct* complex conjugate pairs, Stroh (1958) showed that  $\mathbf{A}$  and  $\mathbf{L}$  are non-singular, and moreover, the matrix  $\mathbf{B}$  is a positive definite Hermitian matrix, where

$$\mathbf{B} = i \mathbf{AL}^{-1} \quad (4.14)$$

Here  $i = (-1)^{1/2}$ . Note that by definition  $\mathbf{B}$  is independent of the normalizing constants of  $\mathbf{A}$ , and has a smooth limit even if the latter is singular. It is also good to bear in mind that  $\mathbf{B}$  has the dimension of compliance. Compiled below are several extraordinary known results involving  $\mathbf{B}$ .

For a *crack* running in the  $x$ -direction in a homogeneous anisotropic medium, the Irwin-type relation is

$$J = G = \mathbf{k}^T (\mathbf{B} + \bar{\mathbf{B}}) \mathbf{k} / 4 \quad (4.15)$$

Here  $J$  is Rice's (1968) conservation integral,  $G$  the energy release rate, and  $\mathbf{k}$  the stress intensity factor defined by the traction direct ahead the crack tip

$$\mathbf{k} = [K_I, K_I, K_{III}]^T = \lim_{r \rightarrow 0} (2\pi r)^{1/2} [\sigma_{21}, \sigma_{22}, \sigma_{23}]^T \quad (4.16)$$

A proof of (4.15) can be found in Stroh (1958), Sih et al. (1965) or Barnett and Asaro (1972), and may also be treated as a special case of the corresponding bimaterial result presented in the next chapter.

Imagine a *straight line dislocation* in the direction normal to the  $(x,y)$ -plane, with Burgers vector  $\mathbf{b}$ . The elastic strain energy per unit length of the dislocation in an annulus  $r_0 < r < R$  centered at the dislocation is (Stroh 1958)

$$U = (2\pi)^{-1} \mathbf{b}^T (\mathbf{B} + \bar{\mathbf{B}})^{-1} \mathbf{b} \ln(R/r_0) \quad (4.17)$$

Observe that both (4.15) and (4.17) are quadratic forms, and the matrices involved are inverse to each other. This coincidence was first noticed by Barnett and Asaro (1972), and can be extended, with some restrictions, to bimaterials.

Rice (1985) showed that the pre-logarithmic factor in the above expression is exactly the  $M$ -integral evaluated around the dislocation

$$M = (2\pi)^{-1} \mathbf{b}^T (\mathbf{B} + \bar{\mathbf{B}})^{-1} \mathbf{b} \quad (4.18)$$

Similar calculations had been previously made on isotropic solids by Freund (1978).

Another remarkably general result due to Rice (1985) is concerned with a line dislocation in a *bimaterial* wedge or notch. The dislocation is embedded in one of the materials. Referred to the polar coordinates with the origin coincident with the notch tip, the radial component of the image force due to interface and the traction-free notch faces is identical to the pre-logarithmic factor, namely,

$$f_r = (2\pi)^{-1} \mathbf{b}^T (\mathbf{B} + \bar{\mathbf{B}})^{-1} \mathbf{b} \quad (4.19)$$

Here  $\mathbf{B}$  is for the material where dislocation is embedded. Notice (this is truly remarkable)

that the elastic constants of the neighboring solid, as well as the notch angle, do not enter the above formula.

All the above results except for the last one are for one-materials. It turns out that a bimaterial analog of  $\mathbf{B}$  can be defined as

$$\mathbf{H} = \mathbf{B}_1 + \bar{\mathbf{B}}_2 \quad (4.20)$$

The subscripts 1 and 2 attached to matrices and vectors are reserved exclusively to indicate the two materials. In the above definition, the interface is assumed along the x-axis. Obviously  $\mathbf{H}$  is a Hermitian matrix. In the next chapter we will show that this matrix plays a central role in formulating interface crack problems. For example, a necessary and sufficient condition for an interface crack displaying no oscillatory behaviors is that  $\mathbf{H}$  is real. Two neat results are quoted below.

It is found (Bassani and Qu 1988) when a bimaterial is such that an interface crack tip displays no oscillation ( $\mathbf{H}$  is real), the Irwin-type relation is

$$G = \mathbf{k}^T \mathbf{H} \mathbf{k} / 4 \quad (4.21)$$

Note for a Hermitian matrix  $\mathbf{B}$ , the relation  $\mathbf{k}^T \mathbf{B} \mathbf{k} = \mathbf{k}^T \bar{\mathbf{B}} \mathbf{k}$  holds. Comparison of (4.21) and (4.15) shows that the Irwin-type relation for a non-oscillatory interface crack is just the average of the corresponding relations for the two one-materials. An immediate application of (4.21) will be given in §F.

For a straight dislocation in an bimaterial interface (e.g., Suo 1989)

$$U = (2\pi)^{-1} \mathbf{b}^T \mathbf{H}^{-1} \mathbf{b} \ln(R/r_0) \quad (4.22)$$

This is valid even if  $\mathbf{H}$  is not real. Comparing with (4.21) suggests that the inverse relation observed in homogeneous materials still holds for an interface crack and dislocation, provided the non-oscillation condition is satisfied.

### C. IN-PLANE ROTATIONS

When the crack and interface are not aligned with the principal material axes, it is

often convenient to invoke in-plane rotations. The fourth-order compliance and stiffness tensors obey the usual tensor rules. The transformation rules for the stiffness and compliance matrices can be deduced accordingly. Here we investigate the transformation rules for the matrices  $\mathbf{A}$ ,  $\mathbf{L}$ ,  $\mathbf{B}$  and  $\mathbf{H}$  under an in-plane rotation.

Observe that the strain energy of a straight dislocation is a scalar invariant to an in-plane rotation of the coordinate system. Examining (4.17) and (4.22), since  $\mathbf{b}$  is a vector and  $U$  is a scalar, one may conclude that the matrices  $\mathbf{B}$  and  $\mathbf{H}$  ought to transform like second order tensors under such an in-plane rotation. Indeed, this conjecture can be readily confirmed by some recent results by Ting.

Consider an in-plane coordinate rotation

$$\mathbf{R} \equiv \begin{bmatrix} \frac{\partial x_i^*}{\partial x_j} \end{bmatrix} = \begin{bmatrix} \cos \phi & \sin \phi & 0 \\ -\sin \phi & \cos \phi & 0 \\ 0 & 0 & 1 \end{bmatrix} \quad (4.23)$$

where (\*) indicates the new coordinate system, and  $\phi$  is the angle measured from  $x$ -axis to  $x^*$ -axis. Ting (1982) showed that the characteristic numbers transform as

$$\mu_j^* = (\mu_j \cos \phi - \sin \phi) / (\mu_j \sin \phi + \cos \phi) \quad (4.24)$$

and each column of  $\mathbf{A}$  and  $\mathbf{L}$  transforms like a vector, namely

$$\mathbf{A}^* = \mathbf{R} \mathbf{A}, \quad \mathbf{L}^* = \mathbf{R} \mathbf{L} \quad (4.25)$$

It is obvious from their definitions that under such an in-plane rotation,  $\mathbf{B}$  and  $\mathbf{H}$  transform like second order tensors, i.e.,

$$\mathbf{B}^* = \mathbf{R} \mathbf{B} \mathbf{R}^T, \quad \mathbf{H}^* = \mathbf{R} \mathbf{H} \mathbf{R}^T \quad (4.26)$$

The second equation holds provided the relative orientation of the two solids are fixed, but the  $x$ -axis, or the interface, is subjected to an in-plane rotation.

These tensor rules allow one to transform results obtained in principal material axes to those in general coordinate systems. Moreover they are useful to prove some general theorems, as will be illustrated in the next chapter.

## D. ANTI-PLANE DEFORMATIONS

Consider materials with x, y-plane as a mirror plane, in which the in-plane and antiplane deformations are decoupled. Such solid may be called monoclinic in consistent with the crystallographic nomenclature. The anti-plane deformation will be studied in this section.

The Hooks law reduces to

$$\begin{Bmatrix} \gamma_{13} \\ \gamma_{23} \end{Bmatrix} = \begin{bmatrix} s_{55} & s_{45} \\ s_{45} & s_{44} \end{bmatrix} \begin{Bmatrix} \sigma_{13} \\ \sigma_{23} \end{Bmatrix} \quad (4.27)$$

In equation (4.3),  $l_3(\mu)$  is identically zero for a material with such a symmetry. The characteristic equation for antiplane deformation thus becomes

$$l_2(\mu) \equiv s_{55}\mu^2 - 2s_{45}\mu + s_{44} = 0 \quad (4.28)$$

The expression  $s_{44}s_{55} - (s_{45})^2$ , a principal minor of the compliance matrix, is positive. Hence there are two complex conjugate roots to (4.28). According to the convention the root with positive imaginary part is chosen, i.e.,

$$\mu_3 = [s_{45} + i(s_{44}s_{55} - s_{45}^2)^{1/2}] / s_{55} \quad (4.28a)$$

Only one holomorphic function  $f_3(z_3)$  is needed to represent antiplane deformations, with  $z_3 = x + \mu_3 y$ . Now all  $3 \times 3$  matrices defined earlier reduce to scalars. Keeping the same notation, one has

$$L = -1, \quad A = iB, \quad B = (s_{44}s_{55} - s_{45}^2)^{1/2} \quad (4.29)$$

Clearly, B can be interpreted as the inverse of an equivalent shear modulus, which reduces to the standard shear modulus as the material degenerates to be transversely cubic, or tetragonal. Subscripts 1 and 2 is attached to B to signify the two materials. The bimaterial matrix, now a scalar,  $H = B_1 + B_2$ , is identically real! Consequently, for a bimaterial with such a symmetry, the mode III near-tip field of an interfacial crack is non-oscillatory. The Irwin-type relation for a mode III interface crack, specialized from (4.21), is

$$G = (B_1 + B_2)K_{III}^2/4 \quad (4.30)$$

Since the in-plane rotation matrix now corresponds to  $R = 1$ ,  $B$  is invariant to such a rotation. This can be understood directly from (4.27). Since the anti-plane strains and stresses transform like vectors under an in-plane rotation, the reduced compliance matrix in (4.27) must be a second order tensor under such a rotation. The two invariants of this tensor are the trace and determinant, and the latter is  $B$ . The invariance of  $B$  implies that when (4.30) is written in one set of the orientation of the interface and the two solids, it remains unchanged for any other set of orientation. For example, for two orthotropic solids, (4.30) can be written as

$$G = (\left[ \sqrt{s_{44}s_{55}} \right]_1 + \left[ \sqrt{s_{44}s_{55}} \right]_2)K_{III}^2/4 \quad (4.30a)$$

where the compliances are referred to the principal material axes. This equation holds regardless of the specific alignment of the interface (and thus crack) and the two solids.

#### E. IN-PLANE DEFORMATIONS OF ORTHOTROPIC SOLIDS

Consider a solid with the monoclinic symmetry first. The characteristic equation for in-plane deformation, specialized from (4.3), is

$$l_4(\mu) \equiv s_{11}\mu^4 - 2s_{16}\mu^3 + (2s_{12} + s_{66})\mu^2 - 2s_{26}\mu + s_{22} = 0 \quad (4.31)$$

Assuming the roots are distinct, one can choose two different roots,  $\mu_1$  and  $\mu_2$ , with positive imaginary parts, to each of which a complex variable  $z_j = x + \mu_j y$  is associated. The field quantities can be expressed by two holomorphic functions  $f_1(z_1)$  and  $f_2(z_2)$ , as obtained by discarding  $f_3(z_3)$  in (4.2). The matrices  $A$ ,  $L$ ,  $B$  and  $H$  are  $2 \times 2$  now. The elements for  $A$  and  $L$  can be specialized from (4.5) and (4.6) with  $\eta_1 = \eta_2 = 0$ , while

$$B \equiv iAL^{-1} = \begin{bmatrix} s_{11} \operatorname{Im}(\mu_1 + \mu_2) & -i(\mu_1 \mu_2 s_{11} - s_{12}) \\ i(\bar{\mu}_1 \bar{\mu}_2 s_{11} - s_{12}) & -s_{22} \operatorname{Im}(\mu_1^{-1} + \mu_2^{-1}) \end{bmatrix} \quad (4.32)$$

In deriving (4.32) the standard relations between roots and coefficients have been used.

To gain more insight, we consider below orthotropic materials. As input data for

several subsequent illustrative calculations, representative elastic constants are give in tables 4.1, 4.2 and 4.3 for cubic crystals, woods and fiber reinforced composites (unit: GPa).

Table 4.1 ELASTIC CONSTANTS FOR CUBIC CRYSTALS

crystal	$E_{11}$	$\mu_{12}$	$v_{12}$
Al(fcc)	63.7	28.5	.36
Cr(bcc)	333.3	100.8	.14
Cu(fcc)	66.8	75.4	.42
Nb(bcc)	151.5	28.7	.35

Table 4.2 ELASTIC CONSTANTS FOR WOODS

specie	$E_L$	$E_R$	$E_T$	$\mu_{RT}$	$\mu_{TR}$	$\mu_{LR}$	$v_{RT}$	$v_{TL}$	$v_{LR}$
ash	15.8	1.50	0.80	0.27	0.89	1.34	.69	.026	.47
balsa	6.3	0.30	0.11	0.03	0.20	0.31	.67	.009	.30
oak	5.7	2.14	0.96	0.39	0.77	1.29	.65	.086	.32
pine	16.3	1.10	0.57	0.07	0.67	1.74	.61	.016	.47

Table 4.3 ELASTIC CONSTANTS FOR COMPOSITES

material	$E_{11}$	$E_{22}$	$\mu_{12}$	$v_{12}$	$v_{23}$
boron/epoxy	201.3	22.1	5.4	.17	-
S-glass/epoxy	60.7	24.8	12.0	.23	-
graphite/epoxy	144.8	10.3	6.9	.28	-
aramid/epoxy	84.1	4.8	2.8	.32	-

First consider the case that the material principal axes are in x and y direction, since other orientations can be treated with an in-plane rotation. Given an orthotropic medium, only four elastic constants,  $s_{11}$ ,  $s_{22}$ ,  $s_{12}$  and  $s_{66}$ , enter the plane problem formulation. Following the notation introduced earlier (Suo, 1988b), we define two nondimensional parameters

$$\lambda = \frac{s_{11}}{s_{22}}, \quad \rho = \frac{2s_{12} + s_{66}}{2\sqrt{s_{11}s_{22}}} \quad (4.33)$$

The two parameters measure the anisotropy in the sense that  $\lambda = 1$  as the material is tetragonal and  $\lambda = \rho = 1$  as the material becomes transversely isotropic. The positive definiteness of the strain energy density requires that

$$\lambda > 0, \quad -1 < \rho < \infty. \quad (4.34)$$

Representative values of  $\lambda$  and  $\rho$  are given in Table 4.4 for both plane strain and plane stress. In the calculation of the plane strain values for the composites, we take  $v_{23} = 0.3$ .

Table 4.4  $\lambda$  AND  $\rho$  VALUES

material	plane stress		plane strain	
	$1/\lambda$	$\rho$	$1/\lambda$	$\rho$
Al(fcc)	1	0.76	1	0.72
Cr(bcc)	1	1.51	1	1.52
Cu(fcc)	1	0.02	1	-0.19
Nb(bcc)	1	2.28	1	2.47
ash(LR)	10.5	1.68	7.9	1.88
balsa(LR)	21.0	2.13	17.8	2.29
oak(LR)	2.7	1.16	2.3	1.21
pine(LR)	14.8	1.09	12.1	1.18
boron/epoxy	9.1	6.14	8.3	6.43
S-glass/epoxy	2.4	1.47	2.3	1.51
graphite/epoxy	14.0	2.73	12.8	2.85
aramid/epoxy	17.4	3.49	16.0	3.64

The specialized characteristic equation is

$$\lambda\mu^4 + 2\rho\sqrt{\lambda}\mu^2 + 1 = 0 \quad (4.35)$$

Hence the roots depend on  $\lambda$  and  $\rho$  only, implying that moduli dependence of in-plane stress components is only through  $\lambda$  and  $\rho$  for a traction prescribed homogeneous body. Written out explicitly, the roots with positive imaginary parts are

$$\begin{aligned}
\mu_1 &= i\lambda^{-1/4}(n + m), \quad \mu_2 = i\lambda^{-1/4}(n - m), \quad \text{for } 1 < \rho < \infty \\
\mu_1 &= \lambda^{-1/4}(in + m), \quad \mu_2 = \lambda^{-1/4}(in - m), \quad \text{for } -1 < \rho < 1 \\
\mu_1 &= \mu_2 = i\lambda^{-1/4}, \quad \text{for } \rho = 1
\end{aligned} \tag{4.36}$$

$$n = \sqrt{(1 + \rho)/2}, \quad m = \sqrt{|1 - \rho|/2}$$

Note as  $\rho = 1$  the roots are degenerate. The significance of this special case has been discussed in Suo (1988, 1989). For simplicity we will only consider the case  $\rho \neq 1$  here.

The matrix  $\mathbf{B}$  for an orthotropic material is

$$\mathbf{B} = \begin{bmatrix} 2n\lambda^{1/4}\sqrt{s_{11}s_{22}} & i(\sqrt{s_{11}s_{22}} + s_{12}) \\ -i(\sqrt{s_{11}s_{22}} + s_{12}) & 2n\lambda^{-1/4}\sqrt{s_{11}s_{22}} \end{bmatrix} \tag{4.37}$$

For an orthotropic bimaterial with principal axes *aligned* in the x and y directions, one has

$$\mathbf{H} = \begin{bmatrix} H_{11} & -i\beta\sqrt{H_{11}H_{22}} \\ i\beta\sqrt{H_{11}H_{22}} & H_{22} \end{bmatrix} \tag{4.38}$$

where

$$\begin{aligned}
H_{11} &= \left[ 2n\lambda^{1/4}\sqrt{s_{11}s_{22}} \right]_1 + \left[ 2n\lambda^{1/4}\sqrt{s_{11}s_{22}} \right]_2 \\
H_{22} &= \left[ 2n\lambda^{-1/4}\sqrt{s_{11}s_{22}} \right]_1 + \left[ 2n\lambda^{-1/4}\sqrt{s_{11}s_{22}} \right]_2 \\
\sqrt{H_{11}H_{22}} \beta &= [\sqrt{s_{11}s_{22}} + s_{12}]_2 - [\sqrt{s_{11}s_{22}} + s_{12}]_1
\end{aligned} \tag{4.39}$$

Here  $\beta$  is a generalization of one of the Dundurs (1969) parameters. Another generalized Dundurs parameter  $\alpha$ , or  $\Sigma$ , can be defined as

$$\Sigma = \frac{\left[ \sqrt{s_{11}s_{22}} \right]_2}{\left[ \sqrt{s_{11}s_{22}} \right]_1}^2 = \frac{1 + \alpha}{1 - \alpha} \tag{4.40}$$

Obviously  $\Sigma$  (and  $\alpha$ ) measures the relative stiffness of the two materials. It can be shown

that, for a composite of two aligned orthotropic materials,  $\alpha$  and  $\beta$  are the only *bimaterial* parameters needed for traction prescribed problems, in addition to two anisotropy measures,  $\lambda$  and  $\rho$ , for each material.

Note that  $\mathbf{B}$  and  $\mathbf{H}$  are still well-behaved even if  $\rho = 1$  ( $\mathbf{A}$  and  $\mathbf{L}$  are singular for this case). Specifically, for an elastically isotropic solid ( $\rho = \lambda = 1$ ), (4.37) and (4.38) yield

$$\mathbf{B} = \frac{1}{\mu} \begin{bmatrix} 1 - \nu & i(1/2 - \nu) \\ -i(1/2 - \nu) & 1 - \nu \end{bmatrix}, \quad \mathbf{H} = \frac{4}{E^*} \begin{bmatrix} 1 & -i\beta \\ i\beta & 1 \end{bmatrix} \quad (4.41)$$

where  $E^*$  and  $\beta$  are bimaterial constants defined in §III. A.

When  $x$ -axis is at an angle  $\phi$  from the 1-axis for an orthotropic solid, one may invoke the tensor rule of §C to obtain the elements for matrix  $\mathbf{B}$

$$\begin{aligned} B_{11} &= 2n (s_{11}s_{22})^{1/2} (\lambda^{1/4} \cos^2 \phi + \lambda^{-1/4} \sin^2 \phi) \\ B_{22} &= 2n (s_{11}s_{22})^{1/2} (\lambda^{-1/4} \cos^2 \phi + \lambda^{1/4} \sin^2 \phi) \\ B_{12} = \bar{B}_{21} &= n(s_{11}s_{22})^{1/2} (\lambda^{1/4} - \lambda^{-1/4}) \sin 2\phi + i[(s_{11}s_{22})^{1/2} + s_{12}] \end{aligned} \quad (4.42)$$

When the solid possesses an in-plane cubic symmetry ( $\lambda = 1$ ), it follows from (4.42) that  $\mathbf{B}$  is invariant under an in-plane rotation. There are many implications. For example, The relation (4.15) connecting energy release rate and stress intensity factors for a cubic material can be specialized to

$$G = ns_{11}(K_I^2 + K_{II}^2) \quad (4.43)$$

where  $n$  and  $s_{11}$  are referred to the principal material axes. It is remarkable that this relation holds even if the crack is not aligned with the principal material axes.

Consider a *symmetric tilt* grain boundary of an orthotropic crystal. The interface coincides with  $x$ -axis, and the tilt angle (the angle between the crystal axis 1 and the interface) is  $\phi$  for both upper and lower phases. With (4.42), one can confirm

$$\mathbf{H} = 4n (s_{11}s_{22})^{1/2} \begin{bmatrix} \lambda^{1/4} \cos^2 \phi + \lambda^{-1/4} \sin^2 \phi & 0 \\ 0 & \lambda^{-1/4} \cos^2 \phi + \lambda^{1/4} \sin^2 \phi \end{bmatrix} \quad (4.44)$$

In conjunction with (4.21), the above equation gives an explicit relation between energy release rate and stress intensity factors for a crack along a symmetric tilt grain boundary. An application of this will be given in the next section.

#### F. SYMMETRIC TILT DOUBLE-LAYERS

Imagine two identical infinite layers cut from an orthotropic solid with an angle  $\phi$  to the principal axis (Fig.4.1). The thickness of the two layers are equal, and is designated as  $h$ . The compliances  $s_{11}$ ,  $s_{22}$ ,  $s_{12}$  and  $s_{66}$ , and the stiffnesses  $c_{11}$ ,  $c_{22}$ ,  $c_{12}$  and  $c_{66}$  are referred to the principal material axes. The two layers are bonded together to form a symmetric tilt boundary, with a semi-infinite crack lying along the interface. The tilt angle is  $\phi$  and the tilt axis, or the crack front, is one of the principal axes of the orthotropic solid. Plane strain problems are considered, with the understanding that transformation (4.8) has been operated on the compliances.

Owing to the local material symmetry, all three modes decouple, and thus the two in-plane stress intensity factors can be defined such that, asymptotically, traction along the tilt boundary a distance  $r$  ahead the crack tip is given by

$$\sigma_{yy} = (2\pi r)^{-1/2} K_I, \quad \sigma_{xy} = (2\pi r)^{-1/2} K_{II} \quad (4.45)$$

The energy release rate is quadratic in  $K_I$  and  $K_{II}$  and is expected to contain no cross product due to the symmetry. The result has been given at the end of the last section, which may be written as

$$G = \sqrt{s_{11}s_{22}} [\tilde{G}_I K_I^2 + \tilde{G}_{II} K_{II}^2]$$

$$\tilde{G}_I = \sqrt{(1+\rho)/2} (\lambda^{-1/4} \cos^2 \phi + \lambda^{1/4} \sin^2 \phi) \quad (4.46)$$

$$\tilde{G}_{II} = \sqrt{(1+\rho)/2} (\lambda^{-1/4} \sin^2 \phi + \lambda^{1/4} \cos^2 \phi)$$

where  $\lambda$  and  $\rho$  are the orthotropy parameters defined in (4.33).

The double layer is loaded in two ways in Figs.4.2 and 4.3, so that G can be easily related to the external loads. Hence one may obtain an explicit relation connecting  $K_I$  and  $K_{II}$  with the external loads. These two loading cases will be treated separately below.

### 1. Edge-Loaded Double-Layers

As indicated in Fig. 4.2, the general edge loads P's (load per unit width) and M's (moment per unit width) are applied. From § III. D we know many fracture specimens are special cases of this arrangement.

G can be evaluated by the edge loads the same way as in § III.D

$$G = \frac{s_{11}^*}{2} \left[ \frac{1}{h} \left( P_1^2 + P_2^2 - \frac{1}{2} P_3^2 \right) + \frac{12}{h^3} \left( M_1^2 + M_2^2 - \frac{1}{8} M_3^2 \right) \right] \quad (4.47)$$

Here  $s_{11}^*$  is the x-component of compliance matrix, which, according to Lekhnitskii (1963, p.45), is related to the principal compliances by

$$s_{11}^* = \sqrt{s_{11}s_{22}} s, \quad s = \lambda^{1/2} \cos^4 \phi + 2\rho \cos^2 \phi \sin^2 \phi + \lambda^{-1/2} \sin^4 \phi \quad (4.48)$$

Comparison of the two energy release rate expressions, (4.46) and (4.47), gives a relation between K and loads. However, this does not allow one to partition  $K_I$  and  $K_{II}$ . To achieve the partition, one may consider two simple loading cases.

Owing to the symmetry, *pure mode I* is attained under the loading that  $M_1 = M_2 = M$  and all other loads vanish. Comparison of (4.46) and (4.47) yields

$$K_I = 2\sqrt{3s/\tilde{G}_I} Mh^{-3/2}, \quad K_{II} = 0 \quad (4.49)$$

Again by symmetry, *pure mode II* is attained when  $P_1 = P_2 = P$ ,  $M_1 = -Ph/2$ ,  $M_2 = Ph/2$ . It follows from (4.46) and (4.47) that

$$K_I = 0, \quad K_{II} = 2\sqrt{s/\tilde{G}_{II}} Ph^{-1/2} \quad (4.50)$$

Other loading cases can be treated by the superposition scheme in § III. D. The final result is

$$K_I = \left( 3s/\tilde{G}_I \right)^{1/2} \left( 2Mh^{-3/2} + Ph^{-1/2} \right), \quad K_{II} = 2 \left( s/\tilde{G}_{II} \right)^{1/2} Ph^{-1/2} \quad (4.51)$$

where  $P$  and  $M$  are linear combinations of the six load parameters. However, due to the two overall equilibrium equations, only four of these loads are independent, say,  $P_1, P_3, M_1$  and  $M_3$ .  $P$  and  $M$ , specialized from (3.58), are given by

$$P = P_1 - \frac{1}{2}P_3 - \frac{3}{4}M_3/h, \quad M = M_1 - \frac{1}{8}M_3 \quad (4.52)$$

Now it is straightforward to consider some special specimens. For the *four-point bend* specimen illustrated in Fig. 3.7a, the result is

$$K_I = (3s/\tilde{G}_I)^{1/2} Mh^{-3/2}, \quad K_{II} = \frac{3}{2}(s/\tilde{G}_{II})^{1/2} Mh^{-3/2} \quad (4.53)$$

The calibration relation for the *delamination specimen* of Fig. 3.8a is

$$K_I = \frac{1}{2}(3s/\tilde{G}_I)^{1/2} Ph^{-1/2}, \quad K_{II} = (s/\tilde{G}_{II})^{1/2} Ph^{-1/2} \quad (4.54)$$

Note that since  $\tilde{G}_I$ ,  $\tilde{G}_{II}$  and  $s$  depend on the two anisotropy measures,  $\lambda$  and  $\rho$ , in non-negligible ways, a calibration relation for an isotropic solid may be inadequate for such tilt double-layers. For example, Cu is a cubic material with  $\lambda = 1$  and  $\rho \approx 0$ . The solution for an isotropic material ( $\rho = 1$ ) will give rise to an error of 50% for tilt angle  $\phi = \pi/4$ . In an earlier article (Suo 1989), the writer suggested to use isotropic solutions to approximately calibrate some fracture specimens of orthotropic materials. This approximation seems to be good only for a crack running in one of the principal axes.

## 2. Clamped Double-Layers

Consider the case when the double-layer is held in rigid grips and subject to a prescribed separation  $2v$  and sliding  $2u$ . The energy release rate can be calculated by taking the strain energy per unit thickness per unit width stored far ahead the crack tip, namely

$$G = c_{22}^* v^2/h + c_{66}^* u^2/h \quad (4.55)$$

where the stiffnesses are referred to the present  $(x,y)$  coordinate system, and relate to the principal stiffnesses by (e.g. Love 1944, Art. 105)

$$c_{22}^* = c_{11} \sin^4 \phi + c_{22} \cos^4 \phi + 2(c_{12} + 2c_{66}) \sin^2 \phi \cos^2 \phi \quad (4.56)$$

$$c_{66}^* = c_{66} + (c_{11} + c_{22} - 2c_{12} - 4c_{66}) \sin^2 \phi \cos^2 \phi$$

Owing to the symmetry, the separation  $v$  will only induce  $K_I$ , while the sliding  $u$  will only induce  $K_{II}$ . Comparison of (4.55) with (4.66) yields

$$K_I = (s_{11}s_{22})^{-1/4} (c_{22}^*/\tilde{G}_I)^{1/2} vh^{-1/2}, \quad K_{II} = (s_{11}s_{22})^{-1/4} (c_{66}^*/\tilde{G}_{II})^{1/2} uh^{-1/2} \quad (4.57)$$

While (4.57) is completely explicit, the anisotropic effect is rather opaque. A specific example is chosen to illustrate the anisotropic effect. Consider the double-layer made of copper. Suppose one tries to approximate the specimen by an isotropic solid with Voigt average elastic constants (for Cu,  $\mu = 54.6$  GPa,  $v = 0.324$ , see Hirth and Lothe 1982). The isotropic result corresponding to (4.57) is (Tada et al. 1985)

$$K_I^{iso} = 2(1 - 2v)^{-1/2} \mu vh^{-1/2}, \quad K_{II}^{iso} = [2/(1 - v)]^{1/2} \mu uh^{-1/2} \quad (5.58)$$

The ratios of  $K_I/K_I^{iso}$  and  $K_{II}/K_{II}^{iso}$  are plotted in Fig. 4.4. The deviation from 1 measures the error of the isotropic approximation. As indicated in Fig. 4.4, a 20% error occurs for mode I when the tilt angle  $\phi$  is zero, and a 40% error for mode II when the tilt angle  $\phi$  is  $\pi/4$ .

## V. Interface Cracks in Anisotropic Media

This chapter is based on a recent article (Suo, 1989). The work was initiate by the effort to calibrate some fracture specimens (Sbaizer et al. 1988 and Suo 1988b) and to understand crack deflection at the interface (Gupta and Suo 1989) in highly anisotropic materials. Another compelling motivation came from some fundamental concerns of fracture mechanics extended to anisotropic bimaterials. For many years, people are puzzled by special boundary value problem solutions produced by pioneers in this field (Gotoh 1967, Clements 1971, Willis 1971). These authors left the impression that 6 rather than 3 parameters were necessary to characterize the near tip fields for the general anisotropic bimaterial interface cracks. As one may have realized, the elastic fracture mechanics is entirely built upon *three* stress intensity factors for homogeneous materials (isotropic or anisotropic), and analogously upon one complex and one real stress intensity factors for isotropic bimaterial interfaces (the real one is for mode III). This inconsistency was removed in Suo (1989) by showing that the interface crack tip field for an anisotropic bimaterial is indeed scaled by three, instead of six, independent factors. The major results in this chapter are summarized below.

For pedagogical reasons, the beginning section is devoted exclusively to an algebraic eigenvalue problem involving Hermitian matrix  $\mathbf{H}$ . The generic treatment of such a problem may be found in any good linear algebra textbook. However, as we will show, it is the *specific* features of this problem that play a central role in the understanding the interface crack tip fields.

Two distinct situations are identified for the Hermitian matrix  $\mathbf{H}$ . When  $\mathbf{H}$  is real, the three eigenvalues are degenerate, and the three singularity modes can be separately defined in a classical manner. The structure of the bimaterial crack tip fields in each half is strikingly simple for this case, and is identical to that for the corresponding one-material crack. When  $\mathbf{H}$  is not real, there are three distinct eigenvalues. Among the three

singularity modes, two are coupled and oscillatory and scaled by a complex stress intensity factor, while the third mode shows a square root singularity and is scaled by a real stress intensity factor. A complete description of near-tip fields for this case is also given.

On the basis of the near-tip fields and well defined stress intensity factors, we state the interface fracture mechanics for anisotropic solids.

Collinear interface crack problems are solved here to provide a collection of stress intensity factors. It is found the solutions have remarkably simple structures. When  $\mathbf{H}$  is real, the complete anisotropic bimaterial solution can be constructed from the mode III solution for an isotropic one-material, and the stress intensity factors are identical to its isotropic one-material counterparts. When  $\mathbf{H}$  is complex, the complete solution can be constructed from that for isotropic bimaterial, and the stress intensity factors can be trivially written out providing one knows the isotropic ones.

The chapter concludes with a section on singularity/crack interaction. Some earlier solutions on dislocation mechanics are re-formulated here, which, in conjunction with the basic crack solutions, are used to construct the interactive solutions.

## A. AN EIGENVALUE PROBLEM

### 1. Structure of Eigenpairs

The following algebraic eigenvalue problem is studied in this section

$$\bar{\mathbf{H}}\mathbf{w} = e^{2\pi\epsilon} \mathbf{H}\mathbf{w} \quad (5.1)$$

where  $\mathbf{H}$  is a  $3 \times 3$  positive definite Hermitian matrix. The vector  $\mathbf{w}$  and number  $\epsilon$  are eigenvectors and eigenvalues, respectively. A specific pair  $(\epsilon, \mathbf{w})$  that satisfies (5.1) will be called an eigenpair. Since  $\mathbf{H}$  is a positive definite Hermitian matrix, each eigenvalue  $e^{2\pi\epsilon}$  is positive, and thus  $\epsilon$  is real. It is always possible to obtain three linearly independent eigenpairs for (5.1). The eigenvalues are the roots of the following 3rd-order polynomial of  $e^{2\pi\epsilon}$ .

$$|\bar{H} - e^{2\pi i} H| = 0 \quad (5.2)$$

When  $H$  is real, i.e.,  $\bar{H} = H$ , any vector  $w$  is an eigenvector, and the three eigenvalues degenerate to be  $\varepsilon = 0$ . Conversely, when the three eigenvalues degenerate to be zero, and thus any  $w$  is an eigenvector,  $H$  must be real. Hence a necessary and sufficient condition for all eigenvalues of (5.1) to be zero is that  $H$  is real. The remaining of this section will be primarily focused on the non-trivial case in which  $H$  is not real, or  $\bar{H} \neq H$ .

Observe that for the specific problem of (5.1), if  $(\varepsilon, w)$  is an eigenpair so is  $(-\varepsilon, \bar{w})$ . Since there are only three eigenvalues,  $\varepsilon = 0$  must be an eigenvalue and the associated eigenvector can be chosen to be real. Therefore, a real number  $\varepsilon$  ( $\neq 0$  iff  $H \neq \bar{H}$ ), a complex vector  $w$ , and a real vector  $w_3$  can be found to form *three distinct* eigenpairs

$$(\varepsilon, w), \quad (-\varepsilon, \bar{w}), \quad (0, w_3) \quad (5.3)$$

satisfying

$$\bar{H}w = e^{2\pi i} Hw, \quad \bar{H}w_3 = Hw_3 \quad (5.4)$$

Any two eigenvectors of (5.3) are orthogonal in the sense

$$w^T H w = w^T H w_3 = \bar{w}^T H w_3 = 0 \quad (5.5)$$

Orthogonality conditions involving  $\bar{H}$  can be obtained by taking the complex conjugation of the above.

Note for any given  $H$ , the roots of the polynomial in (5.2) can be found easily since one of them is 1, and the remaining factor is quadratic.

The two vectors  $w$  and  $w_3$  are fully determined by the eigenvalue problem except for a complex and a real normalizing constants, respectively. In general they may be normalized to be dimensionless. We choose to leave the normalization otherwise unspecified at this point.

A given complex-valued vector  $g$  can be represented as a linear combination of the

three eigenvectors

$$\mathbf{g} = g_1 \mathbf{w} + g_2 \bar{\mathbf{w}} + g_3 \mathbf{w}_3 \quad (5.6)$$

where the complex numbers  $g_i$  are the components of vector  $\mathbf{g}$  with eigenvectors as base vectors. The components may be evaluated by taking inner products, i.e.,

$$g_1 = \frac{\bar{\mathbf{w}}^T \mathbf{H} \mathbf{g}}{\bar{\mathbf{w}}^T \mathbf{H} \mathbf{w}}, \quad g_2 = \frac{\mathbf{w}^T \mathbf{H} \mathbf{g}}{\mathbf{w}^T \mathbf{H} \bar{\mathbf{w}}}, \quad g_3 = \frac{\mathbf{w}_3^T \mathbf{H} \mathbf{g}}{\mathbf{w}_3^T \mathbf{H} \mathbf{w}_3} \quad (5.7)$$

When  $\mathbf{g}$  is real-valued, one may confirm that

$$g_2 = \bar{g}_r \quad g_3 = \text{real} \quad (5.8)$$

and (5.6) can be written as

$$\mathbf{g} = g_1 \mathbf{w} + \bar{g}_1 \bar{\mathbf{w}} + g_3 \mathbf{w}_3 \quad (5.9)$$

Thus, a real-valued vector can be decomposed into two components: one is a real component in the direction  $\mathbf{w}_3$ , and the other is a complex component in the plane spanned by  $\text{Re}[\mathbf{w}]$  and  $\text{Im}[\mathbf{w}]$ .

In §B we will show that the interface crack tip field is such that the interface traction vector can be decomposed into two components. One component is along the direction  $\mathbf{w}_3$  and scaled by a real stress intensity factor  $K_3$ . The other (complex) component is in the plane spanned by  $\text{Re}[\mathbf{w}]$  and  $\text{Im}[\mathbf{w}]$ , coupled and oscillatory, and scaled by a complex stress intensity factor  $K$ . As its isotropic counterpart,  $\epsilon$  will be termed as the oscillatory index.

It is instructive at this point to re-examine the isotropic bimaterials. The  $3 \times 3$  matrix  $\mathbf{H}$  is (cf. §§IV.D and E)

$$\mathbf{H} = \begin{bmatrix} 4/E^* & -4i\beta/E^* & 0 \\ 4i\beta/E^* & 4/E^* & 0 \\ 0 & 0 & \mu_1^{-1} + \mu_2^{-1} \end{bmatrix} \quad (5.10)$$

The oscillatory index  $\epsilon$ , solved from the eigenvalue problem (5.1), is

$$\varepsilon = \frac{1}{2\pi} \ln \frac{1-\beta}{1+\beta} \quad (5.11)$$

and the eigenvectors are

$$\mathbf{w} = [-i/2, 1/2, 0]^T, \quad \mathbf{w}_3 = [0, 0, 1]^T \quad (5.12)$$

The interface traction,  $\mathbf{t} = \{\sigma_{21}, \sigma_{22}, \sigma_{23}\}$ , for example, has the components (in the sense of (5.9))

$$t_1 = \sigma_{22} + i\sigma_{12} \quad t_3 = \sigma_{23} \quad (5.13)$$

Notice that in (5.12) a normalization has been assigned to the two eigenvectors, so that the interface traction components of (5.13) are very familiar-looking.

## 2. Effects of in-Plane Rotations

Since  $\mathbf{H}$  defined in (4.20) obeys tensor rules under an in-plane rotation, several invariance properties can be easily established. For two anisotropic media, three macroscopic degrees of freedom are allowed by in-plane rotations, of which two are of interest. One is the relative orientation of the two solids, and the other is the direction of interface.

For the fixed relative orientation of the two media, when the interface rotates,  $\mathbf{H}$  transforms like a second order tensor. Substitution of (4.26) into (5.2) reveals that the polynomial governing the eigenvalues remains unchanged. This establishes Ting's (1986) result that  $\varepsilon$  is invariant under an in-plane rotation of the interface for an anisotropic bimaterial with a fixed relative orientation.

If the two media undergo an in-plane rotation relative to each other, the above theorem does not hold in general. Yet several important situations are worth mentioning. If one of the solids has in-plane cubic symmetry (tetragonal symmetry), we have shown that the associated  $\mathbf{B}$ -matrix is invariant under an in-plane rotation. Thus for this situation,  $\varepsilon$  is invariant to the two in-plane rotations: relative rotation of the two solids and the interface rotation.

Another situation is concerned with a bimaterial with the in-plane as a mirror plane, so that the in-plane and antiplane deformations decouple. For this situation  $w_3$  is normal to the in-plane. A direct calculation shows that if a material pair has  $\epsilon = 0$  for one relative in-plane angle, it has  $\epsilon = 0$  for any relative in-plane angle.

An important special case is observed earlier by Qu and Bassani (1988). Consider a tilt grain boundary (the two materials are identical but mis-oriented) tilted about a principal material axis so that the in-plane and antiplane deformations decouple. The orientations of the two phases are not necessarily symmetric about the interface. Since  $\epsilon = 0$  when the tilt angle is zero,  $\epsilon$  remains to be zero for any tilt angle, according to the above theorem. As noted by these authors, this is also a special case of the Ting's general result. For a tilt boundary with the tilt axis normal to the in-plane, if in addition it is a symmetric tilt boundary, the symmetry ensures that the three modes decouple, and thus  $\epsilon = 0$ . Asymmetric tilt boundary can be achieved by an in-plane rotation of the interface, which does not change  $\epsilon$ , according to Ting's result.

## B. CRACK TIP FIELDS

Consider a semi-infinite, traction-free crack lying along the interface between two dissimilar homogeneous anisotropic half spaces, with material 1 above the x-axis, and material 2 below. The two half-spaces are bonded along the positive x-axis and the crack is along the negative x-axis. Denote C as the crack line ( $x < 0$ ). No specific length and load are present in this problem. Singular fields are sought to satisfy continuity of traction and displacement vectors  $t(x)$  and  $u(x)$  (defined in (4.13) for each material) across the bonded portion of the interface, as well as traction-free condition along the cracked portion. This is a homogeneous boundary value problem, or an eigenvalue problem.

Let the vector potentials defined in (4.12) for the two blocks be  $f_1(z)$  and  $f_2(z)$ , respectively, where the subscripts denote the two materials. Obviously the traction is

continuous across the whole  $x$ -axis, *both* the bonded and cracked portions, so that

$$\mathbf{L}_1 \mathbf{f}_1'(x) + \bar{\mathbf{L}}_1 \bar{\mathbf{f}}_1'(x) = \mathbf{L}_2 \mathbf{f}_2'(x) + \bar{\mathbf{L}}_2 \bar{\mathbf{f}}_2'(x) \quad (5.14)$$

To facilitate the analytic continuation, (5.14) is rearranged as

$$\mathbf{L}_1 \mathbf{f}_1'(x) - \bar{\mathbf{L}}_2 \bar{\mathbf{f}}_2'(x) = \mathbf{L}_2 \mathbf{f}_2'(x) - \bar{\mathbf{L}}_1 \bar{\mathbf{f}}_1'(x) \quad (5.15)$$

Equation (5.15) implies that

$$\mathbf{L}_1 \mathbf{f}_1'(z) = \bar{\mathbf{L}}_2 \bar{\mathbf{f}}_2'(z), \quad z \in 1 \quad (5.16)$$

Here and later in this chapter, the complex variable is of the generic form  $z = x + i\mu$  ( $\text{Im}\mu > 0$ ), with the convention  $z \in 1$  meaning  $y > 0$  and  $z \in 2$  meaning  $y < 0$ .

Define the displacement jump across the interface as

$$\mathbf{d}(x) = \mathbf{u}(x, 0^+) - \mathbf{u}(x, 0^-) \quad (5.17)$$

With the aid of (5.16), a direct calculation gives

$$\mathbf{t}(x) = \mathbf{L}_1 \mathbf{f}_1'(x) + \mathbf{L}_2 \mathbf{f}_2'(x) \quad (5.18)$$

and

$$i \mathbf{d}'(x) = \mathbf{H} \mathbf{L}_1 \mathbf{f}_1'(x) - \bar{\mathbf{H}} \mathbf{L}_2 \mathbf{f}_2'(x) \quad (5.19)$$

Continuity of the displacement across the bonded interface, as inferred from (5.19), implies the existence of a function  $\mathbf{h}(z)$  analytic in the whole plane except on the crack lines, such that

$$\mathbf{h}(z) = \mathbf{L}_1 \mathbf{f}_1'(z) = \mathbf{H}^{-1} \bar{\mathbf{H}} \mathbf{L}_2 \mathbf{f}_2'(z), \quad z \notin C \quad (5.20)$$

Up to now, by only invoking various continuity conditions, we have expressed the two potential vectors for two halves by one function  $\mathbf{h}(z)$  holomorphic in the whole plane. Hence one can focus on  $\mathbf{h}(z)$ , and once  $\mathbf{h}(z)$  is obtained the full field solution is given by (5.20). In terms of  $\mathbf{h}(z)$ , the traction (5.18) and displacement jump (5.19) can be expressed as

$$\mathbf{t}(x) = \mathbf{h}^+(x) + \bar{\mathbf{H}}^{-1} \mathbf{H} \mathbf{h}^-(x) \quad (5.21)$$

and

$$i \mathbf{d}'(x) = \mathbf{H} [\mathbf{h}^+(x) - \mathbf{h}^-(x)] \quad (5.22)$$

With (5.21), the traction-free condition gives

$$\mathbf{h}^+(x) + \bar{\mathbf{H}}^{-1} \mathbf{H} \mathbf{h}^-(x) = \mathbf{0}, \quad x \in C \quad (5.23)$$

This is a homogeneous Hilbert problem. It is convenient to distinguish two cases:  $\mathbf{H}$  is real or complex.

#### Case 1. Non-oscillatory Fields

When  $\mathbf{H}$  is real ( $\mathbf{H} = \bar{\mathbf{H}}$ , and thus  $\bar{\mathbf{H}}^{-1} \mathbf{H}$  is a unit matrix), an obviously admissible singular solution to (5.23) is

$$\mathbf{h}(z) = (2\pi z)^{-1/2} \mathbf{k}/2 \quad (5.24)$$

where the branch cut for  $\sqrt{z}$  is along the crack line. Upon requiring traction to be real, one concludes that  $\mathbf{k}$  is a *real* vector. The normalization adopted in (5.24) is consistent with the conventional definition of stress intensity factors, with the identification

$$\mathbf{k} = [K_{II}, K_I, K_{III}]^T \quad (5.25)$$

as will be clear in (5.27) below.

The complete asymptotic solution is then given by

$$\mathbf{L}_1 \mathbf{f}_1'(z) = \mathbf{L}_2 \mathbf{f}_2'(z) = \mathbf{h}(z) = (2\pi z)^{-1/2} \mathbf{k}/2 \quad (5.26)$$

Assuming  $\mathbf{L}_1$  and  $\mathbf{L}_2$  are non-singular, one can readily obtain the elastic potentials for the two half spaces. The stresses and displacements can be calculated using the basic representation (4.2), with  $z$  properly reinterpreted of course. Examining (5.26) one immediately discovers that the crack tip fields (stresses, displacements) in each block, aside possibly from  $\mathbf{k}$ , do not depend on the elastic constants of the other block. In other words, the structure of the near-tip field in each block is identical to that of a crack in the corresponding anisotropic one-material. The latter field has been completely tabulated in Sih et al. (1965) and Hoenig (1982).

The interface traction a distance  $r$  *ahead* of the crack tip, and the displacement jump a distance  $r$  *behind* of the crack tip, calculated from (5.21) and (5.22), respectively, are given by

$$\mathbf{t}(r) = (2\pi r)^{-1/2} \mathbf{k}, \quad \mathbf{d}(r) = (2r/\pi)^{1/2} \mathbf{Hk} \quad (5.27)$$

The first of the above is conventionally adopted as a defining equation for the stress intensity factors.

The energy release per unit newly created crack area may be defined by Irwin's closure integral

$$G \equiv \frac{1}{2\Delta} \int_0^\Delta \mathbf{t}^T (\Delta - r) \mathbf{d}(r) dr \quad (5.28)$$

where  $\Delta$  is an *arbitrary* length scale. A direct calculation shows

$$G = \mathbf{k}^T \mathbf{Hk}/4 \quad (5.29)$$

In obtaining (5.29) a special value of the beta function has been used

$$\int_0^1 \left( \frac{t}{1-t} \right)^q dt = \frac{q\pi}{\sin q\pi}, \quad (|\operatorname{Re} q| < 1) \quad (5.30)$$

with  $q = 1/2$ . This identity will be invoked again in the next section.

The problem in the present context was formulated earlier by Bassani and Qu (1988) in a different approach. The necessary and sufficient condition for an interface crack displaying no oscillatory behavior is that  $\varepsilon = 0$  or  $\mathbf{H}$  is real. This was first observed by Ting (1986) and proved formally by Qu and Bassani (1988).

### Case 2. Oscillatory Fields

Now we examine the nontrivial case when  $\mathbf{H}$  is *not* real. Let a solution to (5.23) be of the form

$$\mathbf{h}(z) = \mathbf{w} z^{-1/2+i\varepsilon} \quad (5.31)$$

where  $\mathbf{w}$  is a constant vector and  $\varepsilon$  a constant number, both to be determined. The branch

cut for the multi-valued function in (5.31) is chosen to be along the crack line  $x < 0$ , and the phase angle of  $z$  is measured from the positive  $x$ -axis.

Substituting (5.31) into (5.23), one obtains an algebraic eigenvalue problem defined by (5.1). When  $H$  is not real, there are three eigenpairs of form (5.3), each of which corresponds to a solution of form (5.31). The admissible singular solution to (5.3) is then a linear combination

$$h(z) = z^{-1/2}[a w z^{ie} + b \bar{w} z^{-ie} + c w_3] \quad (5.32)$$

where  $a$ ,  $b$  and  $c$  are three undetermined complex numbers. By requiring traction in (5.21) to be real, one concludes

$$a = e^{2\pi e} \bar{b}, \quad c = \text{real} \quad (5.33)$$

Thus, only *one* complex constant and *one* real constant are independent, chosen to be  $K$  and  $K_3$ , respectively, such that

$$h(z) = \frac{e^{\pi e} K z^{ie} w + e^{-\pi e} \bar{K} z^{-ie} \bar{w}}{2\sqrt{2\pi z} \cosh \pi e} + \frac{K_3 w_3}{2\sqrt{2\pi z}} \quad (5.34)$$

Other constants in (6.14) are embedded in a manner similar to the isotropic bimaterial crack tip fields.

The potentials for the two half spaces are thereby obtained from (5.20)

$$\begin{aligned} L_1 f_1'(z) &= \frac{e^{\pi e} K z^{ie} w + e^{-\pi e} \bar{K} z^{-ie} \bar{w}}{2\sqrt{2\pi z} \cosh \pi e} + \frac{K_3 w_3}{2\sqrt{2\pi z}} \\ L_2 f_2'(z) &= \frac{e^{-\pi e} K z^{ie} w + e^{+\pi e} \bar{K} z^{-ie} \bar{w}}{2\sqrt{2\pi z} \cosh \pi e} + \frac{K_3 w_3}{2\sqrt{2\pi z}} \end{aligned} \quad (5.35)$$

The stresses and displacements around an interface crack tip can be written out with the basic LES representation (4.2) without any difficulty. It is interesting to note that the structure of the singular fields is the same for the two half spaces, except for a change of the combination  $\pi e$  to  $-\pi e$  everywhere.

Substitution of (5.34) into (5.21) gives the interface traction a distance  $r$  ahead of the crack tip

$$\mathbf{t}(r) = (2\pi r)^{-1/2} [K r^{i\epsilon} \mathbf{w} + \bar{K} r^{-i\epsilon} \bar{\mathbf{w}} + K_3 \mathbf{w}_3] \quad (5.36)$$

In words it reads that the interface traction at each fixed point  $r$  can be decomposed into two components: one is along  $\mathbf{w}_3$  and the other is in the plane spanned by  $\text{Re}[\mathbf{w}]$  and  $\text{Im}[\mathbf{w}]$ . The components of the interface traction  $\mathbf{t}$ , in the sense of (5.7), are

$$t_1(r) \equiv \frac{\bar{\mathbf{w}}^T \mathbf{H} \mathbf{t}(r)}{\bar{\mathbf{w}}^T \mathbf{H} \mathbf{w}} = \frac{K r^{i\epsilon}}{\sqrt{2\pi r}}, \quad t_3(r) \equiv \frac{\mathbf{w}_3^T \mathbf{H} \mathbf{t}(r)}{\mathbf{w}_3^T \mathbf{H} \mathbf{w}_3} = \frac{K_3}{\sqrt{2\pi r}} \quad (5.37)$$

where  $t_3$  is the  $\mathbf{w}_3$  component and  $t_1$  is the (complex) planar component. These equations may be taken as defining equations for the complex  $K$  and real  $K_3$ . As  $r$  approaches the tip, the  $\mathbf{w}_3$  component has a square root singularity and the planar component is oscillatory, with  $K_3$  and  $K$  measuring their intensities, respectively. The results are clearly the analog of the corresponding ones for isotropic bimaterial. For an isotropic bimaterial,  $t_1(r) \equiv \sigma_{yy} + i\sigma_{xy}$  is the complex in-plane traction, and  $t_3(r) \equiv \sigma_{yz}$  is the anti-plane traction.

The displacement jump a distance  $r$  behind the tip is

$$\mathbf{d}(r) = (\mathbf{H} + \bar{\mathbf{H}}) \sqrt{\frac{r}{2\pi}} \left[ \frac{K r^{i\epsilon} \mathbf{w}}{(1+2i\epsilon)\cosh \pi\epsilon} + \frac{\bar{K} r^{-i\epsilon} \bar{\mathbf{w}}}{(1-2i\epsilon)\cosh \pi\epsilon} + K_3 \mathbf{w}_3 \right] \quad (5.38)$$

Due to the anisotropy, the matrix  $(\mathbf{H} + \bar{\mathbf{H}})$  may rotate the base vectors, implying that non-oscillatory direction of the displacement jump may not coincide with that of the interface traction, and similarly for the oscillatory planes.

The energy release rate defined by (5.28) is

$$G = \bar{\mathbf{w}}^T (\mathbf{H} + \bar{\mathbf{H}}) \mathbf{w} |K|^2 / (4 \cosh^2 \pi\epsilon) + \mathbf{w}_3^T (\mathbf{H} + \bar{\mathbf{H}}) \mathbf{w}_3 K_3^2 / 8 \quad (5.39)$$

In deriving this the integral identity (5.30) has been used with  $q = 1/2, 1/2 \pm i\epsilon$ .

The structure of the near-tip fields around an interface crack has been identified, with only one real and one complex normalizing factors  $K_3$  and  $K$ . In principle, for a given boundary value problem, these factors should be determined by the external geometry and load, and can be used the similar way as the conventional stress intensity factors in Irwin's

fracture mechanics, as will be pursued a little further at the end of the section. A collection of the stress intensity factors for collinear crack problems will be presented in the next section.

### 3. Crack Tip Fields for Orthotropic Bimaterials

Consider two aligned orthotropic solids with the interface along the material axis 1. Since the in-plane is a mirror plane,  $w_3$  is normal to the in-plane and the associated fracture mode (mode III) is rather trivial. In the following only the in-plane fracture modes will be given.

The  $2 \times 2$  matrix  $\mathbf{H}$  for the aligned orthotropic bimaterial is given in §IV.E. The oscillatory index  $\epsilon$ , solved from the eigenvalue problem (5.1), is

$$\epsilon = \frac{1}{2\pi} \ln \frac{1 - \beta}{1 + \beta} \quad (5.40)$$

and the associated in-plane eigenvector is

$$\mathbf{w} = \left[ -i/2, (H_{11}/H_{22})^{1/2}/2 \right]^T \quad (5.41)$$

Values of  $\epsilon$  for some metal crystals bonded with some non-metals are given in table 5.1. The non-metals are taken to be isotropic, and hence these values are valid for arbitrary orientation of interface and the metal crystals, with the crystal axis [001] kept normal to the in-plane.

Table 5.1. OSCILLATORY INDEX  $\epsilon$

	$\text{Al}_2\text{O}_3$	Boron	Carbon	E-glass	SiC
Al(fcc)	-.047	-.049	-.062	+.017	-.049
Cr(bcc)	-.025	-.031	-.064	+.061	-.028
Cu(fcc)	-.029	-.032	-.049	+.040	-.030
Pb(fcc)	-.034	-.035	-.039	-.006	-.035

The interface traction, for example, has the planer component (in the sense of (5.7))

$$t_1 = (H_{22}/H_{11})^{1/2} \sigma_{22} + i\sigma_{12} = (2\pi r)^{-1/2} Kr^{ie} \quad (5.42)$$

This may serve as a defining equation of the complex stress intensity factor  $K$ . A normalization other than that of (5.41) will change the definition of  $K$  by a complex factor. Since  $H_{22}/H_{11} \neq 1$  for orthotropic materials even if  $\epsilon = 0$ , (5.42) reveals that the interface  $K$ , however defined, does not reduce to the conventional stress intensity factors  $K_I + iK_{II}$  when  $\epsilon = 0$ .

This peculiar feature is due exclusively to anisotropy. For a bimaterial consisting of two transversely cubic material (including isotropic bimaterials as a special case), (4.39) shows  $H_{22}/H_{11} = 1$ , and thus one has more familiar singularity

$$\sigma_{22} + i\sigma_{12} = (2\pi r)^{-1/2} Kr^{i\epsilon} \quad (5.43)$$

This latter expression even holds when the two cubic materials, as well as the interface, are not aligned, since the matrix  $H$  for a cubic bimaterial is invariant to in-plane rotations.

The displacement jump for an aligned orthotropic bimaterial is

$$(H_{11}/H_{22})^{1/2} d_2 + id_1 = 2H_{11}\sqrt{\frac{r}{2\pi}} \frac{Kr^{i\epsilon}}{(1+2i\epsilon)\cosh \pi\epsilon} \quad (5.44)$$

and the energy release rate is related to  $K$  by

$$G = H_{11}|K|^2/(4\cosh^2 \pi\epsilon) \quad (5.45)$$

#### 4. Interface Fracture Mechanics for Anisotropic Bimaterials

Knowing the structure of the crack tip field, we can trivially extend Irwin's fracture mechanics to anisotropic bimaterials.

If the bimaterial under investigation has such symmetry that  $H$  is real, the crack tip field is non-oscillatory. The three real stress intensity factors,  $K_I$ ,  $K_{II}$  and  $K_{III}$ , can be defined in the conventional way, i.e., by normalizing interface traction ahead of the crack tip like (5.27). The stress and displacement fields are linear in these stress intensity factors.

The fracture criterion may be stated as (Hutchinson, private communication)

$$G = G_c(\psi, \phi)$$

Here  $G$  is the energy release rate of the cracked body to be assessed, and  $G_c$  is the interface

toughness, which in general depends on the solid angles,  $\psi$  and  $\phi$ , defined in the ( $K_I$ ,  $K_{II}$ ,  $K_{III}$ ) space.

For a bimaterial with complex  $H$ , the crack tip field can be decoupled into two fields. The 2D field is oscillatory and the 1D field is non-oscillatory, with one complex  $K$  and one real  $K_3$ , defined in the fashion like (5.37). The near-tip stress and displacement fields are linear in  $\text{Re}(K^{ie})$ ,  $\text{Im}(K^{ie})$  and  $K_3$ . The fracture criterion is the same as the above, except that the phase angles are defined in the space ( $\text{Re}[KL^{ie}]$ ,  $\text{Im}[KL^{ie}]$ ,  $K_3$ ), where  $L$  is a fixed length as its counterpart for isotropic bimaterials.

Observe that for a given loaded specimen, for a fixed length  $L$  the solid angles  $\psi$  and  $\phi$  are fixed regardless of the physical units adopted for  $K$ ; when  $L$  changes to  $L_1$ ,  $\phi$  remains unaffected while  $\psi$  rotates by an amount of  $\varepsilon \ln(L_1/L)$ .

### C. COLLINEAR CRACKS

Having obtained a *complete* description of the asymptotic fields, we turn our attention to a class of boundary value problems to obtain stress intensity factors. Consider a set of cracks lying along the interface between two dissimilar anisotropic half-spaces, with self-equilibrated traction  $t = t_0(x)$  prescribed on the crack faces. Suppose there are  $n$  finite cracks in the intervals  $(a_j, b_j)$ ,  $j = 1, 2, \dots, n$  and two semi-infinite cracks in the intervals  $(-\infty, b_0)$  and  $(a_0, +\infty)$ .

The same configuration was solved for an isotropic bimaterial by England, Erdogan, Rice and Sih in 1965, which is also included in §III.A of this work. The anisotropic bimaterial version has been solved by several authors (Gotoh 1967, Clements 1971, Willis 1971 and Tewary 1989a), and can be dated back even earlier if one accepts some of the contact problems in the book by Galin (1961) as limiting cases of interface crack problems (rigid/elastic interfaces). Yet these earlier authors seemed to have missed the inherent simplicity of the solutions, and thus they were not able to interpret their results

in the spirit of fracture mechanics. The solutions formulated here allow one to grasp the simple mathematical structure and read off the stress intensity factors trivially. The method, however, is actually not new. Mathematically, it is a variant of those contained in the above references, and was treated thoroughly in general terms by Muskhelishvili (1953b).

The results of the last section up to the introduction of the traction-free condition (5.23) is still valid. When the crack faces are subjected to the traction  $t_0(x)$ , the Hilbert problem is replaced by a non-homogeneous one

$$h^+(x) + \bar{H}^{-1} H h^-(x) = t_0(x), \quad x \in C \quad (5.46)$$

where  $C$  is the *union* of all cracks. Equation (5.46) does not have a unique solution. Several auxiliary conditions needed are:  $h(z)$  approaches zero faster than  $1/z$  as  $|z|$  goes to infinity; At the crack tips,  $h(z)$  has a singularity as in (5.24) if  $H$  is real, or (5.34) if  $H$  is not real; and moreover, the net Burgers vector for each of the  $n$  finite cracks is zero. From (5.22), this latter statement leads to

$$\int_{a_j}^{b_j} [h^+(x) - h^-(x)] dx = 0, \quad j = 1, 2, \dots, n \quad (5.47)$$

The mathematical problem is then governed by (5.46) and (5.47) and other auxiliary conditions stated above. In the following, the two cases,  $H$  is real or complex, are treated separately.

#### Case 1. $H$ Is Real

When  $H$  is real, and thus  $\bar{H}^{-1} H$  is a unit matrix, notice that the governing equations and the auxiliary conditions for the vector function  $h(z)$  are independent of any elastic constants, and *exactly the same* as those for the mode III potentials in an *isotropic one-material*. A straightforward method thus emerges to *construct* the complete solutions for the above interface crack problems, without much work, from the well-known mode III solutions for isotropic one-materials. Each component of the vector function  $h(z)$

is the same (except for a factor of -1/2) as the mode III potential for collinear cracks in a homogeneous isotropic material, and the latter can be found in Rice (1968). Listed below are the general solutions so constructed for the collinear interfacial cracks

$$h(z) = \frac{\chi_0(z)}{2\pi i} \int_C \frac{t_0(x)dx}{\chi_0^+(x)(x-z)} + P(z)\chi_0(z) \quad (5.48)$$

$$\chi_0(z) = \prod_{j=0}^n (z - a_j)^{-1/2} (z - b_j)^{-1/2}$$

Here the branch cuts are chosen along the crack lines so that the product for each finite crack behaves as 1/z for large z. And P(z) is a vector involving three polynomials, which should be chosen to satisfy the auxiliary conditions. Knowing h(z), one can obtain the complete solutions for the two blocks,  $f_1(z)$  and  $f_2(z)$ , from (5.20). In particular, the stress intensity factors are *identical* to the classical results for the same crack configuration in an isotropic one-material.

Solutions for the two important configurations are written out more explicitly

i) *Semi-infinite crack in the interval (-∞, 0)*

$$\chi_0(z) = z^{-1/2}, \quad P(z) = 0$$

$$L_1 f_1'(z) = L_2 f_2'(z) = \frac{1}{2\pi\sqrt{z}} \int_{-\infty}^0 \frac{\sqrt{-x}}{x-z} t_0(x) dx \quad (5.49)$$

$$k = -\sqrt{\frac{2}{\pi}} \int_{-\infty}^0 \frac{t_0(x)dx}{\sqrt{-x}}$$

ii) *Finite crack in the interval (-a, a)*

$$\chi_0(z) = (z^2 - a^2)^{-1/2}, \quad P(z) = 0$$

$$L_1 f_1'(z) = L_2 f_2'(z) = \frac{1}{2\pi\sqrt{z^2 - a^2}} \int_{-a}^a \frac{\sqrt{a^2 - x^2}}{x-z} t_0(x) dx \quad (5.50)$$

$$k = -\frac{1}{\sqrt{\pi a}} \int_{-a}^a \sqrt{\frac{a+x}{a-x}} t_0(x) dx$$

The solution to the second problem listed above was obtained earlier by Bassani and Qu (1988) with an integral transform.

### Case 2. $\mathbf{H}$ Is Not Real

When  $\mathbf{H}$  is not real, the governing equation (5.46) depends on the material constants. Writing (5.46) in its components, or equivalently, taking the inner product of (5.40) with  $\bar{\mathbf{w}}^T \mathbf{H}$ ,  $\mathbf{w}^T \mathbf{H}$  and  $\mathbf{w}_3^T \mathbf{H}$ , one obtains

$$\left. \begin{aligned} h_1^+(x) + e^{-2\pi x} h_1^-(x) &= t_{01}(x) \\ h_2^+(x) + e^{+2\pi x} h_2^-(x) &= \bar{t}_{01}^-(x) \\ h_3^+(x) + h_3^-(x) &= t_{03}(x) \end{aligned} \right\}, \quad x \in C \quad (5.51)$$

The components are defined in the sense of (5.7) (notice that  $\mathbf{h}$  is complex but  $t_0$  is real). These equations are decoupled. Furthermore, since they contain no explicit material dependence besides  $\epsilon$ , one may conjecture that they should be identical to those for isotropic bimaterials. Indeed they are (cf. equation (3.9)). Constructed from the known solutions for isotropic bimaterials, the complete solution is

$$\mathbf{h}(z) = h_1(z)\mathbf{w} + h_2(z)\bar{\mathbf{w}} + h_3(z)\mathbf{w}_3 \quad (5.52)$$

and

$$\begin{aligned} h_1(z) &= \frac{\chi(z)}{2\pi i} \int_C \frac{t_{01}(x)dx}{\chi^+(x)(x-z)} + \chi(z)P_1(z) \\ h_2(z) &= \frac{\bar{\chi}(z)}{2\pi i} \int_C \frac{\bar{t}_{01}^-(x)dx}{\bar{\chi}^+(x)(x-z)} + \bar{\chi}(z)P_2(z) \\ h_3(z) &= \frac{\chi_0(z)}{2\pi i} \int_C \frac{t_{03}(x)dx}{\chi_0^+(x)(x-z)} + \chi_0(z)P_0(z) \end{aligned} \quad (5.53)$$

In the above  $\chi_0(z)$  and  $\chi(z)$  are the standard functions defined in (5.48) and (3.10), respectively. The three polynomials in (5.53) may be determined by the auxiliary conditions. Knowing  $\mathbf{h}(z)$ , one can obtain the full field solution via (5.20).

The stress intensity factors can be extracted by comparison with the asymptotic

solution . As a matter of fact, by construction the answer should have the same structure as their isotropic bimaterial counterparts. For example, looking back at the solutions listed at the end of §III.A, one finds that the stress intensity factors for a *semi-infinite crack* are

$$K_3 = - (2/\pi)^{1/2} \int_{-\infty}^0 (-x)^{-1/2} t_{03}(x) dx \quad (5.54)$$

$$K = - (2/\pi)^{1/2} \cosh \pi \epsilon \int_{-\infty}^0 (-x)^{-1/2-i\epsilon} t_{01}(x) dx$$

and for an *internal crack* the stress intensity factors are

$$K_3 = - \frac{1}{\sqrt{\pi a}} \int_{-a}^a \sqrt{\frac{a+x}{a-x}} t_{03}(x) dx \quad (5.55)$$

$$K = - \sqrt{\frac{2}{\pi}} \cosh \pi \epsilon (2a)^{-1/2-i\epsilon} \int_{-a}^a \left( \frac{a+x}{a-x} \right)^{1/2+i\epsilon} t_{01}(x) dx$$

The complex  $t_{01}$  and the real  $t_{03}$  are the components of the applied traction  $t_0$  in the sense of (5.7).

Without actually re-solving the problems, one can easily write done any other solutions for collinear crack problems in an anisotropic bimaterial, providing one knows the solutions for an isotropic bimaterial. Notice such a constructive rule is only valid for collinear cracks between two half spaces.

#### D. SINGULARITY/CRACK INTERACTIONS

In this section, the interaction problem is considered using the same scheme as in §III.B for isotropic bimaterials. The aim is to obtain the solution of a traction-free crack in the presence of a singularity, such as a line force or a dislocation. This is done by superposing the following two problems: a singularity in a bimaterial without crack (problem A), and an interface crack without singularity but with traction prescribed on the crack faces to nullify that due to problem A (problem B). Problem B has been discussed in the above section. The remaining work in this process is to solve problem A, and

evaluation the integral involved in problem B.

### 1. Line Force and Dislocation in a Homogeneous Medium

The solution for a singularity in an *infinite homogeneous* medium is a building block for the interaction solutions. Consider a dislocation line in the direction perpendicular to  $x,y$ -plane, with Burgers vector  $\mathbf{b}$ , and consider a line force uniformly distributed along that direction, with force per unit length  $\mathbf{p}$ . Both singularities are at the point  $(x_0, y_0)$ . The solution is of the form (Eshelby et al. 1953)

$$f_j(z) = q_j \ln(z - s_j), \quad s_j = x_0 + \mu_j y_0 \quad (5.56)$$

where the coefficient vector  $\mathbf{q} = \{q_j\}$  is to be determined in terms of  $\mathbf{b}$  and  $\mathbf{p}$ . The branch points for the  $\ln$ -functions are at  $s_j$ , while, for definiteness, the branch cuts are chosen in the negative  $x$ -direction, and the phase angle is measured from the positive  $x$ -direction. With the aid of (4.2), by definition one has

$$\mathbf{b} = \mathbf{u}^+ - \mathbf{u}^- = 2\pi i (\mathbf{A}\mathbf{q} - \bar{\mathbf{A}}\bar{\mathbf{q}}), \quad \mathbf{p} = \mathbf{T}^- - \mathbf{T}^+ = 2\pi i (\mathbf{L}\mathbf{q} - \bar{\mathbf{L}}\bar{\mathbf{q}}) \quad (5.57)$$

Solving for  $\mathbf{q}$  from the above algebraic equations, one finds

$$\mathbf{q} = (2\pi)^{-1} \mathbf{L}^{-1} (\mathbf{B} + \bar{\mathbf{B}})^{-1} \mathbf{b} - (2\pi)^{-1} \mathbf{A}^{-1} (\mathbf{B}^{-1} + \bar{\mathbf{B}}^{-1})^{-1} \mathbf{p} \quad (5.58)$$

Hence a complete description of the solution is achieved.

### 2. A Singularity in a Bimaterial

Now the interaction problem A is taken up. Suppose we know, somehow, the solution for an isolated singularity in an infinite homogeneous medium, designated as  $\mathbf{f}_0(z)$ , not necessarily of the form (5.56). The aim is to construct the solution for the same singularity embedded in the bonded half planes. Without loss of generality, the singularity is taken to be in material 2, and thus the material constants involved in  $\mathbf{f}_0(z)$  are for material 2. This problem was posed and solved by Tucker (1969), and studied recently by Tewary et al. (1989b). Adapted below is a derivation consistent with the present notation.

Write the solution for the two blocks formally as

$$\mathbf{f}(z) = \begin{cases} \mathbf{f}^1(z), & z \in 1 \\ \mathbf{f}^2(z) + \mathbf{f}_0(z), & z \in 2 \end{cases} \quad (5.59)$$

The task is to solve for  $\mathbf{f}^1(z)$  and  $\mathbf{f}^2(z)$ , analytic in upper and lower half planes, respectively, in terms of  $\mathbf{f}_0(z)$ . From (4.13), the continuity of forces across the interface requires that

$$\mathbf{L}_1 \mathbf{f}^1(x) + \bar{\mathbf{L}}_1 \bar{\mathbf{f}}^1(x) = \mathbf{L}_2 [\mathbf{f}^2(x) + \mathbf{f}_0(x)] + \bar{\mathbf{L}}_2 [\bar{\mathbf{f}}^2(x) + \bar{\mathbf{f}}_0(x)] \quad (5.60)$$

Rearranging the above one obtains

$$\mathbf{L}_1 \mathbf{f}^1(x) - \bar{\mathbf{L}}_2 \bar{\mathbf{f}}^2(x) - \mathbf{L}_2 \mathbf{f}_0(x) = \mathbf{L}_2 \mathbf{f}^2(x) - \bar{\mathbf{L}}_1 \bar{\mathbf{f}}^1(x) - \bar{\mathbf{L}}_2 \bar{\mathbf{f}}_0(x) \quad (5.61)$$

This equation holds along the whole x-axis. Moreover, the functions at the left-hand side are analytic in the upper half plane, while those on the right-hand side are analytic in the lower half plane. By standard analytic continuation arguments one reaches

$$\mathbf{L}_1 \mathbf{f}^1(z) - \bar{\mathbf{L}}_2 \bar{\mathbf{f}}^2(z) - \mathbf{L}_2 \mathbf{f}_0(z) = \mathbf{0}, \quad z \in 1 \quad (5.62)$$

Continuity of the displacements across the interface, with the same arguments, gives

$$\mathbf{A}_1 \mathbf{f}^1(z) - \bar{\mathbf{A}}_2 \bar{\mathbf{f}}^2(z) - \mathbf{A}_2 \mathbf{f}_0(z) = \mathbf{0}, \quad z \in 1 \quad (5.63)$$

Solving from (5.62) and (5.63) for  $\mathbf{f}^1(z)$  and  $\mathbf{f}^2(z)$ , one finds

$$\mathbf{f}^1(z) = \mathbf{L}_1^{-1} \mathbf{H}^{-1} (\bar{\mathbf{B}}_2 + \mathbf{B}_2) \mathbf{L}_2 \mathbf{f}_0(z), \quad z \in 1 \quad (5.64)$$

$$\mathbf{f}^2(z) = \mathbf{L}_2^{-1} \bar{\mathbf{H}}^{-1} (\bar{\mathbf{B}}_2 - \bar{\mathbf{B}}_1) \bar{\mathbf{L}}_2 \bar{\mathbf{f}}_0(z), \quad z \in 2$$

Substitution into (5.59) gives the complete solution. When calculating the field quantities via (4.2), one has to substitute  $z$  by  $z_j = x + \mu_j y$  respectively for each component of  $\mathbf{f}(z)$  of (5.59). Notice that this relation to *construct* a bimaterial solution from a one-material solution is universal in that no specific information about the singularity is needed.

A singularity in a half-space interacting with a traction-free surface,  $y = 0$ , can be constructed similarly on the basis of the infinite plane solution,  $\mathbf{f}_0(z)$ . The result is

$$\mathbf{f}(z) = \mathbf{f}_0(z) - \mathbf{L}^{-1}\bar{\mathbf{L}}\bar{\mathbf{f}}_0(z) \quad (5.65)$$

Another interesting case is a singularity in a half plane interacting with a rigidly held surface on  $y = 0$ . The solution is

$$\mathbf{f}(z) = \mathbf{f}_0(z) - \mathbf{A}^{-1}\bar{\mathbf{A}}\bar{\mathbf{f}}_0(z) \quad (5.66)$$

The general solution developed above has been used by Gupta and Suo (1989) to study a crack running perpendicular into an interface and crack deflection at an interface. Dislocation solution in a half space was used by Suo (1988b) as kernels in an integral equation formulation of delamination in composites.

### 3. Singularity/Crack Interactions

Now the interaction problem can be readily solved by the superposition scheme discussed in the opening remarks of this section. The only relatively non-trivial part is the integral involved in the process. We will not pursue the interaction problem for the general singularity, as has been done for isotropic materials in §III.B. Instead, we will concentrate on a special problem to illustrate the process. The technique, though, is generally applicable.

Consider, for example, a dislocation or a line force, embedded in material 2, interacting with the traction-free semi-infinite interface crack. The non-oscillatory condition  $\mathbf{H} = \bar{\mathbf{H}}$  is assumed. For problem A, from (5.59) the traction in the interface is

$$\mathbf{t}_0(x) = \mathbf{C}\mathbf{f}_0'(x) + \bar{\mathbf{C}}\bar{\mathbf{f}}_0'(x), \quad \mathbf{C} = \mathbf{H}^{-1}(\mathbf{B}_2 + \bar{\mathbf{B}}_2)\mathbf{L}_2 \quad (5.67)$$

where  $\mathbf{f}_0(z)$  is of the form (3.1), and  $\mathbf{C}$  is an abbreviation.

The negative of this traction is prescribed on the crack faces. The solution for this problem has been examined in the last section. The key is to evaluate the integral (5.48). In the present context, it is

$$\mathbf{h}(z) = -\frac{\chi_0(z)}{2\pi i} \int_{-\infty}^0 \frac{\mathbf{C}\mathbf{f}_0'(x) + \bar{\mathbf{C}}\bar{\mathbf{f}}_0'(x)}{\chi_0^+(x)(x-z)} dx \quad (5.68)$$

where  $\chi_0(z) = 1/\sqrt{z}$ , with the branch cut along the crack. The integral can be evaluated by a

contour integral used in §III. B. The final result is

$$\mathbf{h}(z) = -[\mathbf{C}\mathbf{f}_0'(z) + \bar{\mathbf{C}}\bar{\mathbf{f}}_0'(z) - z^{-1/2}\mathbf{CD}\mathbf{f}_0'(z) - z^{-1/2}\bar{\mathbf{CD}}\bar{\mathbf{f}}_0'(z)]/2 \quad (5.69)$$

$$\mathbf{D} = \text{diag}[\sqrt{s_1}, \sqrt{s_2}, \sqrt{s_3}]$$

where  $s_j$  are defined in (5.56) and  $\text{diag}[\ ]$  denotes a diagonal matrix. The complete solution can be obtained using (5.20). Comparison of (5.69) and (5.24) gives the stress intensity factors induced by a dislocation or line force

$$\mathbf{k} = -2(2\pi)^{1/2} \text{Re} \left\{ \mathbf{H}^{-1}(\mathbf{B}_2 + \bar{\mathbf{B}}_2) \mathbf{L}_2 [q_1 s_1^{-1/2}, q_2 s_2^{-1/2}, q_3 s_3^{-1/2}]^T \right\} \quad (5.70)$$

where  $q_j$  and  $s_j$  are defined in (5.56) with elastic constants for material 2.

The dislocation interacting with a crack was treated in a homogeneous medium by Atkinson (1966). The Green function for an internal interface crack was obtained recently by Tewary et al. (1989a).

## Bibliography

- Argon, A.S., Gupta, V., Landis, H.S. and Cornie, J.A., 1989, *J. Mater. Sci.*, **24**, 1403-1412.
- Atkinson, C. 1966 *Int. J. Fracture Mech.*, **2**, 567-575.
- Barnett, D.M. and Asaro, R.J. 1972 *J. Mech. Phys. Solids*, **20**, 353-366.
- Bassani, J.L. and Qu, J. 1988 Finite crack on bimaterial and bicrystal interfaces, to appear in *J. Mech. Phys. Solids*.
- Cao, H.C. and Evans, A.G. 1989 An experimental study of the fracture resistance of bimaterial interface, *Mechanics of Materials*, in press.
- Charalambides, P.G., Lund, J., Evans, A.G. and McMeeking, R.M., 1989, *J. Appl. Mech.* **56**, 77-82.
- Charalambides, P.G., Cao, H.C., Lund, J. and Evans, A.G., 1988, to be published.
- Clements, D.L. 1971 *Int. J. Engng. Sci.*, **9**, 257-265.
- Dundurs, J. 1968 in *Mathematical Theory of Dislocations*, ASME, New York.
- England, A.H. 1965 *J. Appl. Mech.*, **32**, 400-402.
- Erdogan, F. 1965 *J. Appl. Mech.*, **32**, 403-410.
- Eshelby, J.D., Read, W.T. and Shockley, W. 1953 *Acta Met.*, **1**, 251-259.
- Eshelby, J.D. 1957 *Proc. Roy. Soc., A* **241**, 376-396.
- Evans, A.G., Ruhle, M., Dalgleish, B.J. and Charalambides, P.G. 1989 The fracture energy of bimaterial interfaces, to be published.
- Freund, L.B. 1978 *Int. J. Solids Struct.*, **14**, 241-250.
- Galin, L.A. 1961 *Contact Problems in the Theory of Elasticity*, § I.11, translated by H. Moss, School of Physical Sciences and Applied Mathematics, North Carolina State College Publications.
- Gotoh, M. 1967 *Int. J. Fracture Mech.*, **3**, 253-260.
- Green, A.E. and Zerna, W. 1954 *Theoretical Elasticity*, Oxford at the Clarendon Press.
- Gupta, V., Argon, A.S. and Cornie, J.A. 1989 Interfaces with controlled toughness as

- mechanical fuses to isolate fibers from damage, *J. Mater. Sci.*, in press.
- Gupta, V. and Suo, Z. 1989 Crack deflection in composite materials, work in progress.
- Hirth, J.P. and Lothe, J. 1982 *Theory of Dislocations*, 2nd ed., John Wiley & Sons, New York.
- Hoenig, A. 1982 *Engng. Fracture Mech.*, **16**, 393-403.
- Hutchinson, J.W. 1989 Mixed mode fracture mechanics of interface, *Scripta Met.*, in press.
- Hutchinson, J.W. 1974 On steady quasi-static crack growth, Harvard Report DEAP S-8.
- Lekhnitskii, S.G. 1963 *Theory of Elasticity of an Anisotropic Body*, Holden-Day, Inc.
- Love, A.E.H. 1944 *A Treatise on the Mathematical Theory of Elasticity*, 4th ed., Dover Publications, New York.
- Malyshev, B.M. and Salganik, R.L. 1965 *Int. J. Frac Mech.*, **5**, 114-128.
- Muskhelishvili, N.I. 1953a *Some Basic Problems of the Mathematical Theory of Elasticity*, P. Noordhoff Ltd., Groningen, Holland.
- Muskhelishvili, N.I. 1953b *Singular Integral Equations*, P. Noordhoff Ltd., Groningen, Holland.
- Oh, T.S., Cannon, R.M. and Ritchie, R.O., 1987, *J. Am. Ceram. Soc.* **70**, C-352-355.
- Park, J.H. and Earmme, Y.Y, 1986 *Mech. Mater.*, **5**, 261-276.
- Qu, J. and Bassani, J.L. 1988 Cracks on bimaterial and bicrystal interfaces, to appear in *J. Mech. Phys. Solids*.
- Rice, J.R. 1988 *J. Appl. Mech.*, **55**, 98-103.
- Rice, J.R. 1985 in *Fundamentals of Deformation and Fracture*, B.A. Bibly, K.M. Miller and J.R. Willis, eds., Cambridge University Press.
- Rice, J.R. 1968 in *Fracture, An Advanced Treatise, II*, H. Liebowitz, ed., Academic Press.
- Rice, J.R., Wang, J.-S. and Suo Z. 1989 Mechanics and thermodynamics of interfacial

failure, to be published in *Scripta Met.*

- Rice, J.R. and Sih, G.C. 1965 *J. Appl. Mech.*, **32**, 418-423.
- Sbaizer, O., Charalambides, P.G. and Evans, A.G. 1988 to be published.
- Shih, C.F. 1974 in *Fracture Analysis*, ASTM STP **560**, 187-210.
- Shih, C.F. and Asaro, R.J. 1988 *J. Appl. Mech.*, **55**, 299-316.
- Shih, C.F. and Asaro, R.J. 1989 to be published in *J. Appl. Mech.*
- Sih, G.C., Paris, P.C. and Irwin, G.R. 1965 *Int. J. Fracture Mech.*, **1**, 189-203.
- Stroh, A.N. 1958 *Phil. Mag.*, **7**, 625-646.
- Suga, T., Elssner, E. and Schmander, S. 1988 *J. Composite Materials*, **22**, 917-934.
- Suo, Z. 1988a Singularities interacting with interfaces and cracks, Harvard University Report Mech-134, to appear in *Int. J. Solids and Struct.*
- Suo, Z. 1988b Delamination specimens for orthotropic materials, Harvard University Report Mech-135, to be published.
- Suo, Z. 1989 Singularities, interfaces and cracks in dissimilar anisotropic media, Harvard University Report Mech-137, to be published.
- Suo, Z. and Hutchinson, J.W. 1989 *Mater. Sci. Engng.*, **A107**, 135-143.
- Suo, Z. and Hutchinson, J.W. 1988a Interface crack between two elastic layers, Harvard University Report Mech-118, to appear in *Int. J. Fracture*.
- Suo, Z. and Hutchinson, J.W. 1988b Steady-state cracking in brittle substrates beneath adherent films, Harvard University Report Mech-132, to appear in *Int. J. Solids Struct.*
- Tada, H., Paris, P.C. and Irwin, G.R. 1985 *The Stress Analysis of Cracks Handbook*, Del Research, St. Louis, MO.
- Tewary, V.K., Wagoner, R.H. and Hirth, J.P. 1989a,b *J. Mater. Res.*, **4**, 113-136.
- Thomson, R. 1986 *Solid State Physics*, **39**, 1-129.
- Ting, T.C.T. 1986 *Int. J. Solids. Struct.*, **22**, 965-983.
- Ting, T.C.T. 1982 *Int. J. Solids. Struct.*, **18**, 139-152.

- Tucker, M.O. 1969 *Phil. Mag.*, **19**, 1141-1159.
- Varchenya, S.A., Simanovskis, A. and Stolyarova, S.V. 1989 *Thin Solid Films*, **164**, 147-152.
- Wang, J.S. and Suo, Z. 1989 Experimental determination of interface toughness as a function of phase angle, work in progress.
- Wang, S.S. 1984 *AIAA J.*, **22**, 256-264.
- Williams, M.L. 1959 *Bull. Seismol. Soc. Am.*, **49**, 199-204.
- Willis, J.R. 1971 *J. Mech. Phys. Solids*, **19**, 353-368.

## **Figure Captions**

- Fig. 2.1a The admissible domain of the Dundurs' parameters.
- Fig. 2.1b Dundurs' parameters calculated by Suga et al. (1988).
- Fig. 2.2 Crack tip geometry and convention.
- Fig. 2.3 Angular distributions of the crack tip field.
- Fig. 3.1 Integration Contours.
- Fig. 3.2 Generic sandwich set-up.
- Fig. 3.3 Interlayer and crack in a tensile specimen.
- Fig. 3.4 Superposition scheme for a double-layer.
- Fig. 3.5 A double-cantilever beam subjected to edge moments.
- Fig. 3.6 A thin film under residual tension.
- Fig. 3.7 A four-point bend specimen.
- Fig. 3.8 A delamination specimen.
- Fig. 4.1 Two strips cut from an orthotropic material.
- Fig. 4.2 A symmetric double-layer subjected to edge loads.
- Fig. 4.3 A symmetric double-layer held in rigid grips.
- Fig. 4.4 Errors of the isotropic average approximation.

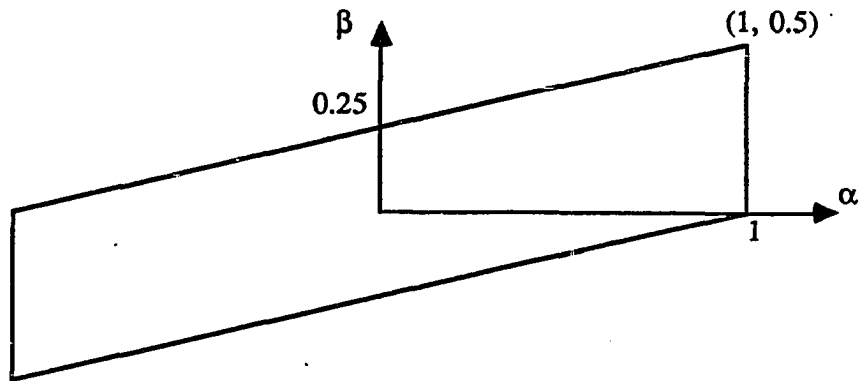


Fig. 2.1a The admissible domain of the Dundurs' parameters.

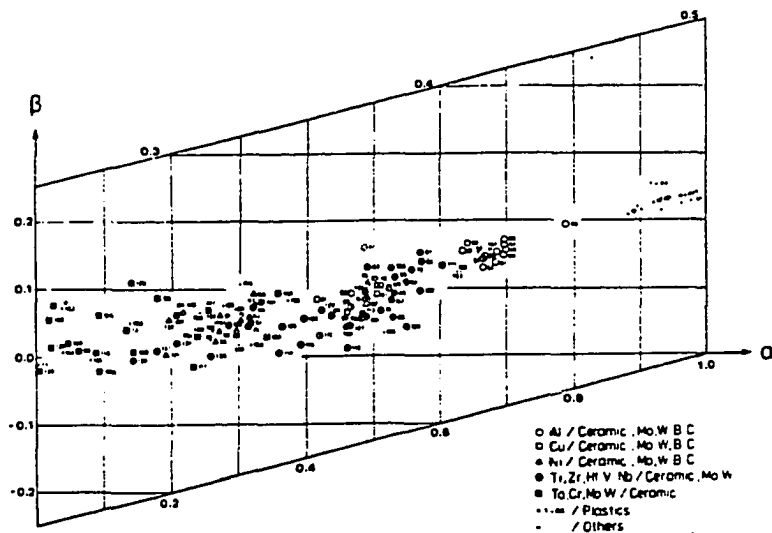


Fig. 2.1b Dundurs' parameters calculated by Suga et al. (1988).

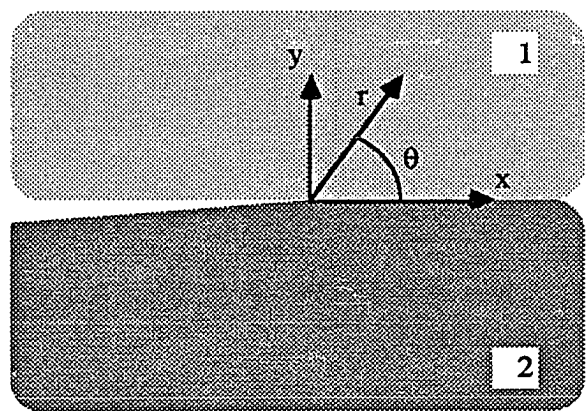


Fig. 2.2 Crack tip geometry and convention.

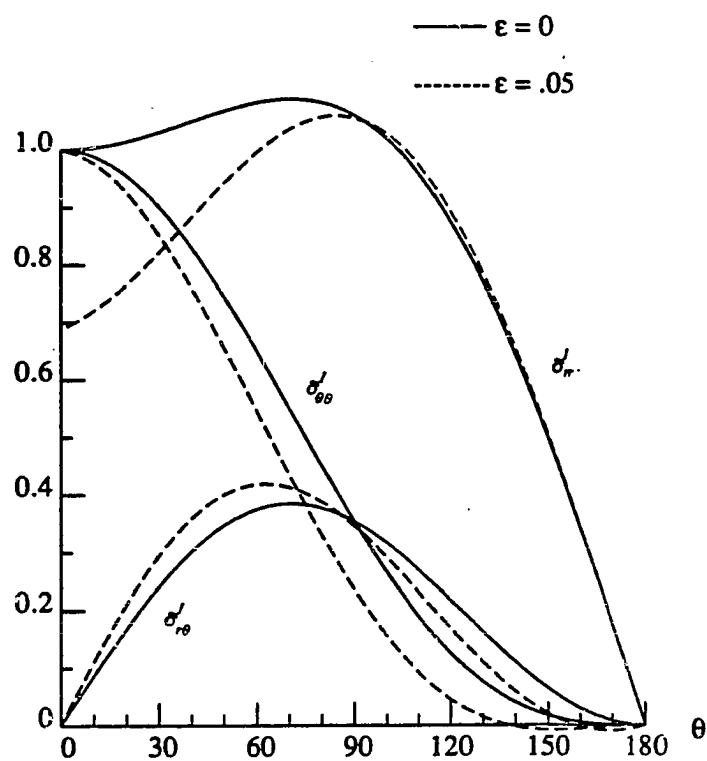


Fig. 2.3a

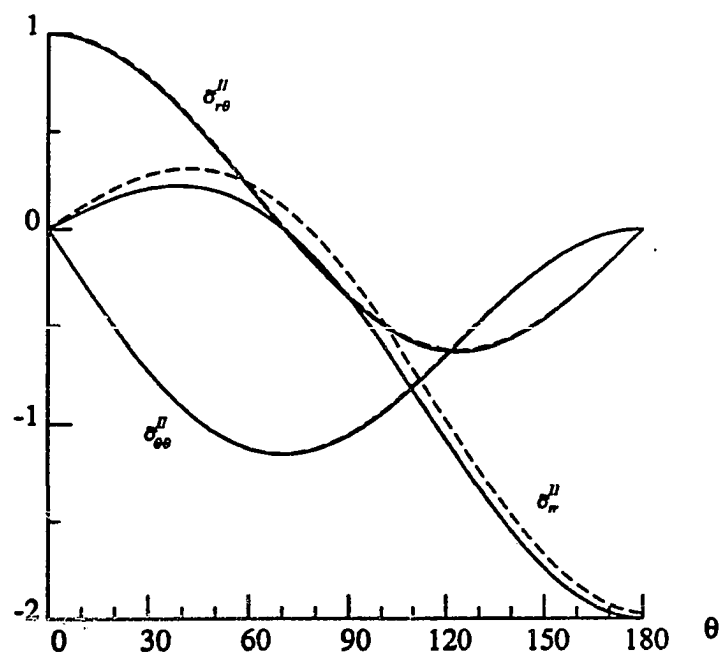


Fig. 2.3b

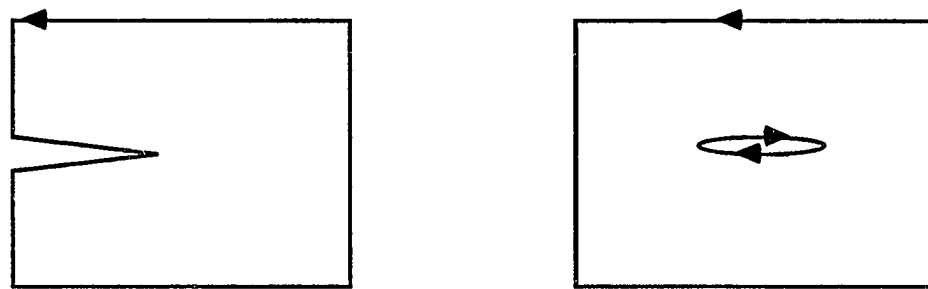
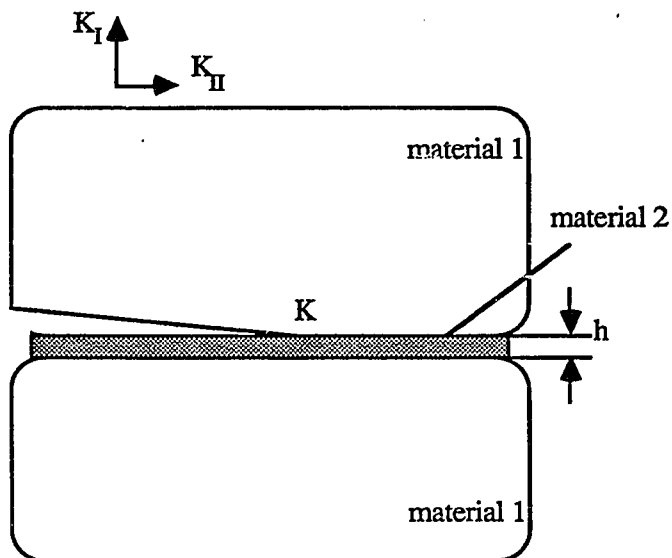


Fig. 3.1 Integration Contours.



$$\sigma_{yy} + i\sigma_{xy} = (2\pi r)^{-1/2} (K_I + iK_{II}), \quad r \rightarrow \infty$$

$$\sigma_{yy} + i\sigma_{xy} = (2\pi r)^{-1/2} Kr^{ie}, \quad r \rightarrow 0$$

Fig. 3.2 Generic sandwich set-up.

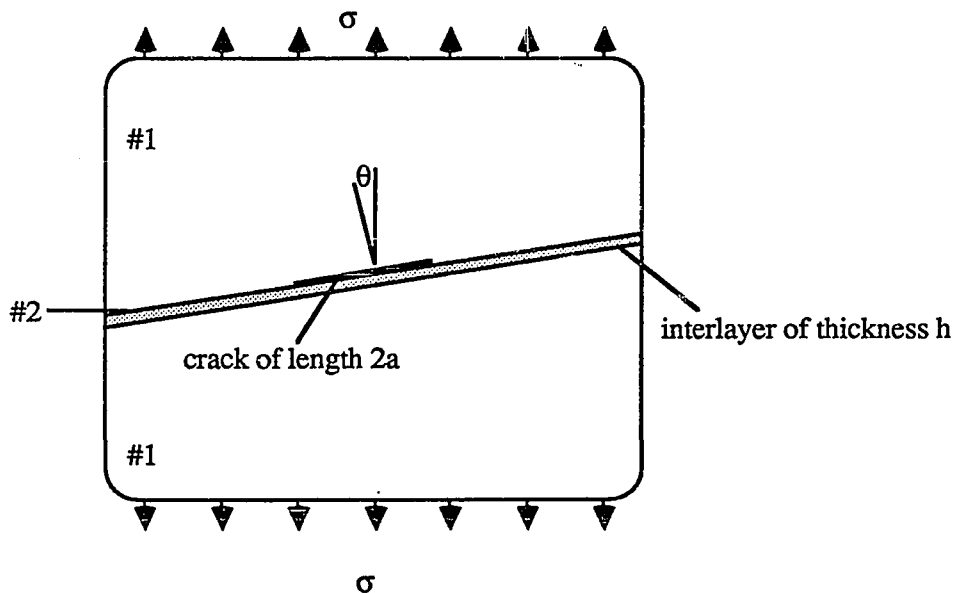


Fig. 3.3 Interlayer and crack in a tensile specimen.

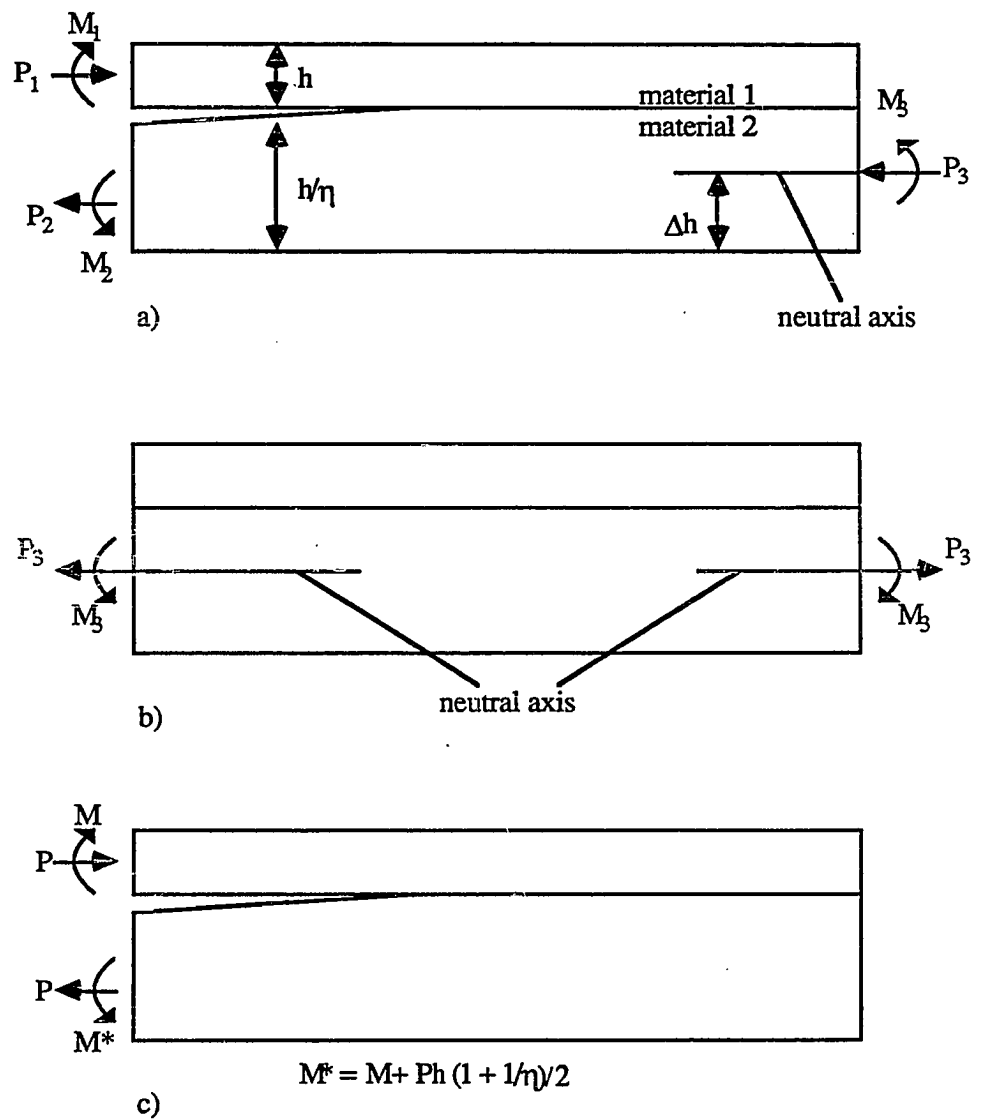
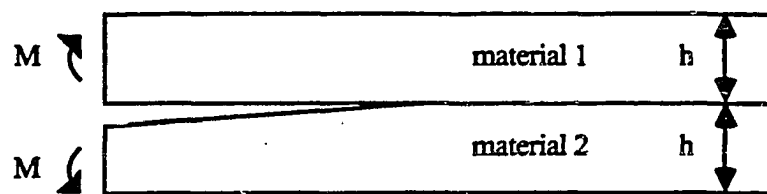
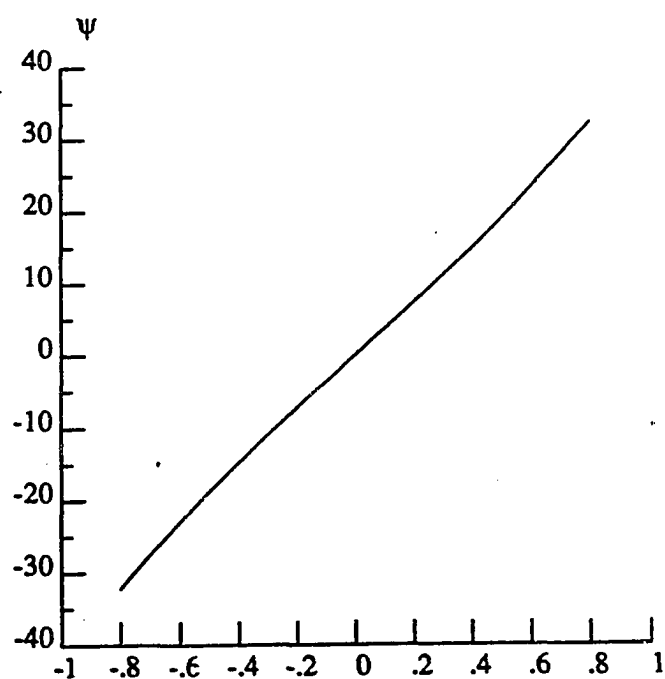


Fig. 3.4 Superposition scheme for a double-layer.



a)



b)

Fig. 3.5 A double-cantilever beam subjected to edge moments

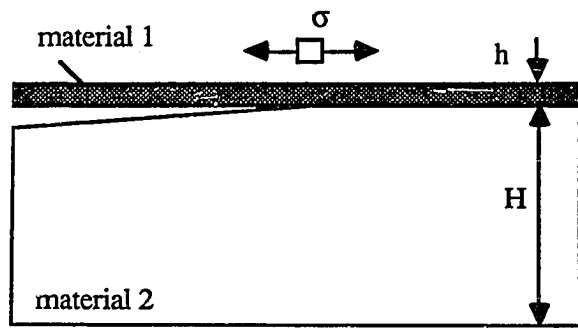
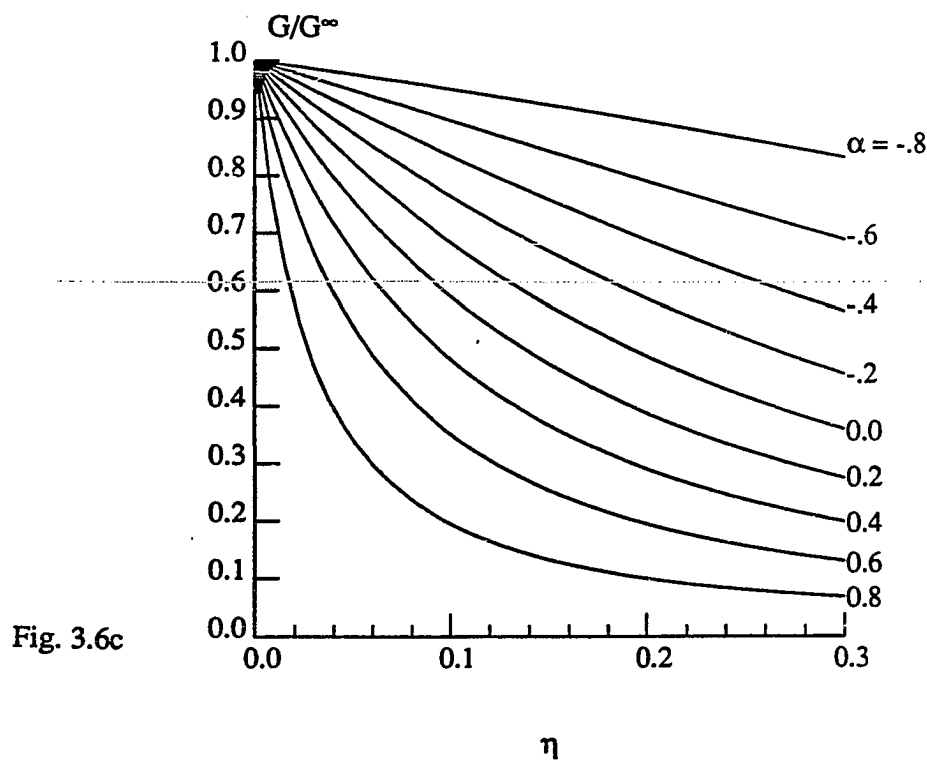
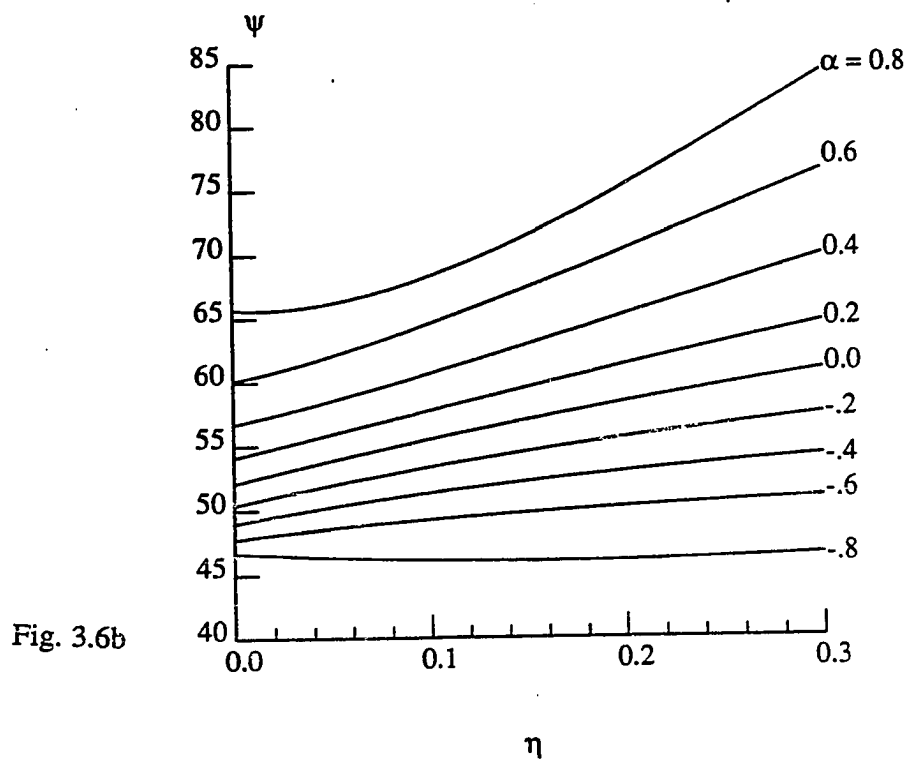


Fig.3.6a A thin film under residual tension.



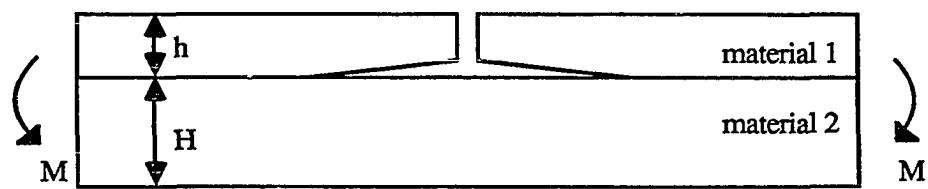
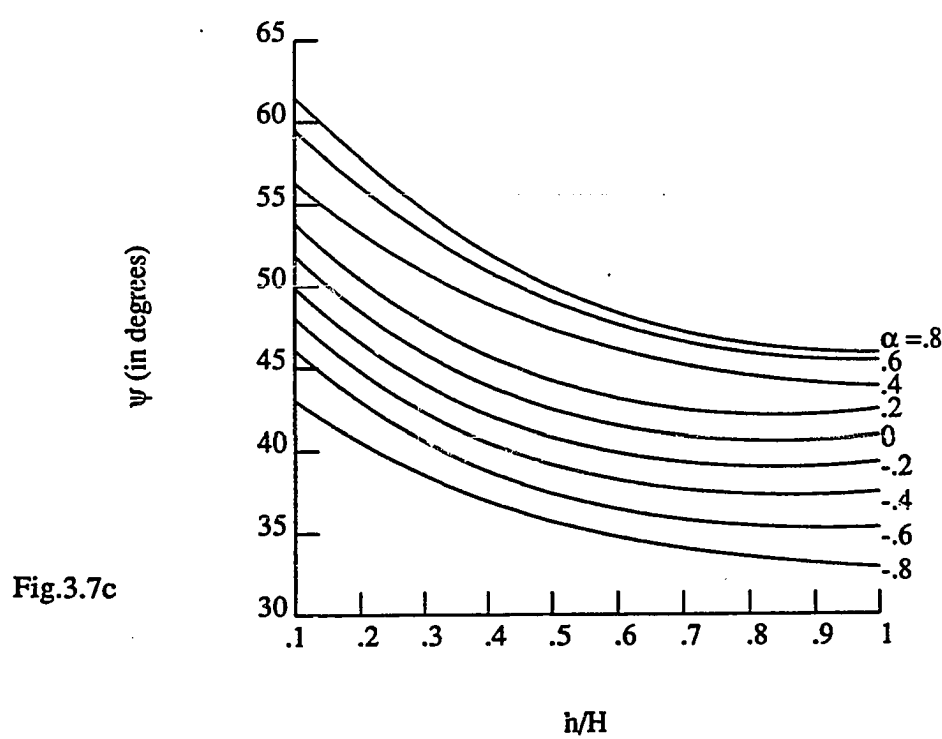
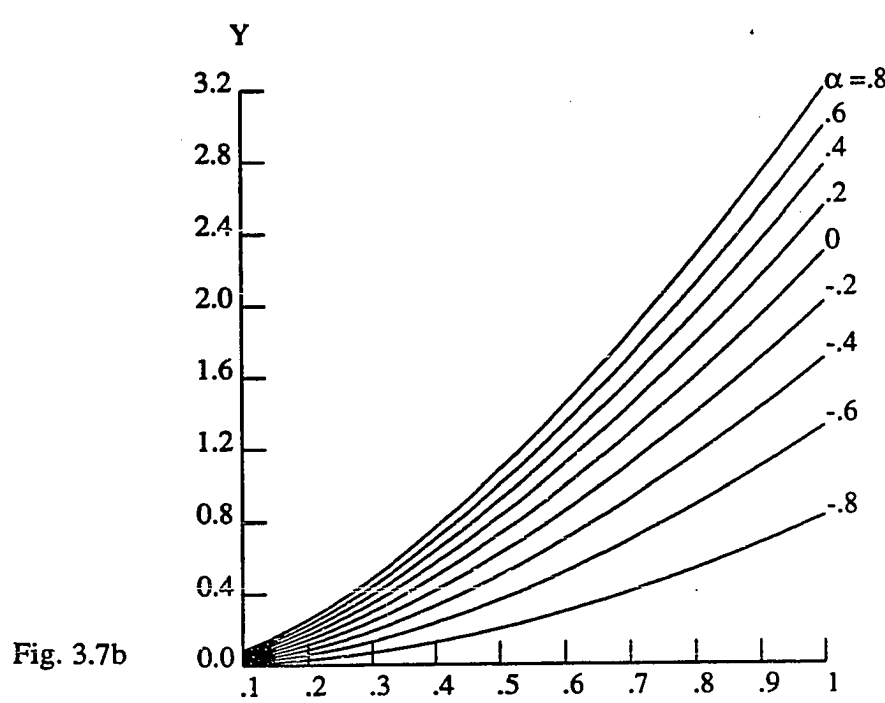


Fig. 3.7a A four-point bend specimen.



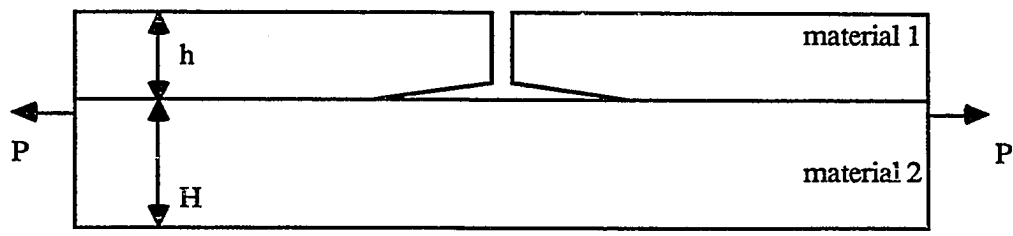


Fig. 3.8a A delamination specimen.

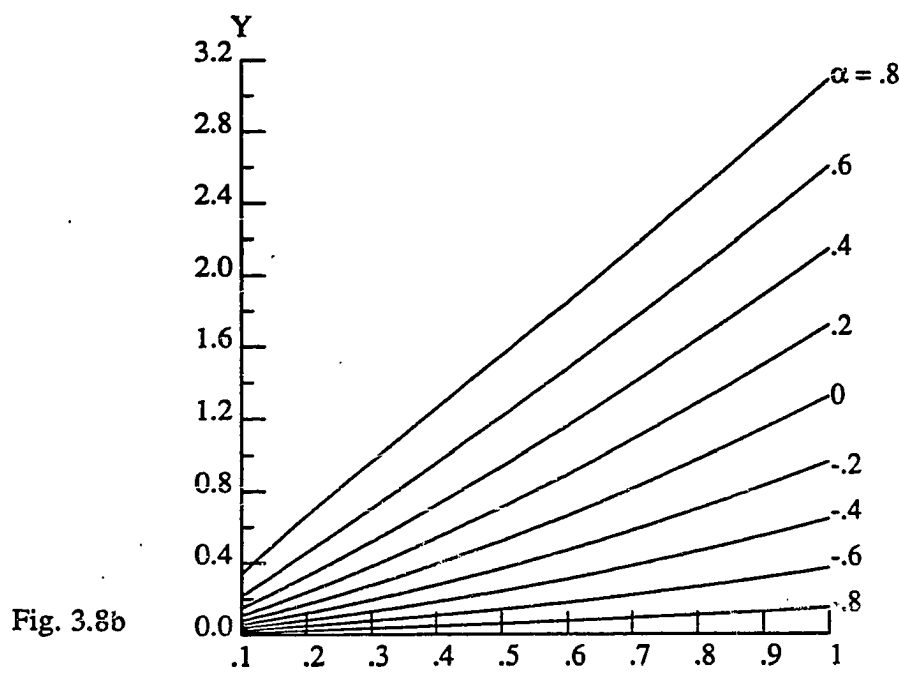


Fig. 3.8b

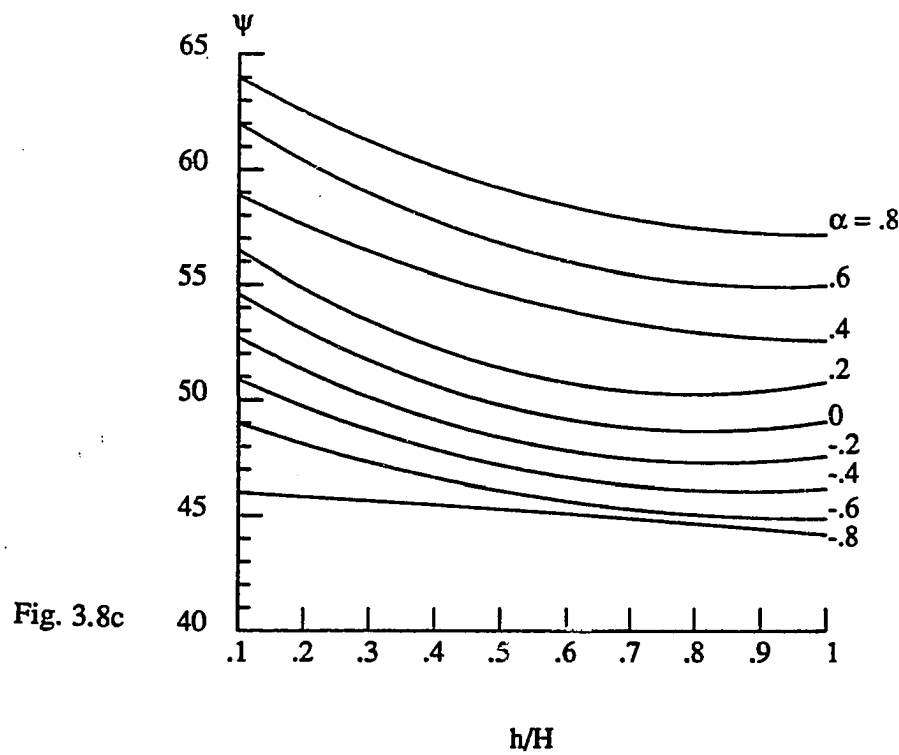


Fig. 3.8c

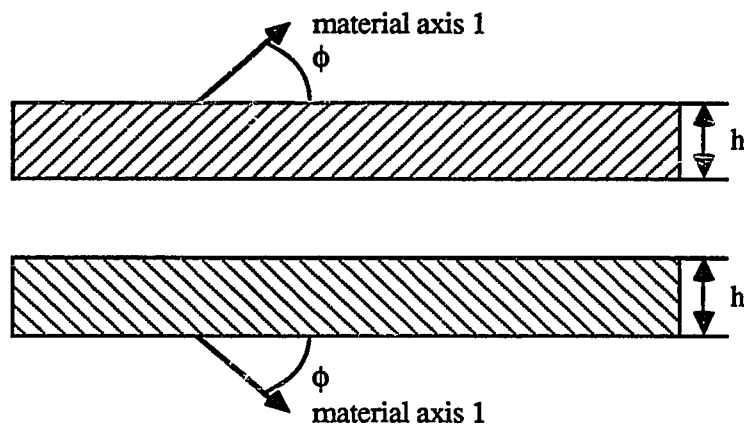


Fig. 4.1 Two strips cut from an orthotropic material.

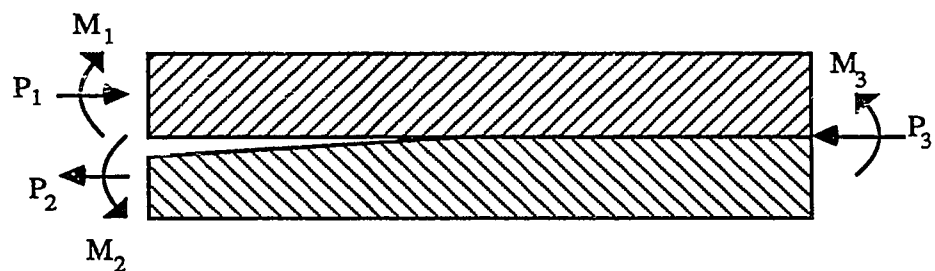


Fig. 4.2 A symmetric double-layer subjected to edge loads.

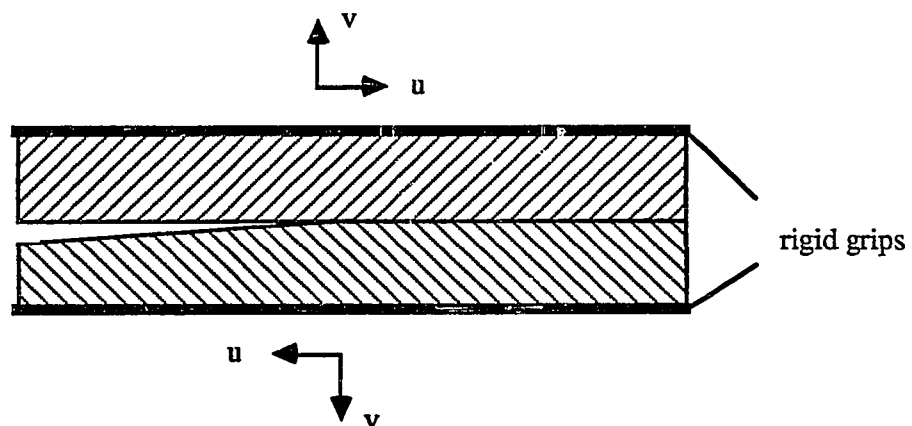


Fig. 4.3 A symmetric double-layer held in rigid grips.

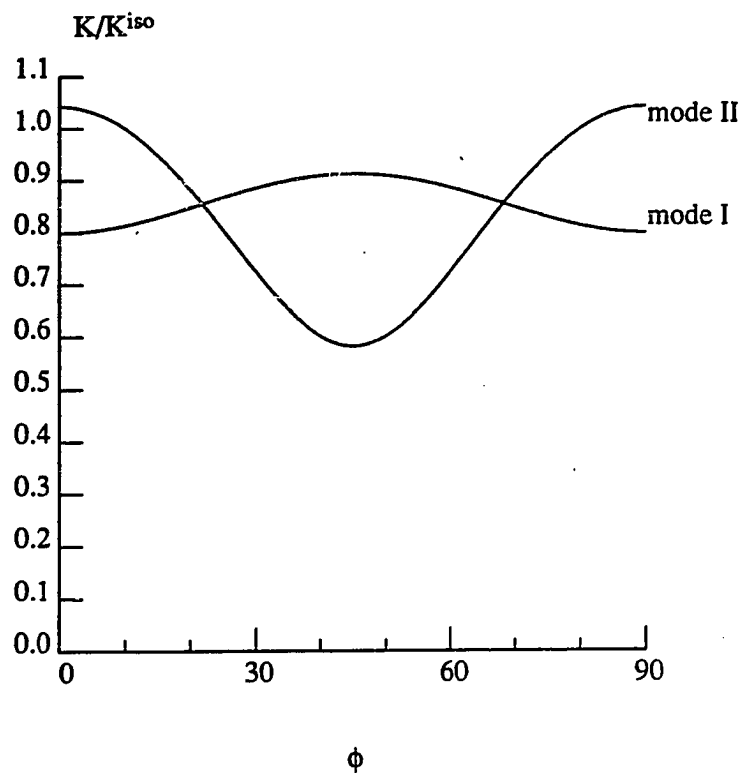


Fig. 4.4 Errors of the isotropic average approximation.